Earth Syst. Dynam. Discuss., doi:10.5194/esd-2016-32, 2016
Manuscript under review for journal Earth Syst. Dynam.
Published: 10 August 2016

Earth System Dynamics
Discussions
Open Access

Climate engineering by mimicking the natural dust climate control: the Iron Salt Aerosols method

Authors:

Franz Dietrich OESTE *[1], Renaud de_RICHTER [2], Tingzhen MING [3], Sylvain CAILLOL [2]

* corresponding author

Affiliations & Addresses:

1 gM-Ingenieurbüro, Tannenweg 2, D-35274 Kirchhain, Germany. Email: oeste@gm-ingenieurbuero.com

2 Institut Charles Gerhardt Montpellier − UMR5253 CNRS-UM2 − ENSCM-UM1 – Ecole Nationale Supérieure de Chimie de Montpellier, 8 rue de l'Ecole Normale, 34296 Montpellier Cedex 5, France.

3 School of Civil Engineering and Architecture, Wuhan University of Technology, No. 122, Luoshi Road, Hongshan District, Wuhan, 430070 China.

Abstract

Power stations, ship, and air traffic are among the most potent greenhouse gas emitters and primarily responsible for global warming. Iron salt aerosols (ISA) exert a cooling effect on climate in several ways. This article aims firstly to examine all direct and indirect natural climate cooling mechanisms driven by tropospheric aerosol particles composed partly of iron and chloride, showing their cooperation and interaction within the different environmental compartments.

It then looks at a proposal to enhance the cooling effects by ISA in order to reach the CoP 21 optimistic target level of a global temperature increase of between 1.5 and 2 °C.

Using mineral dust as a natural analogue tool, the proposed ISA method might be able to reduce climate warming by mimicking the same method used by nature during the glacial periods. The first estimations made in this article show that by doubling the current natural ISA emissions into the troposphere, i.e. by about 0.3 Tg Fe per year, artificial ISA would enable the prevention or even reversal of global warming.

The ISA method proposed integrates technical and economically feasible tools.

Keywords

Iron salt aerosols, cooling the earth, reverse global warming, methane removal, CO_2 removal phytoplankton fertilization, cloud albedo, carbon capture and storage (CCS), climate engineering

Earth Syst. Dynam. Discuss., doi:10.5194/esd-2016-32, 2016
Manuscript under review for journal Earth Syst. Dynam.
Published: 10 August 2016

Earth System Dynamics
Discussions
Open Access

1. Introduction

The 5th assessment report of the Intergovernmental Panel on Climate Change (IPPC), released in November 2014, is clear on the anthropogenic nature of climate change.

Global warming (GW) has already begun to dramatically change continental and marine ecosystems.

A recently noticed risk is that the vertical mixing in the oceans decreases and even reaches a stagnation point (de Lavergne et al., 2014), thus weakening the net oceanic cumulative uptake of atmospheric CO_2 (Bernardello et al., 2014a; Bernardello et al., 2014b).

A consequence of the decrease of vertical ocean mixing is a reduced or interrupted oxygen supply to the depths of the ocean. Currently, the formation of low-oxygen areas in the oceans is increasing (Capone and Hutchins, 2013; Kalvelage et al., 2013). Furthermore, the climate warming entails both a heating of the upper oceanic water layer and a desalting caused by freshwater injection from increasing ice melt. This desalting phenomenon weakens the thermohaline circulation (THC) by promoting density stratification (Hansen et al., 2015) which triggers the formation of oxygen-depleted zones (Voss et al., 2013) that also emit nitrous oxide (N_2O), a potent GHG and a powerful ozone depleting agent.

Warming surface waters and decreasing input of cold oxygenated surface water trigger a temperature rise of the sediments, transforming solid methane hydrate into gaseous methane emissions in seawater (Phrampus et al., 2014). Methane oxidation consumes additional oxygen, decreasing the oxygen content above those areas (Yamamoto et al., 2014).

The same effects are expected with an anticipated increase in spring and summer coastal upwelling intensity, associated with increases in the rate of offshore advection, decreasing the nutrient supply and producing a spatial or temporal (phenological) mismatch between production and consumption in the world's marine most productive ecosystems (Bakun et al., 2015).

These facts have the threatening consequence of a sprawling lack of oxygen in the oceans. In such low-oxygen areas (sub-oxic to anoxic) only bacterial life is possible, higher life forms do not exist there. Accordingly, an early result of the climate warming progression could lead to a dramatic limitation of the oceanic food sources that will be needed for the projected 9-10 billion people by 2050. The same deleterious consequences on seafood supply can also result in ocean surface acidification by increased CO_2 dissolution in sea water and decreased flow of surface water currents to the ocean basin bottoms, limiting reef fish and shelled mollusks survival (Branch et al., 2013).

Any decrease of the THC has severe consequences on all kinds of ecosystems because it further triggers climate warming by different interactions. THC decrease induces a reduction or eventual disappearance of the phytoplankton fertilizers on the ocean surface Si, P, N and Fe extracted from their resources at the bottom of the ocean basins. Hydrothermal fluid

cycling by mid-ocean ridges, off-axis hydrothermal fluid fluxes, subduction-dependent hydrothermal convection fluids, hydrothermal fluxes at hot spot sea mount and fluid emissions from anaerobic sediments, contain said elements as dissolved or colloidal phase (Dick et al., 2015; Hawkes et al., 2013; Holm and Neubeck, 2009; Martin and Russell, 2007; Orcutt et al., 2011; Postec et al., 2015; Resing et al., 2015; Sousa et al., 2013). The deeper water of all ocean basins is enriched by the fertilizers. A THC decrease within the ocean basins will result in a decrease of the assimilative transformation of CO_2 into organic carbon. Moreover, any THC decrease would further trigger the acidification of the ocean surface by lowering or preventing the neutralization of dissolved CO_2 and HCO_3^-, because the alkalinity decreases from hydrothermal sources (Monnin et al., 2014; Orcutt et al., 2011).

During the convective water flow through the huge alkaline ocean crust volume estimated to about 20 - 540 x 10^3 km³/yr (Nielsen et al., 2006) ocean water is depleted in O_2, but enriched in its reductant content like methane (Kawagucci et al., 2011; Orcutt et al., 2011). Even further elements are enriched in this convective water flow through crust rocks, all essential for the existence of life. The re-oxygenation of this huge water volume becomes retarded or even impossible with a minimized THC.

According to model calculations of Watson et al. (Watson et al., 2015) the THC might have significantly changed between last glacial and interglacial periods. During the Cenozoic epoch with ice covered pole caps the incorporation of carbon in the form of carbonate into the oceanic crust became much lower than during the warm Late Mesozoic (Coogan and Gillis, 2013). The findings of Coogan & Gillis show, that during ice-free periods, THCs were possible with much higher effectivity than recently. Even during those warm periods with low temperature gradients between polar and equatorial oceans, an effective production of brines leading to buoyancy differences necessary for development of effective THC, may be generated (Otto-Bliesner et al., 2002). However, increased inflow rates of high density brines coming from shallow shelf regions with high evaporation rates, induced several collapses or vertical reductions of the strong Cretaceous THC. From here and for more than a million years, the lower parts of ocean basins have been filled up with anoxic brines.

Remnants of these anoxic events are black shale sediments (Takashima et al., 2006). During such THC collapses, the uptake of CO_2 into the oceanic crust stayed restricted to organic carbon sediments. Additionally, the organic carbon productivity of the remaining oxic zone was decreased, because phytoplankton fertilizer production was limited to continental weathering.

These examples point out the sensitivity of the THC to disturbances. Without action, the weakness of our recent THC may worsen. Any THC collapse would not only result in severe damages to ecosystems, food chains, and food resources of the oceans, but would also lead to an acceleration of the increase of atmospheric CO_2 concentration, resulting in a faster

Earth Syst. Dynam. Discuss., doi:10.5194/esd-2016-32, 2016
Manuscript under review for journal Earth Syst. Dynam.
Published: 10 August 2016

Earth System Dynamics
Discussions

climate warming than forecasted.

The best means to prevent such disturbing situations and consequences is to stop GW.

A realistic chance of averting this development is the controlled application of a climate cooling process used several times by nature throughout the last ice ages with high efficiency and based on loess dust. Loess is a wind-blown dust sediment formed by progressive accumulation and composed generally of clay, sand and silt (approximately a ratio of 20:40:40 respectively), loosely cemented by calcium carbonate.

The dust concentration in the troposphere increased during every cold period in ice ages and reached a multiple of today's levels (Martínez-Garcia et al., 2011). Dust deposition in the Southern Ocean during glacial periods was 3 to 10 times greater than during interglacial periods, and its major source region was probably Australia or New Zealand (Lamy et al., 2014). The windblown dust and its iron content effect on marine productivity in the Southern Ocean is thought to be a key determinant of atmospheric CO_2 concentrations (Maher and Dennis, 2001). During high dust level periods, the global average temperature fell down to 10°C (Lamy et al., 2014; Martin, 1990; Martínez-Garcia et al., 2011), which is 4.5°C lower than current global average temperature. Loess sediments in the northern and southern hemisphere on continents and ocean floors originate from these cold dusty periods.

Former geoscientists had the predominant conception that the cold glacial temperatures had caused dustiness, and not the reverse (Maher et al., 2010). Meanwhile more evidence accumulates that mineral dust was a main factor in the cause of the cold periods and that the iron (Fe) fraction of wind-blown dust aerosol fertilized the oceans' phytoplankton, activating the assimilative conversion of CO_2 into organic carbon (Anderson et al., 2014; Lamy et al., 2014; Martin, 1990) (Maher et al., 2010; Martínez-García et al., 2014; Ziegler et al., 2013) and carbonate which composes the main dry body substance of phytoplankton, together with silica, another component of dust (Tréguer and Pondaven, 2000). Evidence about the responsibility of iron-containing dust that triggered ice ages during the late Paleozoic epoch are in discussion (Sur et al., 2015).

The process of iron fertilization by injection of iron salt solution into the ocean surface had already been in discussion as an engineering system scheme proposed to mitigate global warming (Smetacek and Naqvi, 2008). But iron fertilization experiments with $FeSO_4$ conducted over 300 km^2 into the Subantarctic Atlantic Ocean, although they doubled primary productivity of Chlorophyll a, did not enhance downdraft particles' flux into the deep ocean (Martin et al., 2013). The researchers attribute the lack of fertilization-induced export to the limitation of silicon needed for diatoms. Thus, ocean fertilization using only iron can increase the uptake of CO_2 across the sea surface, but most of this uptake is transient and will probably not conduct to long-term sequestration (Williamson et al., 2012). In other experiments, the authors (Smetacek et al., 2012) find that iron-fertilized diatom blooms may

sequester carbon for centuries in ocean bottom water, and for longer in the sediments, as up to half the diatom bloom biomass sank below 1 km depth and reached the sea floor. Meanwhile dissolution of olivine, a magnesium-iron-silicate, with a Mg:Fe ratio of nearly 9:1, and containing silica, conducted to 35% marine carbon uptake (with the hypothesis of 1% of the iron dissolved and biologically available), with communities of diatoms being one of the phytoplankton winners (Köhler et al., 2015).

The small content of water-soluble iron salts (IS) in the dust particles triggers this fertilization effect (Duggen et al., 2007) and the soluble iron deposition during glaciations had been up to 10 x modern deposition (Conway et al., 2015). According to Spolaor (Spolaor et al., 2013), most of the bioavailable water soluble Fe(II) has been linked, during the last 55,000 years, to the fine dust fraction, as it was demonstrated from ice cores from Antarctica. During late Paleozoic epochs, glacial stage dust fluxes of ~400 to 4,000 times those of interglacial times had been found (Soreghan et al., 2014), which gives an estimated carbon fixation ~2-20 times that of modern carbon fixation due to dust fertilization. Photochemistry sunshine is the main trigger of the transformation of the primary insoluble iron fraction of dust aerosols into soluble iron salt (Johnson and Meskhidze, 2013), and the understanding of how the different iron content and speciation in aerosols affect the climate is growing (Al-Abadleh, 2015). Currently, increased subglacial melt water and icebergs may supply large amounts of bioavailable iron to the Southern Ocean (Death et al., 2014). The flux of bioavailable iron associated with glacial runoff is estimated at 0.40–2.54 Tg per year in Greenland and 0.06–0.17 Tg per year in Antarctica (Hawkings et al., 2014), which are comparable with Aeolian dust fluxes to the oceans surrounding Antarctica and Greenland, and will increase by enhanced melting in a warming climate. But CO_2 uptake by the oceans is not the only effect of iron dust.

The full carbon cycle is well described in the literature; meanwhile the iron biogeochemical cycle is only described in the ocean by few scientific publications (Boyd and Ellwood, 2010; Mahowald et al., 2005; Mahowald et al., 2009). This review aims to describe the multi-stage chemistry of the iron cycle on the atmosphere, oceans, land, sediments and ocean crust. This article is a comprehensive review of the evidence for connections between the carbon cycle and the iron cycle and their direct and indirect planetary cooling effects. Numerous factors influence the Fe-cycle and the iron dissolution: iron speciation, photochemistry, biochemistry, red-ox chemistry, mineralogy, geology. In order to perform an accurate prediction of the impact of Fe-containing dusts, sea salt, and acidic components, the atmospheric chemistry models need to incorporate all relevant interaction compartments of the Fe-cycle with sun radiation, chlorine, sulphur, nitrogen and water. This review advocates a balanced approach to make profit of the Fe-cycle to fight global warming by enhancing natural processes.

Earth Syst. Dynam. Discuss., doi:10.5194/esd-2016-32, 2016
Manuscript under review for journal Earth Syst. Dynam.
Published: 10 August 2016

Breakdown of sections:

The next three sections describe about a dozen different climate cooling processes induced by iron salt aerosols (ISA) and their interaction for modelling parameter development (sections 2, 3 and 4). Then estimation of the requirements in terms of ISA, to stop global warming will be given in section 5, followed by the description of a suggested ISA enhanced method to fight global warming and induce planetary cooling in section 6, followed by a general discussion and concluding remarks in section 7. To our knowledge, this review completes the previous global iron cycle vision of Parekh (Parekh et al., 2004) and advocates a balanced approach to make profit of the iron cycle to fight global warming by enhancing natural processes.

Components of the different natural cooling mechanism by ISA

The best known cooling process induced by ISA is the phytoplankton fertilizing stage described in the introduction. But this process is only part of a cascade of at least 12 climate cooling stages presented in this article. These stages are embedded within the coexisting multi-component complex networks of different reciprocal iron induced interactions across the borders of atmosphere, surface ocean, sediment and igneous bedrock as well as across the borders of chemistry, biology, and physics and across and along the borders of illuminated, dark, gaseous, liquid, solid, semi-solid, animated, unanimated, dead and different mix phase systems. Some impressions according to the complexity of iron acting in the atmospheric environment have been presented by Al-Abadleh (Al-Abadleh, 2015).

The ISA-induced cooling effect begins in the atmosphere. Each of the negative forcing stages unfolds a climate-cooling potential for itself. Process stages 1-6 occur in the troposphere (chapter 2), stage 6 at sunlit solid surfaces, stages 7-8 in the ocean (chapter 3), and stages 9-12 in the oceanic sediment and ocean crust (chapter 4). The 12 stages of this cooling process cascade operate as described below.

2. Tropospheric natural cooling effects of the iron cycle

2.1. ISA-induced cloud albedo increase

Aerosols have a climate impact through aerosol–cloud interactions and aerosol–radiation interactions (Boucher, 2015). By reflecting sunlight radiation back to space, some types of aerosols increase the local albedo (which is the fraction of solar energy that is reflected back to space), producing a cooling effect (Bauer and Menon, 2012). If the top of clouds reflect back a part of the incident solar radiation received, the base of clouds receive the longwave radiation emitted from the Earth surface and reemit downward a part of it. Usually, the higher a cloud is, in the atmosphere, the greater its effect on enhancing atmospheric greenhouse

Earth Syst. Dynam. Discuss., doi:10.5194/esd-2016-32, 2016
Manuscript under review for journal Earth Syst. Dynam.
Published: 10 August 2016

Earth System Dynamics Discussions

warming, and therefore the overall effect of high altitude clouds, like cirrus, is a positive forcing. Meanwhile, the net effect of low altitude clouds (stratocumulus) is to cool the surface, as they are thicker and prevent more sunlight from reaching the surface. The overall effect of other types of clouds like cumulonimbus is neutral: neither cooling nor warming.

More outgoing long-wave radiation is possible when the cirrus cover is reduced. Efficient ice nuclei (such as bismuth tri-iodide) seeding of cirrus cloud might artificially reduce their cover (Mitchell and Finnegan, 2009; Storelvmo et al., 2013).

In order to enhance the cooling effects of low altitude clouds, marine cloud brightening has been proposed (Latham et al., 2012a), for instance by injecting sea salt aerosols over the oceans. The effect depends on both particle size and injection amount, but a warming effect is possible (Alterskjær and Kristjánsson, 2013).

Aerosol effects on climate are complex because aerosols both reflect solar radiation to space and absorb solar radiation. In addition, atmospheric aerosols alter cloud properties and cloud cover depending on cloud type and geographical region (Koch and Del Genio, 2010). The overall effect of aerosols on solar radiation and clouds is negative (a cooling effect), which masks some of the GHGs-induced warming. But some individual feedbacks and forcing agents (black carbon, organic carbon, and dust) have positive forcing effects (a warming effect). For instance, brown clouds are formed over large Asian urban areas (Ramanathan et al., 2007) and have a warming effect. The forcing and feedback effects of aerosols have been clarified (Bauer and Menon, 2012) by separating direct, indirect, semi-direct and surface albedo effects due to aerosols.

Hygroscopic salt aerosols act as cloud condensation nuclei (CCN) (Karydis et al., 2013; Levin et al., 2005). ISA particles are hygroscopic. High CCN particle concentrations have at least three different cooling effects (Rosenfeld and Freud, 2011; Rosenfeld et al., 2008). Each effect triggers the atmospheric cooling effect by a separate increase of earth reflectance (albedo) (Rosenfeld et al., 2014):

- Cloud formation (even at low super saturation);
- Formation of very small cloud droplets, with an elevated number of droplets per volume, which causes elevated cloud whiteness;
- Extending the lifetime of clouds, as the small cloud droplets cannot coagulate with each other to induce precipitation fall.

Figure 1 illustrates this albedo change due to ISA-CCN particles.

Earth Syst. Dynam. Discuss., doi:10.5194/esd-2016-32, 2016
Manuscript under review for journal Earth Syst. Dynam.
Published: 10 August 2016

Earth System Dynamics
Discussions
Open Access

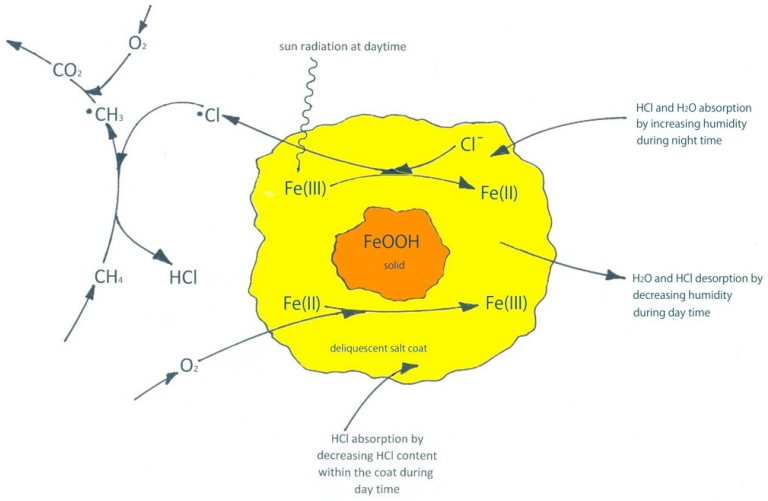

Figure 1. Process of tropospheric cooling by direct and indirect increasing of the quantity of different cloud condensation nuclei (CCN) inducing albedo increase by cloud formation at low supersaturation, cloud whitening and cloud life elongation.

Additional to climate cooling effects, CCN-active aerosols might induce a weakening of tropical cyclones. The cooling potential of the ocean surface in regions of hurricane genesis and early development, by cloud whitening potential (Latham et al., 2012b) shall be casual. Further effects like delayed development, weakened intensity, early dissipation, and increased precipitation have been found (Wang et al., 2014c; Zhang et al., 2009).

2.2. Oxidation of methane and further GHGs

Currently, methane (CH_4) in the troposphere is destroyed mainly by the hydroxyl radical °OH. Only 3 to 4 % CH_4 (25 Tg/yr) become oxidized by °Cl in the troposphere (Allan et al., 2007; Graedel and Keene, 1996).

Absorption of photons by semi-conductor metal oxides can provide the energy to produce an electron-hole pair able to produce either a reduced or an oxidized compound. At suitable conditions UV and visible light can reduce a variety of metal ions in different environments (Monico et al., 2015; Oster and Oster, 1959) (Thakur et al., 2015). Photo-reduced metal compounds may further act as effective chemical reductants (Ola and Maroto-Valer, 2015; Xu et al., 2015) and the oxidized compounds like hydroxyl radicals or chlorine atoms, can further

Earth Syst. Dynam. Discuss., doi:10.5194/esd-2016-32, 2016
Manuscript under review for journal Earth Syst. Dynam.
Published: 10 August 2016

act as effective oxidants. Zamaraev et al. (Zamaraev et al., 1994) proposed the decomposition of reducing atmospheric components like methane by photolytically induced oxidation power of the oxides of iron, titanium and some further metal oxide containing mineral dust components. In this sense Zamaraev designated the dust generating deserts of the globe as “kidneys of the earth” (Zamaraev, 1997) and the atmosphere as a giant photocatalytic reactor where numerous physicochemical and photochemical processes occur (Zamaraev et al., 1994). Researches have proposed giant photocatalytic reactors to clean the atmosphere of several GHGs, like N_2O (de Richter et al., 2016b), CFCs and HCFCs (de Richter et al., 2016a) and even CO_2 after direct air capture (Kiesgen de_Richter et al., 2013), as almost all GHGs can be transformed or destroyed by photocatalysis (de Richter and Caillol, 2011).

Oeste suggested (Oeste, 2004) and Wittmer et al. confirmed (Wittmer et al., 2015a; Wittmer et al., 2015b; Wittmer and Zetzsch, 2016) the emission of methane depleting chlorine atoms. This can be induced by 3 ways: sunlight photo reduction of Fe(III) to Fe(II) from $FeCl_3$ or FeOOH containing salt pans, from $FeCl_3$ or FeOOH-containing sea spray aerosols and from pure FeOOH aerosol in contact with air containing ppbv amounts of HCl. Because the H abstraction from the GHG CH_4 as the first oxidation step by °Cl is at least 16 times faster compared to the oxidation by °OH, which is the only CH_4 oxidant acting in the ISA-free atmosphere, concentration of CH_4 can be significantly reduced by ISA emission. Figure 2 illustrates by a simplified chemical reaction scheme this climate cooling mechanism by the ISA method: a direct cooling of the troposphere by methane oxidation induced by ISA particles.

Earth Syst. Dynam. Discuss., doi:10.5194/esd-2016-32, 2016
Manuscript under review for journal Earth Syst. Dynam.
Published: 10 August 2016

Earth System Dynamics
Discussions
Open Access

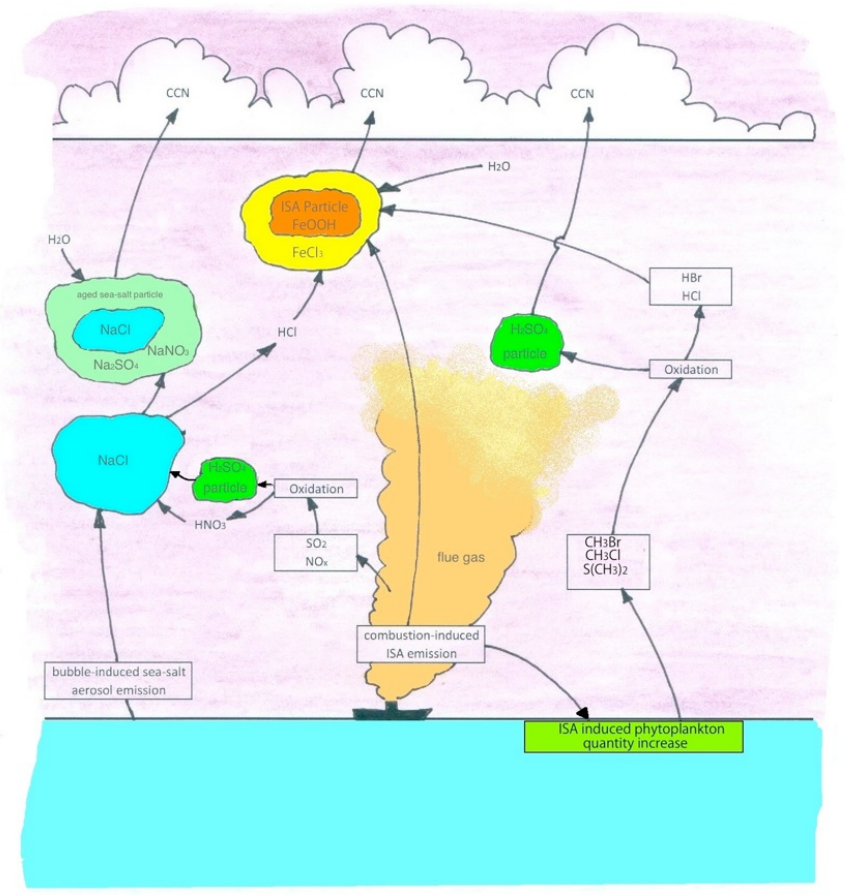

Figure 2. simplified chemical reaction scheme of the generation of chlorine radicals by iron salt aerosols under sunlight radiation and the reaction of the chlorine radicals with atmospheric methane.

At droplet or particle diameters below 1 µm, between 1 µm and 0,1 µm, contact or

coagulation actions between the particles within aerosol clouds are retarded (Ardon-Dryer et al., 2015; Rosenfeld and Freud, 2011; Santachiara et al.; Wang et al., 1978). Otherwise the aerosol lifetime would be too short to bridge any intercontinental distance or even arrive in polar regions. That reduces the possible Cl^- exchange by particle contact. But absorption of gaseous HCl by reactive iron oxide aerosols resulting in Fe(III) chloride formation at the particle surfaces is possible (Wittmer and Zetzsch, 2016). Gaseous HCl and further gaseous chloro-compounds are available in the troposphere: HCl (300 pptv above the oceans and 100 pptv above the continents) (Graedel and Keene, 1996), $ClNO_2$ (up to 1500 pptv near flue gas emitters) (Osthoff et al., 2008; Riedel et al., 2014) and CH_3Cl (550 pptv remote from urban sources) (Khalil and Rasmussen, 1999; Yokouchi et al., 2000). By or after sorption and reactions like photolysis, oxidation, and reduction, any kind of these chlorine species can induce chloride condensation at the ISA particle surface. Acid tropospheric aerosols and gases like H_2SO_4, HNO_3, oxalic acid, and weaker organic acids further induce the formation of gaseous HCl from sea-salt aerosol (Drozd et al., 2014; Kim and Park, 2012; Pechtl and von Glasow, 2007). Since 2004, evidence and proposals for possible catalyst-like sunshine-induced cooperative heterogeneous reaction between Fe(II), Fe(III), Cl^-, °Cl, and HCl fixed on mineral dust particles and in the gaseous phase on the CH_4 oxidation are known (Oeste, 2004; Wittmer and Zetzsch, 2016). Further evidence of sunshine-induced catalytic cooperation of Fe and Cl came from the discovery of °Cl production and CH_4 depletion in volcanic eruption plumes (Baker et al., 2011; Rose et al., 2006). Wittmer et al. presented sunshine-induced °Cl production by iron oxide aerosols in contact with gaseous HCl (Wittmer and Zetzsch, 2016). Further evidence comes from °Cl found in tropospheric air masses above the South China Sea (Baker et al., 2015). It is known that the troposphere above the South China Sea is often in contact with Fe-containing mineral dust aerosols (~18 g m^{-2} a^{-1}) (Wang et al., 2012). This is further evidence that the Fe oxide-containing mineral dust aerosol might be a source for the °Cl content within this area.

HCl, water content and pH within the surface layer of the aerosol particles depend on the relative humidity. Both liquid contents, H_2O and HCl, grow with increasing humidity (von Glasow and Sander, 2001). In spite of growing HCl quantity with increasing humidity, pH increases because of decreasing HCl concentration within the surface layer. Hence, since the radiation induced °Cl production decreases with decreasing pH, the °Cl emission decreases in humid conditions (Wittmer and Zetzsch, 2016). Under dry conditions, even sulphate may be fixed as solid Na-sulphate hydrates. Solubilized sulphate slightly inhibits the iron induced °Cl production (Bleicher et al., 2014).

Night or early morning humidity produces similarly the maximum chloride content on the liquid aerosol particles surface. During day time, the humidity decrease induces ISA photolysis and Cl^- conversion to °Cl production by decreasing water content and pH. The ISA

particle surface layer comes to Cl^- minima levels during or after noon hours. In the continental troposphere low sea salt aerosol level, these effects enable the pure ISA iron oxide aerosol particles to coat their surface with chloride solution at night and to produce chlorine atom emission at daytime.

Freezing has different effects on the primary wet ISA particles. Changing by CCN action to cloud droplets with solubilized chloride and iron content and when arriving to freezing conditions, the frozen ice becomes covered by a mother liquor layer with elevated concentration of both iron and chlorine. Some acids like HCl do not decrease the mother liquor pH proportional to concentration and the behavior of the ice surfaces, grown from low salt content water, are different from high salt content water, thus the different kinds of ISA shall behave differently. (Bartels-Rausch et al., 2014; Kahan et al., 2014; Wren and Donaldson, 2012). Direct measurements of molecular chlorine levels in the Arctic marine boundary layer in Barrow, Alaska, showed up to 400 pptv levels of molecular chlorine (Liao et al., 2014). The Cl concentrations fell to near-zero levels at night but peaked in the early morning and late afternoon. The authors estimated that the Cl radicals oxidized on average more CH_4 than hydroxyl radicals, and enhanced the abundance of short-lived peroxy radicals.

Further investigations have to prove how the different types of ISA particles behave in clouds below the freezing point or in the snow layer at different temperatures: the primary salt-poor Fe-oxide, the poor $FeCl_3$-hydroyzed and the $FeCl_3$-NaCl mixture, because the °Cl emission depends on pH, Fe and Cl concentration.

Additional to iron photolysis, in a different and day-time independent chemical reaction, iron catalyzes the formation of °Cl or Cl_2 from chloride by tropospheric ozone (Sadanaga et al., 2001). Triggering the methane decomposition, both kinds of iron and chlorine have a cooperative cooling effect on the troposphere: less GHG methane in the atmosphere reduces the GH effect and allows more outgoing IR heat to the outer space.

These reactions had been active during the glacial period: Levine et al. (Levine et al., 2011) found elevated $^{13}CH_4$ / $^{12}CH_4$ isotope ratios in those Antarctic ice core segments representing coldest glacial periods. The much greater °Cl preference for $^{12}CH_4$ oxidation than $^{13}CH_4$ oxidation than by the °OH is an explanation for this unusual isotope ratio. Additional evidence gives the decreased CH_4 concentration during elevated loess dust emission epochs (Skinner, 2008).

As shown in more detail in the next section 2.3 ISA produces °Cl and much more hydrophilic °OH and ferryl as further possible CH_4 oxidants by the Fenton and photo-Fenton processes (Al-Abadleh, 2015). To gain the optimal reaction conditions within the heterogeneous gaseous / liquid / solid phase ISA system in the troposphere the reductant (methane) and oxidant (Fenton and photo-Fenton oxidant) have to be directed in a way, that oxidant and

Earth Syst. Dynam. Discuss., doi:10.5194/esd-2016-32, 2016
Manuscript under review for journal Earth Syst. Dynam.
Published: 10 August 2016

reductant can act within the identical medium.

Table 1: the Henry's law constants (Sander, 2015) for the different components of the ISA.

Element	Henry's law constant
CH4	1.4 x 10^{-5} mol m^{-3} $Pa^{-}1$
°Cl	2.3 x 10^{-2} mol m^{-3} Pa^{-1}
°OH	3,8 x 10^{-1} mol m^{-3} Pa^{-1}
Fe(II), Fe(III), Fe(IV) (dissolved and/or solid)	>10^{6} mol m^{-3} Pa^{-1}

As seen on table 1, according to the CH_4 Henry's law constant the preference of the 1.8 ppm tropospheric CH_4 is undoubtedly the gaseous phase. °Cl has a preference for the gaseous phase. Iron is completely part of the liquid or solid phase, so the Henry's law constant is estimated to more than 10^6 mol m^{-3} Pa^{-1} (Sander, 2015). While ferryl keeps tightly bound to the condensed phases °OH may change into the gaseous phase (Nie et al., 2014) and may contribute to the oxidation of CH_4 during clear dry conditions without liquid phase at the Fe(III) surfaces.

Like the water-soluble Ammonia (5.9 x 10^{-1}), °OH has a similar Henry's law constant. Therefore °OH has the tendency to stay within hydrous phases during humid conditions. This tendency is 16 times lower for °Cl. This property is combined with the 16 times higher reactivity in comparison to °OH. At an equal production of °Cl and °OH, the reaction of °Cl with CH_4 has a probability of up to 250 times (16 x 16) that of °OH with CH_4 when the ISA particles are wet and 16 times that of °OH with CH_4 when the ISA particles are dry. The probability of CH_4 oxidation by ISA derived °Cl against ISA derived °OH, may be restricted by the pH increase tendency within ISA during humid episodes (decreased °Cl generation on ISA with rising pH), to values fluctuating between the extremes 1 and 250. Independent of the kind of oxidants produced by ISA – during dry, clear sky, and sunshine episodes - the ISA deriving oxidants produce maximum oxidant concentrations within the CH_4-containing gaseous phase, producing optimum CH_4 depletion rates.

The °Cl reactivity on most VOC other than CH_4 is at least one order of magnitude higher than that of °OH (Young et al., 2014). Halogen organics like dichloromethane (Pena et al., 2014) as well as the environmental persistent and bioaccumulating perfluoro organics like perfluoro octane sulphonate may be depleted by sunlit ISA (Jin et al., 2014).

2.3. Oxidation of organic aerosol particles containing black and brown carbon

Andreae & Gelencsér (Andreae and Gelencsér, 2006) defined the differences between the carbons: black carbon contains insoluble elemental carbon, brown carbon contains at least

partly soluble organic carbon. Black carbon contains as well additional extractable organics of more or less volatility and/or water-solubility (Andreae and Gelencsér, 2006; Nguyen and Ball, 2006)..

Black and brown carbonaceous aerosols have a positive radiative forcing (warming effect) on clouds (Ramana et al., 2010) as seen in sub-section 2.1, and also after deposition on snow, glaciers, sea ice or on the polar regions, as the albedo is reduced and the surface is darkened (Hadley and Kirchstetter, 2012). One of the most effective methods of slowing global warming rapidly on short-term is by reducing the emissions of fossil-fuel particulate black carbon, organic matter and reducing of tropospheric ozone (Jacobson, 2002).

Both aerosol types have adverse effects to health (human, animal, livestock, vegetal) and reducing its levels will save lives and provide many benefits (Shindell et al., 2012).

Thus any tropospheric lifetime reduction of both dark carbons would gain cooling effects and further positive effects.

Both carbons are characterized by aromatic functions. The black carbons contain graphene structures, the brown ones have low-molecular weight humic-like aromatic substances (HULIS). HULIS derive from tarry combustion smoke residues and/or from aged secondary organic aerosol (SOA). The source of SOA are biogenic VOCs like terpenes (Fry et al., 2014). HULIS contain polyphenolic red-ox mediators like catechol and nitro-catechols (Claeys et al., 2012; Hoffer et al., 2004; Ofner et al., 2011; Pillar et al., 2014).

The polyphenolic HULIS compounds are ligands with very strong binding to iron. Rainwater-dissolved HULIS prevent Fe(II) from oxidation and precipitation when mixing with seawater (Willey et al., 2008). Wood smoke derived HULIS nano-particles penetrate into living cell walls of respiratory epithelia cells. After arrival in the cells the HULIS particles extract the cell iron from the mitochondria by formation of HULIS iron complexes (Ghio et al., 2015).

Beside iron, other metals like manganese and copper have oxygen transport properties which improve the oxidation power of H_2O_2 by Fenton reactions generating °OH (Chemizmu and Fentona, 2009). H_2O_2 is a troposphere-borne oxidant (Vione et al., 2003).

Polyphenolic and carboxylate ligands of HULIS enhance the dissolution of iron oxides. These ligands bind to undissolved iron oxides (Al-Abadleh, 2015).

Iron and catechols are both reversible electron shuttles:

$Fe^{2+} \leftrightarrow Fe^{3+} + e$ (Eq. 1);

catechol $\leftrightarrow$ quinone + 2e (Eq. 2).

The HULIS – iron connection enhances the oxidative degradation of organic compounds like aromatic compounds (Al-Abadleh, 2015).

Oxidant generation by reaction of oxidizable dissolved or un-dissolved metal cations like Fe(II), Cu(I) and Mn(II) with H_2O_2 had first been discovered for instance for Fe(II) in 1894

Earth Syst. Dynam. Discuss., doi:10.5194/esd-2016-32, 2016
Manuscript under review for journal Earth Syst. Dynam.
Published: 10 August 2016

(Fenton, 1894). Since then these reactions are known as Fenton reactions. Mechanisms and generated oxidants of the Fenton reactions are still under discussion.

According to the participating metal ligand oxidants like °OH, $Fe(IV)O^{2+}$ (= Ferryl), °Cl, $°SO_4^-$, organic peroxides and quinones may appear (Barbusiński, 2009).

According to Barbusinsky et al. the primary reaction intermediate from Fe^{2+} and H_2O_2 is the adduct $\{Fe(II)H_2O_2\}^{2+}$ which is transformed into the ferryl complex $\{Fe(IV)(OH)_2\}^{2+}$. The latter stabilizes as $\{Fe(IV)O\}^{2+} + H_2O$. Reductants may also react directly with $\{Fe(IV)O\}^{2+}$ or after its decomposition to Fe^{3+} + °OH + OH- by °OH. Fe^{3+} reacts with H_2O_2 to Fe^{2+} via $°O_2H$ development; the latter decays into $O_2 + H_2O$.

Light enhances the Fenton reaction effectiveness. It reduces Fe^{3+} to Fe^{2+} by photolysis inducing °OH or °Cl generation, the latter in the case of available Cl^-, which reduces the H_2O_2 demand (Machulek Jr et al., 2009; Southworth and Voelker, 2003).

This process is illustrated by figure 3.

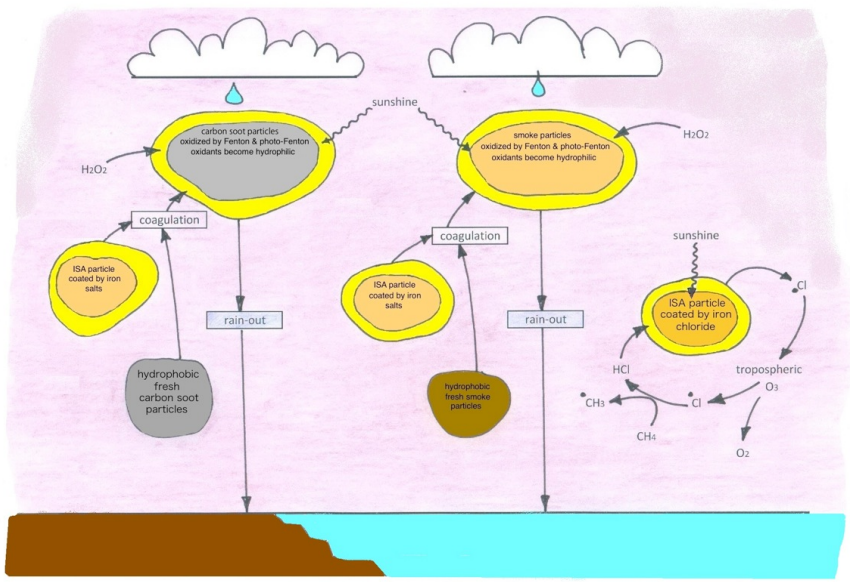

Figure 3. Schematic representation of the cooling of the troposphere, by inducing the decrease of ozone and organic aerosol particles like soot and smoke.

The Fenton reaction mechanism is dependent on pH and on the kinds of ligands bound to the Fenton metal. The reaction mechanism or oxidants of SO_4^{2-}, NO_3^-, Cl^- and 1,2-dihydroxy benzene ligands had been studied (De Laat et al., 2004).

In biological systems, 1,2-dihydroxy benzenes (catecholamines) regulate the Fenton reaction and orient it toward different reaction pathways (Salgado et al., 2013).

Additionally, the fractal reaction environments like surface rich black and brown carbons and ISA are of considerable influence on the Fenton reaction. By expanding the aqueous interface, accelerations of the reaction velocity up to three orders of magnitude had been measured (Enami et al., 2014). This may be one of the reasons why iron-containing solid surfaces made of fractal iron oxides, pyrite, activated carbon, graphite, carbon nanotubes, vermiculite, pillared clays, zeolites have been tested as efficient Fenton reagents (Pignatello et al., 2006; Pinto et al., 2012; Teixeira et al., 2012).

Even the oxidation power of artificial Fenton and photo-Fenton systems is known to be high enough to hydroxylate aliphatic C-H bonds, inclusive CH_4 hydroxylation to methanol (Gopakumar et al., 2011; Hammond et al., 2012; Yoshizawa et al., 2000).

But the HULIS itself becomes depleted by the Fenton oxidation when it remains as the only reductant (Salgado et al., 2013).

Like HULIS or humic substances, the different kinds of black carbons act as red-ox mediators because of their oxygen functionalities bound to the aromatic hexagon network like hydroxyl, carbonyl, and ether (Klüpfel et al., 2014; Oh and Chiu, 2009). These functionalities act similarly as hydroquinone, quinone, aromatic ether, pyrylium and pyrone at the extended graphene planes as electron acceptor and donor moieties. Soot also possesses such red-ox mediator groups (Drushel and Hallum, 1958; Studebaker et al., 1956). Again these are ligands with well-known binding activity on iron compounds. Their difference to the HULIS ligands is that they are attached to stacks of aromatic graphene hexagon networks instead of mono- or oligo-cyclic aromatic hexagons of HULIS. As well as the HULIS red-ox mediator ligands these hydroxyl and ketone groups transfer electrons from oxidants to reductants and vice versa. Like the HULIS – iron couple, the black carbon - iron couple enhances the red-ox mediation above the levels of every individual electron shuttle (Kim et al., 2013; Lima et al., 2013; Wang et al., 2014b). Accordingly, any ISA doping of black carbons generates effective oxidation catalysts (Oeste, 1977; Song et al., 2015).

Lit by sunlight the ISA doped soot represents an oxidation catalyst to adsorbed organics producing its own oxidants by the photo-Fenton reaction. In spite of the higher chemical stability of the graphene network of soot compared to HULIS soot, by wet oxidation further oxygen groups are fixed to the soot graphene stacks (Moreno-Castilla et al., 2000) increasing soot's hydrophilic property, which is necessary to arrange its rain-out. The hydroxyl radical attack resulting from the photo Fenton reaction at last breaks the graphene network into parts (Bai et al., 2014; Zhou et al., 2012). Photo-Fenton is much more efficient in °OH generation than Fenton, because Fe(III) reduction as regeneration step occurs by Fe(III) photo reduction, rather than consuming an organic reductant.

Earth Syst. Dynam. Discuss., doi:10.5194/esd-2016-32, 2016
Manuscript under review for journal Earth Syst. Dynam.
Published: 10 August 2016

The oxidized hydrophilic carbon particles are more readily washed out of the atmosphere by precipitation (Zuberi et al., 2005). ISA accelerates this oxidation process because the iron-induced Fenton and photo-Fenton reaction cycles produce hydroxyl and chlorine radical oxidants, speeding up the soot oxidation.

Fe(III) forms colored complexes with hydroxyl and carboxylic hydroxyl groups too, particularly if two of them are in 1,2 or 1,3 position, like oxalic acid. The latter belong to the group of dicarboxylic acids known to be formed as oxidation products from all kind of volatile, dissolved or particular organic carbons in the atmosphere (Kawamura et al., 2003). Dicaboxylate complexes with iron are of outstanding sensitivity to destruction by photolysation (Eder, 1880, 1906; Weller et al., 2014; Zhu et al., 1993): photolysis reduces Fe(III) to Fe(II) by producing H_2O_2 and oxidation of the organic complex compounds. Then Fe(II) is re-oxidized to Fe(III) by H_2O_2 in the Fenton reaction by generation of °OH (Cunningham et al., 1988). According to their elevated polarity oxidation products containing hydroxyl and carboxyl groups have increased wettability, are more water soluble and are thus rapidly washed out from the atmosphere.

Because of their elevated reactivity compared to CH_4 the gas phase oxidation of airborne organic compounds by ISA-generated °OH or °Cl is enhanced. By eliminating black and brown carbon aerosols, ISA contributes to global warming reduction and to decreasing polar ice melting by surface albedo reduction caused by black-carbon snow contamination (Flanner et al., 2007; Ramanathan and Carmichael, 2008).

The generation of ISA by combusting fuel oil with ferrocene or other oil soluble iron additives in ship engines or heating oil burners has additional positive effects, because soot becomes catalytically flame-oxidized in the presence of flame-borne ISA (detailed in chapter 6) as a combustion product of the iron additive (Kasper et al., 1998; Weiser et al.).

2.4. Tropospheric Ozone depletion by ISA

An additional GHG is the tropospheric ozone (Jacobson, 2002). Since long, °Cl and °Br are known as ~~a~~ catalysts for ozone destruction in the Stratosphere (Crutzen and Oppenheimer, 2008). Investigations both in laboratory and nature have shown that °Br is a much more active catalyst of ozone depletion within the troposphere than °Cl (Le Bras and Platt, 1995; Liao et al., 2014; Wayne et al., 1995).

The ISA-induced increase of °Br concentration at sea-salt containing tropospheric conditions has been confirmed (Wittmer et al., 2015a). This establishes ISA as part of an ozone-depleting reaction cycle and additional cooling stage. This depletion effect of the GHG tropospheric ozone is worth noting.

As discussed at the end of chapter 2.6 clear evidence exists, that the ozone depleting “bromine explosions” known as regular phenomenon developing from cost-near snow layers

Earth Syst. Dynam. Discuss., doi:10.5194/esd-2016-32, 2016
Manuscript under review for journal Earth Syst. Dynam.
Published: 10 August 2016

at sunrise in the polar spring (Blechschmidt et al., 2016; Pratt et al., 2013) are likely to be induced by the photolysed precipitation of iron containing dust. According to Pratt bromide enriched brines covering acidified snow particles become oxidized by photolyzation to °Br.

2.5. ISA induced phytoplankton fertilization albedo increase (by enhancing DMS-emissions) and CH_4 oxidation efficiency (by increasing MC- and DMS-emissions)

One of the largest reservoirs of gas-phase chlorine is the about 5 Tg of methyl chloride (MC) in the Earth's atmosphere (Khalil and Rasmussen, 1999). Methyl-chloride is released from phytoplankton (Hu et al., 2013) and from coastal forests, terrestrial plants and fungi (Khalil et al., 1999).

Dimethylsulphide (DMS) is a volatile sulphur compound that plays an important role in the global sulphur cycle. Through the emission of atmospheric aerosols, DMS may control climate by influencing cloud albedo (Charlson et al., 1987).

Currently, researchers (Lana et al., 2011) estimate that 28.1 (17.6–34.4) Tg of sulphur in the form of DMS are transferred annually from the oceans into the atmosphere.

Ocean acidification has the potential to exacerbate anthropogenic warming through reduced DMS emissions (Six et al., 2013). On the contrary, increased emissions of DMS and MC into the troposphere are a consequence of the ISA-induced phytoplankton growth and DMS + MC release into the troposphere. DMS is oxidized in the troposphere to sulphuric and sulphonic acid aerosols, which are highly active CCN. This process enhances the direct ISA cooling effect according to cooling section 2.1 (Charlson et al., 1987).

In contact with this acidic aerosol with sea spray aerosol, sulphate and sulphonate aerosols are formed and gaseous HCl is produced. Sulphate aerosols are known to have a negative radiative forcing (a cooling effect) (Crutzen, 2006).

A further HCl source is the oxidation of MC. Both effects induce the tropospheric HCl level to rise. According to cooling stage described in section 2.2, with the risen HCl level, additional chlorine atoms are produced by reaction with ISA. This effect further accelerates the methane oxidation and its removal from the atmosphere, reducing its radiative forcing.

2.6. Oxidation of CH_4 and further GHGs by sunlit solid surfaces

Mineral aerosol particles adhere strongly to sunlit, dry and solid surfaces of rocks and stones. A well-known remnant of the dust deposit in rock or stone deserts and rocky semi-arid regions is the orange, brown, red or black colored "Desert Varnish" coat covering stones and rocks. The hard desert varnish is the glued together and hardened residue of the primary dust deposit. Daily sun radiation and humidity change, as well as microbe and fungi influence grows up the varnish changing the primary aerosol deposit (Perry et al., 2005) by photolytic Fe(III) and Mn(IV) reduction during daytime and night time oxidation of Fe(II) and Mn(II). The

oxidation is triggered further by Mn and Fe oxidizing microbes adapted to this habitat (Allen et al., 2001; Hungate et al., 1987). Desert varnish preserves the Fe and Mn photo reduction ability of the aerosol: lit by light the varnish can produce chlorine from chloride containing solutions (Johnson and Eggleston, 2013). The photo, humidity, and microbial induced permanent Fe and Mn valence change between night and day (Matsunaga et al., 1995) accompanied by adequate solubility changes seem to trigger the physico-chemical hardening of every new varnish layer.

The varnish is composed of microscopic laminations of Fe and Mn oxides. Fe plus Mn represent about 1/5 of the varnish. Meanwhile 4/5 of the laminations are composed of SiO_2, clay and former dust particles. Dominant mineral is SiO_2 and/or clay (Dorn, 2009; Liu and Dorn, 1996). There is little doubt that desert varnish can build up even from pure iron oxides or iron chloride aerosol deposits like ISA. The optimum pH to photo-generate the methane oxidizing chlorine atoms from ISA is pH 2 (Wittmer et al., 2015a). Established by the gaseous HCl content of the troposphere (Graedel and Keene, 1996), a pH drop to pH 2 at the varnish surface is possible on neutral alkaline-free surfaces like quartz, quartzite and sandstone. The humidity controlled mechanism acting between gaseous HCl and HCl dissolved in the liquid water layer absorbed on the solid iron oxide surface of ISA particles as explained in the section 2.2 acts at the varnish surface analogue: a $FeCl_3$ stock can pile up by Fe(II) oxidation and humidity-triggered HCl absorption during night time. The $FeCl_3$ stock at the varnish surface is consumed during daytime by photolytic Fe(II) and chlorine atom generation.

ISA aerosol particles emit HCl during dry conditions. Like oxidic ISA desert varnish absorbs H_2O and HCl from the atmosphere gathering it during night time as surface-bound H_2O, OH^-, and Cl^- coat. During sunlit day time, chloride and water desorbs from Fe(III) as °Cl, °OH and H_2O, leaving Fe(II) in the varnish surface. The surface Fe(II) (and Mn(II)) is bound by oxygen bridges to the varnish bulk of Fe(III) (and Mn(IV)); may be like the combination of Fe(II) and Fe(III) within magnetite. During night time the Fe(III) (and Mn(IV)) surface coat is regenerated by microbial and/or abiotic oxidation with O_2. It is worth mentioning, that desert varnish can exist only within dry regions.

Figure 4 illustrates the interactions of ISA at the phase borders of tropospheric aerosols, ocean surface, and dry solid surfaces.

Earth Syst. Dynam. Discuss., doi:10.5194/esd-2016-32, 2016
Manuscript under review for journal Earth Syst. Dynam.
Published: 10 August 2016

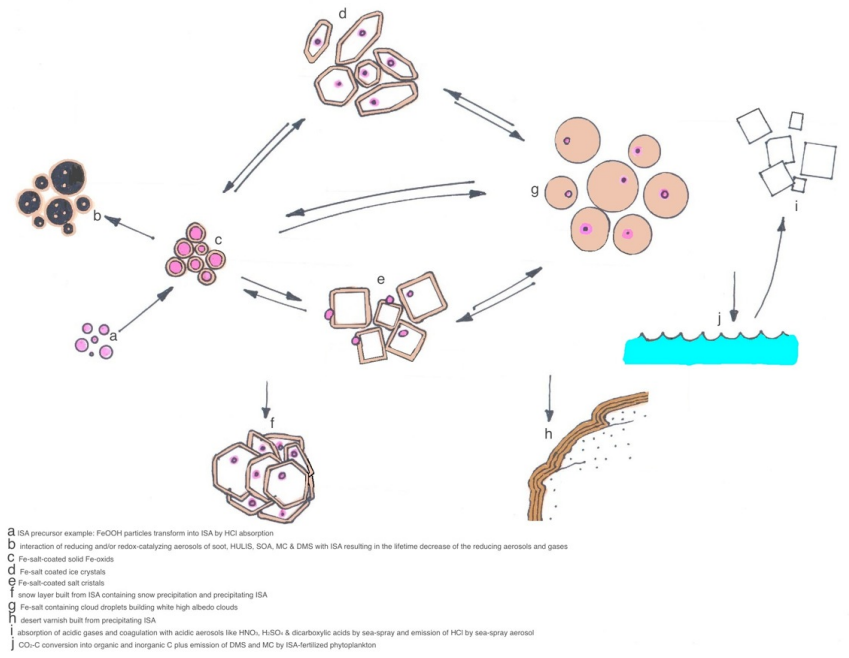

Figure 4. Schematic representation of iron salt aerosols interactions with different solid surfaces:

a,b ISA particles composed of FeOOH or FeOOH, H_2O, and chloride

c Interaction of reducing and/or red-ox-catalyzing aerosols of soot, HULIS, SOA, MC and DMS with ISA resulting in the lifetime decrease of the reducing aerosols, vapors and gases

d ISA-coated ice crystals

e ISA-coated salt crystals

f snow layer build from ISA containing snow and/or ISA precipitate

g ISA containing cloud or fog droplets

h desert varnish build from precipitating ISA

i precipitating ISA at the ocean surface accelerate the CO_2-C conversion into organic and carbonate C plus emission of DMS, MC and SOA by fertilization of the phytoplankton

j the ISA induced DMS, MC and SOA production increase is responsible for an additional production of H_2SO_4, sulphonic acids and dicarboxylic acids containing aerosol and gaseous HCl. By reaction with sea-spray the acid aerosols produce additional gaseous HCl enhancing the further activation of ISA

Similar daytime dependent microbial activated abiotic photo-reduction and photo-oxidation reaction cycles are known from aquifer environments (Gammons et al., 2007). Thus the methane depletion of the former ISA deposits will persist even after change into desert

Earth Syst. Dynam. Discuss., doi:10.5194/esd-2016-32, 2016
Manuscript under review for journal Earth Syst. Dynam.
Published: 10 August 2016

Earth System Dynamics
Discussions

varnish. As explained chapter 2.2 continental HCl (300 pptv above the oceans and 100 pptv above the continents) (Graedel and Keene, 1996), $ClNO_2$ (up to 1500 pptv near flue gas emitters) (Osthoff et al., 2008; Riedel et al., 2014) and CH_3Cl (550 pptv remote from urban sources) (Khalil and Rasmussen, 1999; Yokouchi et al., 2000) and in deserts chloride salt containing dusts are direct and indirect sources of chloride which could provide desert varnishes with Cl^-.

Furthermore, analogue to ISA deposited on solid desert surfaces even ISA depositions on dry snow, snow cover and ice occurring in permanent snow-covered Mountain regions or within polar and neighboring regions shall preserve its methane destruction activity during sunlit day, spring, and summer times (Liao et al., 2014).

The global area of the desert varnish surface does not change with changing dust precipitation rates. It only depends on the precipitation frequency. It grows through desertification and shrinks with increasing wet climate. Until now quantitative measurements about the specific amount of methane depletion per square meter of desert varnish are not known. Without these data, estimation about its influence on the methane depletion and climate is impossible.

The photochemical actions inducing CH_4 depletion of the desert varnish surfaces resulting from dust precipitation are concurrent with the surfaces of deserts and semi deserts made of sand or laterite soils. Their surface is colored by ochre to red iron oxide pigments. Their iron components should act in principle by the same CH_4 depleting photochemistry like ISA and desert varnish.

As mentioned in chapter 2.4 the Cl and Br activation by iron photolysis changes after division of the ingredients by freezing or drying of the former homogenous liquid between solid salt-poor ice and liquid brine coat or solid salt and liquid brine coat. This inhomogeneous partition phenomenon of the predominant transformation of aerosol droplets into solid and vice versa applies even to snow or salt layers containing a proportion of ISA.

It has been shown that even cooling precipitation of the buffering influence of salts like carbonates, sulphates and chlorides of bromide and chloride rich mother liquors on arctic snow packs or ice particles can minimize their buffering capacity against pH change (Bartels-Rausch et al., 2014; Blechschmidt et al., 2016; Sander et al., 2006). Similar mechanisms may act when liquid aerosol particles become solid by drying.

Then the uptake and contact of solid iron-bearing particles and airborne organic and inorganic acids and acid precursors on or with ice crystal surfaces over time may drop the pH of the former alkaline particle surface into the reaction conditions of the bromide oxidation by iron(III) photo reduction.

According to Kim et al. (Kim et al., 2010) the photogeneration of Fe(III) oxides, proceeding slow at pH 3.5 in bulk solution, becomes significant accelerated in polycrystalline arctic ice.

This effect is accompanied by an acceleration of the physical dissolution of the Fe(III)oxides by freezing ice (Jeong et al., 2012; Kim et al., 2010).
The contact of arctic snow layers with iron oxides is confirmed by Kim (Kim et al., 2010). Dorfman (Dorfman et al., 2015) found recent loess dust sedimentation rates in the Alaskan Arctic Burial Lake of 0.15 mm/a. According to the research results from artificial iron doped salt pans (Wittmer et al., 2015b), iron salt doped sea-salt aerosols (Wittmer et al., 2015a), sea-salt doped iron oxide aerosols or pure iron oxide aerosols in contact with gaseous HCl (Wittmer and Zetzsch, 2016), chloride and bromide in sun-lit surfaces become oxidized to °Cl and °Br by photo-reduced Fe(III) if the pH of the reaction media is 3.5 or lower.
As known from the bromine explosions they appear on acidified first-year tundra and first-year sea ice snow lit by sunlight (Pratt et al., 2013). According to Kim et al. and Dorfman et al. the year-old snow layers contain even Iron(III). This confirms, that sufficient reaction conditions exist to produce bromine explosions by oxidation of Iron(III) photoreduction.
Continents have considerable areas where the outflowing water is drained into “endorheic” water bodies and not into the oceans. Endorheic lakes have no outlets other than evaporation and thus dissolved salts and nutrients concentrate over time. Large surfaces of these basins are covered by salt crusts, salt marshes, salty soils, or salt lakes. Most of these areas are situated within desert or semi-desert areas (Hammer, 1986). These salt environments gain iron from precipitating dust or even from iron containing brines they have precipitated from. As far as these environments become acidic they oxidize methane by iron photolysis induced °Cl (Wittmer et al., 2015b).

3. Oceanic natural cooling effects of the iron cycle

3.1. Biotic CO_2 conversion into organic and carbonate carbon

Vegetation uses the oxidative power of organic metal compounds induced by photon absorption oxidizing water to oxygen and reducing CO_2 by organic carbon generation (photosynthesis by chlorophyll, a green Mg-Porphyrin complex). This assimilation process is retarded by prevailing iron deficiency in the oceans which retards the phytoplankton growth.
Meanwhile there is no doubt that ISA-containing dust precipitation fertilizes the phytoplankton which in turn affects the climate (Albani et al., 2016).
ISA triggers the phytoplankton reproduction and increases the formation of organic carbon from the GHG CO_2 (Martínez-García et al., 2014). The vast majority of the oxygen thus formed and only slightly water soluble (11 mg O_2 / l) escapes into the atmosphere. In contrast, the formed organic carbon remains completely in the ocean forming the basis of the marine food and debris chain.
From the primary produced phytoplankton carbon only a small fraction arrives at the ocean

Earth Syst. Dynam. Discuss., doi:10.5194/esd-2016-32, 2016
Manuscript under review for journal Earth Syst. Dynam.
Published: 10 August 2016

bottom as organic debris and becomes part of the sediment. Cartapanis et al. (Cartapanis et al., 2016) and Jaccard et al. (Jaccard et al., 2016) found direct evidence that during the glacial maxima, the accumulation rate of organic carbon was consistently higher (50 %) than during inter-glacials. This resulted from the high dust concentrations during the glacial maxima fertilizing the phytoplankton with ISA.

The build-up of Ca-carbonate shell and frame substances by the calcification process at the ocean surface extracts additional CO_2-C from the troposphere. The bulk of calcification can be attributed to corals, foraminifera and coccolithofores; the latter are believed to contribute up to half of current oceanic $CaCO_3$ production (Mackinder et al., 2010).

Both carbon fixation processes increase the removal of the GHG CO_2 and thus contribute to cool the troposphere. The Fe-fertilizing process worked during the ice age, as the evaluations of Antarctic ice cores show: the minimum CO_2 concentrations and temperatures in the troposphere are connected to the high dust phases (Skinner, 2008).

It has been discussed that the alkalinity loss by phytoplankton calcification and $CaCO_3$ loss with phytoplankton debris from the ocean surface is said to produce calcium and alkalinity deficit at the ocean surface (Meyer and Riebesell, 2015; Rost and Riebesell, 2004) producing additional acidification at the ocean surface by CO_2 generation:

$$Ca(HCO_3)_2 \rightarrow CaCO_3 + H_2O + CO_2$$

At least in part this acidification is compensated by assimilative generation of organic carbon by CO_2 consumption. Both organic debris and $CaCO_3$ become part of the ocean sediment. But if the organic debris is re-oxidized during its journey downwards, some acidification could result. Acidification could result too if more CO_2 is absorbed by the ocean, then is assimilated and changed to organic debris. According to the ISA-induced phytoplankton productivity, both, sedimentation of organic debris and $CaCO_3$, increase.

The increasing amount of $CaCO_3$ sedimentation within iron fertilized ocean regions had been discussed by Salter (Salter et al., 2014). In a sufficient mixed ocean, alkalinity loss at the surface is more than compensated by the different sources of alkali and earth alkali cations at the ocean bottom and through continental weathering: in the first place these are the mechanisms of alkalinity generated by the ocean water reactions within the ocean sediments and their bed-rock, the oceanic crust. The latter mechanisms are described in more detail in chapters 4.1 – 4.3. The convection of the primary oxic ocean bottom water through the ocean crust generates alkalinity by reduction of sulphate, nitrate and hydrogen carbonate, by dissolution of silicates by with reduced humic acids and further by serpentinization of basalt and peridotite silicates (Alt and Shanks, 2003; Früh - Green et al., 2004). The alkalinity extracted from the oceanic crust keeps mainly positioned in the dark water layers of the ocean basins if the decreased THC is not able to elevate the alkaline extract into the phytoplankton layer in sufficient quantities.

Earth Syst. Dynam. Discuss., doi:10.5194/esd-2016-32, 2016
Manuscript under review for journal Earth Syst. Dynam.
Published: 10 August 2016

The THC activation by the ISA method is described in the chapters 4.1 – 4.3.

When any time lag induced Ca level decreases by sudden ISA-induced phytoplankton growth the increase does no harm to the phytoplankton because calcium is not essential to phytoplankton. Just the opposite is true: phytoplankton uses the calcification as a detoxification measure to get rid of calcium ions from their bodies (Müller et al., 2015). As a consequence of this effect only the relation between Ca carbonate sequestration and organic carbon sequestration will decrease during the time lag.

By additional direct alkalinity production of the phytoplankton itself at least parts of the acidity production by the lime shell production may be compensated: ISA-controlled phytoplankton growth induce synthesis increase of organic sulphur and of chlorine compounds (Matrai and Keller, 1994) , emitted as dimethylsulphide (DMS) and methyl chloride (MC) (Carpenter et al., 2012). Synthesis of organic sulphur and halogen organics as precursors of the volatile DMS and MC emission is realized by the phytoplankton by reduction of sulphate to organic sulphides and oxidation of chloride to carbon chlorine compounds. This precursor synthesis excretes equivalent Na^+ and/or Ca^{2+} alkalinity, because Na_2SO_4 reduction/formation to DMS generates Na alkalinity; NaCl oxidation/formation to MC generates Na alkalinity too: cations former bound to SO_4^{2-} or Cl^- lost their anions producing alkalinity. According to (Chen et al., 1996; Fujita, 1971) the sulphur content of phytoplankton exclusively exceeds the Ca^{2+}, Mg^{2+}, and K^+ alkaline load of phytoplankton lost with the phytoplankton debris. Only half of the organic carbon assimilated by phytoplankton derives from dissolved CO_2. The other half derives from the ocean water $NaHCO_3$ anion content (Cassar et al., 2004). The chemical reduction (reduction of HCO_3^- to organic C + O_2 by assimilation of HCO_3^- anions produces alkalinity as further compensation of the alkalinity loss by calcification. $NaHCO_3$ reduction/formation to organic carbon generates Na alkalinity. The cation previously bound to HCO_3^- loses its anion and produces alkalinity.

These considerations demonstrate that any of the proposed enhanced weathering measures to prevent ocean acidification by increasing the alkalinity (Taylor et al., 2015) might be not necessary if the ISA method is in action and keeps the vertical ocean mixture sufficiently active.

During the down-dripping of the very fine-shaped phytoplankton debris bacterial oxidation, fish and further food chain links minimize the organic debris up to an order of magnitude (Weber et al., 2016). Even the solution of the small carbonate debris reduces the carbonate fraction until arriving at the sediment surface. In order to maximize the effect of the ISA method within the main ISA precipitation regions the oxidation and dissolution of the organic and carbonate phytoplankton debris during its dripping down through the ocean water column can be reduced. To meet this aim we suggest farming fixed filter feeders like mussels and oysters within the ISA precipitation region.

Mussels and oysters produce faeces and so called “Pseudo-faeces” in the shape of rather solid pellets. Compared to the time of sedimentation of the unconditioned phytoplankton debris this expands the sedimentation time difference between excreted filter feeder faeces and the phytoplankton faeces pellets sedimentation on the ocean floor by order of magnitude. Bivalve farming would reduce the oxidative and solution loss of phytoplankton debris attack significantly. Mussel and oyster farming are well-known practices which have been employed for long time as a measure to produce protein rich food. They have even been proposed as an element of climate engineering (Dimitrova et al., 2015; Lenton and Sen Gupta, 2010).

To further optimize the CO_2-C conversion to sediment-bound C the biomass of oysters and mussels including their shells and fixing systems might be periodically dumped into the sediment.

Additional floating supports such as coral habitats, sponges, sea lilies and sea anemones between the mussel supports might complete and again optimize the ISA precipitation areas. The oceanic water deserts may become changed into productive ecosystems and protein sources for an increasing population by these measures, among others, for an optimized CO_2 fixation induced by ISA.

A further proposal in order to maximize the CO_2 fixation induced by ISA is our suggestion to integrate the solution of the waste problem on the ocean surfaces into the ISA method. About 5 to 13 million metric tons of solid plastic waste per year are entering the oceans (Jambeck et al., 2015). Over the last years the plastic waste drifting on the ocean has developed into a huge problem for the oceanic ecosystems (Law et al., 2014). Even plastic keeps sunlight away from phytoplankton hampering it from effective growth. The plastic waste drifts with the ocean currents. It then collects within accumulation zones predicted by a global surface circulation model (Cózar et al., 2014). Most plastic-covered ocean surfaces are concentrated in central-oceanic regions with low iron content with predestination for applying the ISA method. Because of the trash there would be a reduction in the ISA efficiency so we propose the integration of the plastic depletion problem into our ISA method: On both the side of and outside a container ship vessel specific technology can be installed: plastic trash collection, plastic trash sorting, plastic trash extrusion, plastic trash burning, ISA production and emission. The aforementioned processes are well known and need no description here. Trash or waste burning has the advantages of delivering an effective hot carrier gas with high buoyancy for uplift of ISA and of delivering HCl as co-catalyst of ISA. With the plastic extruder most carrier parts of floating supports on the reef coral, sponge, and mussel habitats could be produced.

Beside the larger plastic fragments, the floating plastic fine debris with particle diameters in the µm range is a further problem (van Sebille et al., 2015). Instead of doing the micro-trash

separation by technical means, the mussel and oyster farming may clean away this ocean surface environmental problem. The floating micro-trash particles are collected by the bivalves and excreted as pseudo-faeces pellets and at last become part of the sediment layer at the ocean bottom.

Within the iron cycle, the photolytic driven oxidant production with iron participation may not be reduced to °Cl and °OH in the troposphere and O_2 by assimilation: When iron is cycled through the mantle at temperatures above 2500 K, Fe(III) becomes reduced to Fe(II) by release of O_2 (Bykova et al., 2016). This phenomenon may be driven even by the blackbody radiation containing a great fraction of photons with wave length shorter than 2 µm at and above this temperature level.

3.2. ISA activates the O_2 input to the deep ocean

Ocean ecosystems are based on certain balances between oxidizing and reducing agents. As a result of the ISA-triggered additional input of organic carbon in the ISA emission region (i.e. the ISA precipitation region), as described in chapter 3.1, oxygen consumption by increasing organic debris precipitation could increase. The recent oxygen decline in some oceanic regions may result at least in part from the deposition of soluble iron deriving from flue gas pollution. Equally discussed in chapter 3.1 is the decrease of the oxidation efficiency within the water column by measures to increase the sinking velocity of the organic containing debris, this effect of ISA might compensate completely.

Recently and without ISA influence, oxygen deficiency seems to develop in many parts of the ocean as described in the introduction. Oxygen deficiency is usually due to insufficient vertical water exchange owing to increased vertical density gradient rather than the result of increased phytoplankton production.

Oxygen deficiency (hypoxia) is found frequently between the oxic surface layer (the oxygenated one) and the oxic deep water layer (Bruland, 2006; Capone and Hutchins, 2013). Due to the climate warming the localities with a lack of oxygen seem to intensify and expand already today (Kalvelage et al., 2013).

The deepest water layer of most ocean basins results from the Antarctic wintertime **ocean** surface ice generation by fractionating sea water into salt-poor sea ice and salt-rich dense brine. This results in the production of cold high density oxic brines which sink to the bottom of the south ocean. The cold high density oxic brines spread as a thin oxic bottom layer up to the ocean basins north of the equator. The most recent severe climate warming which induced disturbance of the THC is likely to have been activated by the increasing inflow of the soft and cold melt water from Greenland into the North Atlantic. This inflow disturbs the down flow of the Gulf Stream water (Rahmstorf et al., 2015). According to the increased melt even of Antarctican glaciers the ocean surface around Antarctica became decreased in its

salt content. This effect increased the ocean surface covered by sea ice (Bintanja et al., 2013). This freezing of the salt-poor melt water layer decreases the production of dense brines. This again decreases the down flow of brine reducing again the vertical components of the ocean currents.

Through the ISA induced cooling, the oxygen and CO_2 flux into the deep ocean basins will be restored because of the input of the cold dense oxygen and CO_2 enriched polar surface water: Reduced melt water production of the Greenlandic and Antarctic ice shields by falling surface layer temperatures will restore and intensify the thermohaline circulation within the northern polar regions by increasing the amount of Gulf Stream dumped and by producing the circum Antarctic sea ice cover without melt water dilution, which induces the production of cold high density brines sinking to the ocean basin bottoms (Ohshima et al., 2013; Rahmstorf, 2006).

3.3. Phytoplankton fertilizer extraction from ocean sediments and underlying crust

The oceanic crust is composed of peridotites, basalts and serpentine rock and has a layer of sediment on top. Sediments and bed rock contain reductive and alkaline components extractable by sea water. The sea water circling through these rocks loses oxygen, sulphate, nitrate and even hydrogen carbonate by reduction and precipitation and becomes enriched with methane and further reductants (Evans, 2008; Janecky and Seyfried, 1986; Kelemen et al., 2011; Müntener, 2010; Oelkers et al., 2008; Sanna et al., 2014; Schrenk et al., 2013; Sissmann et al., 2014). The cause of the ocean water flow through the sediment layer and base rock is the temperature difference driven convection. Sediment compaction by gravity, subduction-induced compaction and subduction-induced hydroxyl mineral dehydration may be further reasons for water movement through the sediment layer at the ocean bottom.

Olivine is one of the main mineral components of oceanic crust rock layers below the sediment layer. Hauck (Hauck et al., 2016) simulated the effects of the annual dissolution of 3 Gt olivine as a geoengineering climate cooling measure in the open ocean, with uniform distribution of bicarbonate, silicic acid and iron produced by the olivine dissolution. An additional aim of this work was the development of a neutralization measure against the increasing acidification of sea water. All the components of olivine, SiO_2, Fe(II) and Mg are phytoplankton fertilizers. They calculated that the iron-induced CO_2 removal saturates at on average ~1.1 PgC yr^{-1} for an iron input rate of 2.3 Tg Fe yr^{-1} (1% of the iron contained in 3 Pg olivine), while CO_2 sequestered by alkalinisation is estimated to ~1.1 PgC yr^{-1} and the effect of silicic acid represents a CO_2 removal of ~0.18 PgC yr^{-1}. These data represent the enormous potential of the ocean crust rock as source of phytoplankton fertilizer.

The flow of sea water through anoxic sediments and bed rock results in the reduction of its SO_4^{2-} content as well as extraction of the soluble fraction from the sediment like Mn(II), Fe(II), NH_4^+ and PO_4^{3-}. The chemical and physical extraction processes are enhanced by the action of microbial attack at the border lines between oxic sea water and anoxic sediment parts within this huge aqueous system.

At suboxic conditions soluble Fe(II) and Mn(II) have optimum solubility or may be fixed as solid $Fe(II)_3(PO_4)_2$, $FeCO_3$, $MnCO_3$, FeS_2, S^0 and further Fe-S compounds (Ohman et al., 1991; Roden and Edmonds, 1997; Slomp et al., 2013; Swanson, 1988; Wallmann et al., 2008).

Silicon is mobilized too, from the dissolution of silicates and SiO_2 at methanogenic conditions by complexation with reduced humic acid (HA) (Vorhies and Gaines, 2009; Wallmann et al., 2008). In the reduced conditions HA is characterized by catechol and further polyphenolic functions, which allows HA to complex with silicon (Belton et al., 2010; Demadis et al., 2011; Jorgensen, 1976) and with further metal cations.

Silicate dissolution mobilized Ca^{2+}, Mg^{2+}, Ba^{2+}, Fe^{2+}, Na^+, K^+. Fe^{2+}, Mn^{2+} and PO_4^{3-} become more or less precipitated as sulphides, carbonates, within the sediment ($Fe(II)S_2$, $CaCO_3$, $MgCa(CO_3)_2$, $Fe(II)CO_3$, $Mn(II)CO_3$, $Fe(II)_3(PO_4)_2$), and within its suboxic surface ($BaSO_4$) or at its oxic surface (SiO_2, Fe(III)OOH, $Mn(IV)O_2$, clay minerals). The authigenic formed ferromanganese nodules (Kastner, 1999) are formed by in situ microbial precipitation from sediment pore water squeezed out to the seafloor on the sediment layer (Nayak et al., 2011; Wu et al., 2013). Main components of the nodules are the phytoplankton fertilizer components SiO_2, Fe- and Mn-oxides (Nayak et al., 2011).

Having left the borderline between anoxic and suboxic near-surface sediment the HA catechols are changed by reversible oxidation into quinone or quinhydrone configurations by decay of the Si catechol complex. Like most of the chemical reactions within the sediment compartment even oxidation of the HA-Si complex is directed by microorganisms. The microorganisms involved use HA as external red-ox ferment (Benz et al., 1998; Bond and Lovley, 2002; Coates et al., 1998; Kappler et al., 2004; Lovley and Blunt-Harris, 1999; Lovley et al., 1999; Piepenbrock et al., 2014; Straub et al., 2005). After arrival of the pore water originating from the anoxic deeper sediment or bed rock at the suboxic surface-near sediment layers the oxidized HA releases $Si(OH)_4$ and, NO_3^- produced by microbial NH_4^+ nitrification (Daims et al., 2015; van Kessel et al., 2015). Depending on the produced $Si(OH)_4$ concentration this can trigger the precipitation of layered silicates like smectites, glauconite, and celadonite as well as silica (Bjorlykke, 2010; Charpentier et al., 2011; Gaudin et al., 2005; Polgári et al., 2013; Pufahl and Hiatt, 2012; Zijlstra, 1995). Similar to HA, the clay mineral formation within the sediment, and the usage of the red-ox potential of these

Earth Syst. Dynam. Discuss., doi:10.5194/esd-2016-32, 2016
Manuscript under review for journal Earth Syst. Dynam.
Published: 10 August 2016

authigenic minerals are, at least in part, the result of microbial action (Konhauser and Urrutia, 1999; Kostka et al., 1996).

The deep ocean currents take up the pore water percolates out of the sediment and considerable amounts of the disolved, colloidal or suspended sediment originating elements are THC-conveyed to the surface (Lam and Bishop, 2008) and activate there the phytoplankton production again. This as well triggers the CO_2-conversion to organic C resulting in cooling the troposphere according to chapter 3.1. Repeatedly it also cools the troposphere by increasing the DMS formation according to chapters 2.5 and 3.1.

4. Natural cooling effects of the iron cycle on the ocean crust

4.1. Carbon storage as authigenic carbonate in the ocean crust

The mechanism described in this chapter has the highest influence on the climate, because its carbon storage capacity is much greater than that of their sediment layer. The convective water flow through the huge alkaline ocean crust volume is estimated to about 20 - 540 x 10^3 km³/yr (Nielsen et al., 2006). The oceanic crust comprises the largest aquifer system of the Earth with an estimated rock volume of 2,3 x 10^9 km³ and a fluid volume of 2 % of the total ocean or ~10^7 km³ (Orcutt et al., 2011). The system of the mid-ocean rifts (MOR) and subduction zones and the sector between these volcanic active regions are part of the Earth Mantle convection cycle and part of said interconnected aquifer system. The bottom water of the ocean basins are in close contact to this conveyor belt-like moving rock layer of the oceanic crust. New oceanic crust is produced at the MOR, during its cooling it is pulled apart from the MOR by the moving underlying mantel and at last the moving mantle draws the crust down into the deeper mantle below the subduction zones. The oceanic crust has a sediment layer on top of its assemblage of multi-fractured crystalline and volcanic rocks. Both, sediment and igneous bed rock interior are in an anoxic reduced and alkaline state; temperature on top of the sediment surface at the ocean bottom is round about 0 °C but temperature increases up to >1000 °C within the igneous bedrock basement. Because there is no effective sealing between cold bottom water and high temperature zone, the water content of sediments and fractured basement flows through the crust in multiple thermal convection cycles positioned between cold surface and hot deep. Figure 5 illustrates the oceans friction factor inducing climate warming due to the ocean basins vertical mixing circles.

Earth Syst. Dynam. Discuss., doi:10.5194/esd-2016-32, 2016
Manuscript under review for journal Earth Syst. Dynam.
Published: 10 August 2016

Earth System Dynamics
Discussions
Open Access

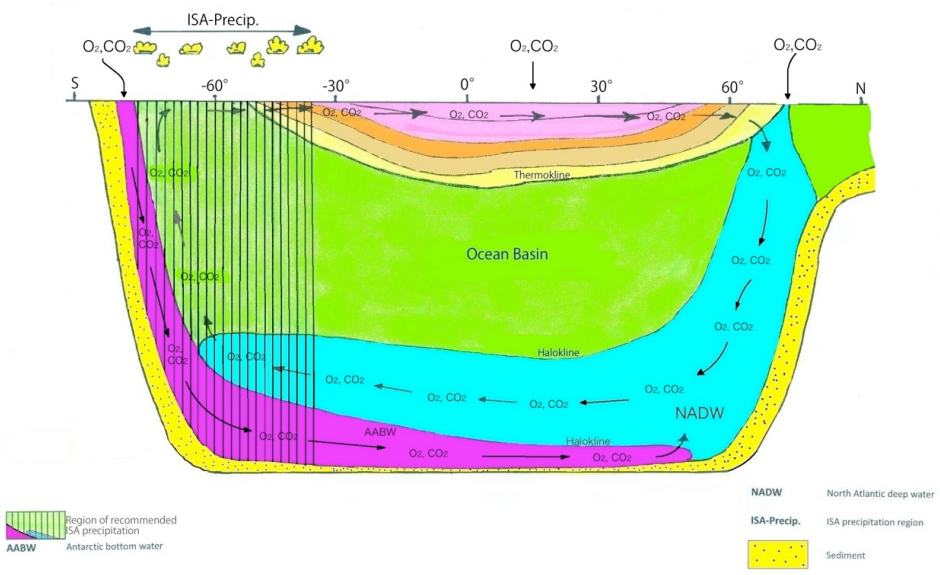

Figure 5. The motor of the Antarctic bottom water (AABW) current is the sea ice production of the Southern Ocean area bordering Antarctica. The North Atlantic Deep Water (NADW) current is driven by decreasing Gulf Stream temperature on its way north. Climate warming especially the faster temperature rise at higher latitudes shifts the region of the Gulf Stream down flow as NADW further to the north as a result of the lowering Δt between equatorial and polar surface water. This shift sets additional Greenlandic coast regions in contact with warm Gulf Stream water and even the rising air temperatures as further component poor increasing amounts of fresh melt water on the ocean surface. The rising melt water volume and the further north flowing Gulf Stream increases the contact region between Gulf Stream water with fresh melt water. This produces increasing amounts of original Gulf Stream water but too low in density to sink and to become part of NADW.

Temperature rise at higher latitudes reduce the salt content of ocean surface water around Greenland and Antarctica inducing reduced NADW and AABW volumes. According to the reduced down flow current volumes, the amounts of CO_2 and O_2 to the deep ocean basin are reduced as well as the vertical fertilizer transport from the ocean basin bottom, to the phytoplankton at the surface.

Alkalinity and alkalinity-inducing compounds of the ocean crust rock layers extract CO_2 and HCO_3^- from sea water by carbonate precipitation in the fissures during sea water percolation through the multi-fractured rock (Coggon et al., 2012). A carbon uptake of 22 to 29 Mt C/year

Earth Syst. Dynam. Discuss., doi:10.5194/esd-2016-32, 2016
Manuscript under review for journal Earth Syst. Dynam.
Published: 10 August 2016

is estimated during the hydrothermal alteration of the oceanic crust (Kelemen and Manning, 2015). This is more than the carbon uptake by the overlying sediment layer of the oceanic crust which is estimated to 13 to 23 Mt C/year (Kelemen and Manning, 2015). The oceanic crust is composed of peridotites, basalts and serpentine rock with a sediment layer on top. Said rock layers contain reductive and alkaline components. Sea water circling through these rock layers loses its contents of oxygen, sulphate, nitrate and even parts of hydrogen carbonate by reduction and precipitation and becomes enriched with methane and further reductants. (Evans, 2008; Janecky and Seyfried, 1986; Kelemen et al., 2011; Müntener, 2010; Oelkers et al., 2008; Sanna et al., 2014; Schrenk et al., 2013; Sissmann et al., 2014).

Because of the opposing chemical milieu differences between the oxic ocean water inflow and anoxic reduced and alkaline sediment and basement the ocean water convection cycles through the ocean crust act as a continuous chemical reaction systems and forms habitats of intensive acting microbial action (Ivarsson et al., 2016). The most intensive chemical reaction intensity is found at MOR, subduction zones and at volcanic sea mounts, between MOR and subduction within the abyssal plain convection cycling occurs (Orcutt et al., 2011). Because the hydrogen carbonate load of the ocean water inflow comes to precipitation as carbonates of Ca, Mg, Fe, and Mn within the alkaline rock interior and by chemical reduction of sulphate, nitrate and hydrogen carbonate, the ocean basements acts as huge CO_2-Carbon storages. No doubt, the ocean crust carbonate depot is the most effective carbon storage, more effective than any other organic carbon storages.

Within the huge ocean crust contact volume, sea water changes the alkaline pyroxenes and basalts into serpentine, diabase and carbonates; by producing heat, rock volume expansion and by permanent production of numerous fissures. The ocean water sulphates react with the silicate components to magnetite, pyrite and barite. The sea waters hydrogen carbonate load precipitates within the rock fissures as magnesite, calcite, siderite and dolomite. By heat transfer from hot rock and chemical reaction, heat circling through the primary and new generated multiple fissures in the former mantle rock the sea water inflow heats up, producing convective flow. At fissures where the alkalized flow of hot CH_4 and H_2 containing convection water comes out with pH 9 to 11 and contacts the fresh sea water, carbonate precipitates and builds up skyscraper high carbonate chimneys (Kelley et al., 2005).

The convective seawater flowing only through the MOR system is estimated to about 20 to 540 x 10^3 km^3/yr (Nielsen et al., 2006). This volume is even more than the global river flow of about 50 km^3/yr (Rast et al., 2001).

The weathering reaction conditions and the sea water alkalization during the intense sea water contact with the alkaline MOR rocks are much more aggressive so respectively more effective comparing to reaction conditions and alkalization during the precipitation water contact during weathering reactions of continental rocks. This is confirmed by the alkaline pH

of up to 11 of the "White Smoker" MOR outflow in spite of its haline salt buffered seawater origin (Kelley et al., 2005). Even the most alkali run-off from limestone karst spring fresh-waters or within karst cave fresh-waters does not exceed pH levels of 8.5 (Li et al., 2010; Raeisi and Karami, 1997; Righi-Cavallaro et al., 2010)

There is no doubt that the efficiency of the pH dependent CO_2 absorption and carbonic acid neutralizing at the ocean surfaces and the hydrogen carbonate precipitation to carbonate processes at and within the oceanic crust are dependent on the activity of the THC within the ocean basins. During cold climate epochs with undisturbed THC the CO_2 conversion to ocean crust carbonate is activated as well as the CO_2 conversion to the organic fraction of ocean sediments. The continuous availability of chemical activity, as chemical reaction vessel and as an alkalinity reservoir of the oceanic crust is maintained by the continuous generation of new crustal rock material of 21 km³/year (Orcutt et al., 2011). This huge rock volume production capacity has enough alkalinity and fertilizer reserves to maintain the absorption, neutralization and precipitation of a multiple of the recent incoming CO_2 and HCO_3^-.

THC is the main transport medium of carbon from the atmosphere into the deep on Earth. This makes THC to the most prominent climate stabilization element.

The realization of the significance of THC as stabilization element of our recent climate induces questions about the stability of the THC. As stated in chapter 1 the main factors for destabilizing the THC seems to be the desalting of surface ocean layers by freshwater injection from increasing ice melt (Hansen et al., 2015) A melt increase might drive the destabilization of THC. And at first the top layers of the ocean basins will suffer from acidification and the deep layers will become alkaline and anoxic.

By starting the ISA process, the induced climate cooling will decrease the Greenland glacier melt. The minimized freshwater inflow to the North Atlantic Ocean reduces the dilution of the salty Gulf Stream and increases the down flow quantity of oxic and CO_2 containing salty surface water. In parallel the surface increase of sea-ice produced on the South Ocean surrounding the Antarctic continent is followed by increased down-flow of oxic and CO_2 containing cold brine onto the bottoms of the oceanic basins. Both effects do increase the THC activation: the flow of alkaline, phytoplankton fertilizer enriched, and oxygen depleted deep-ocean water to the surface. This activates CO_2 absorption from the atmosphere by phytoplankton growth and by CO_2 absorption

One of the proposed alternative climate engineering measures aims to absorb atmospheric CO_2 by reducing the surface ocean acidity and by producing phytoplankton fertilizers. To transfer 1.1 x 10^9 t/year CO_2 carbon into the ocean a crushing of 3 x 10^9 t/year of the ocean crust and mantel rock mineral olivine to a particle diameter of 1 µm and suspend it at the ocean surface would be necessary (Hauck et al., 2016; Köhler et al., 2013; Köhler et al.,

2010). These numbers seem to be two orders of magnitude too high. Keleman & Manning calculate a carbon mass subduction of about 50 x 10^6 t C/year (C in oceanic crust, bedrock and sediment layer) (Kelemen and Manning, 2015). Independently of which of both calculations has a mistake – technical activities to do the Hauck et al. proposal are far from any economic reality.

The proposed reaction of CO_2 with olivine is done with much better effectiveness by nature without any costs within the ocean crust in sufficient quantity. To minimize CO_2 emission it has been proposed to minimize power stations flue gas CO_2 by absorption by lime suspension (Haas et al., 2014). This measure seems to be unnecessary when the ISA method comes into practice.

The fertilizing elements the phytoplankton needs, like Si, P, and Fe, are all present in the ocean crust (Lyubetskaya and Korenaga, 2007) and property of the ocean crust water extract. Intensification of the THC would also increase the fertilizer concentration at the ocean surface in the phytoplankton layer. As demonstrated the undisturbed THC is essential to keep the climate stabilized (Coogan and Gillis, 2013).

The ocean crust from the warm Mesocoic epoch which had no frozen polar regions contained about five times more authigenic carbonate than ocean crust younger than 60 million years (Coogan and Gillis, 2013). Coogan interpreted this as possible consequences of higher bottom water temperature and/or different seawater composition. Insua et al. (Insua et al., 2014) found evidence, that the salinity of the ocean bottom water during the Last Glacial Maximum had been up to 4 % greater than today. It seems evident that the cause of the latter had been the higher volume of brine produced during sea-ice freezing. This fact demonstrates that even disturbed or weakened THCs might be the cause of reduced carbonate C uptake of the ocean crust. The quantity of carbonate precipitation depends on the CO_2 and/or HCO_3^- input with seawater. As a consequence, the quantity of the ocean crust CO_3 uptake varies according to the activities of the THCs: strong THCs increase the crust carbon content; weak THCs decrease it.

During the time lag between the onsets of the ISA method cooling and the appearance of the alkalinity and fertilizer increase at the ocean surface the cooling effect of ISA remains reduced. But after this time lag the ISA method increases to optimal efficiency. Even from an economic viewpoint it seems better to compensate this by increasing the ISA emission at the beginning during the time lag, than doing the proposed suspending of olivine dust at the ocean's surface. Even lime shell wearing phytoplankton is able to accept small pH changes of CO_2 induced dependent acidification because it uses the build-up of calcium carbonate shells as a detoxification measure to get rid of calcium ions from their bodies (Müller et al., 2015). As a consequence of this effect only the relation between Ca carbonate sequestration and organic carbon sequestration may decrease during the time lag.

Earth Syst. Dynam. Discuss., doi:10.5194/esd-2016-32, 2016
Manuscript under review for journal Earth Syst. Dynam.
Published: 10 August 2016

4.2. Carbon storage as organic and inorganic marine debris and as authigenic carbonate in the ocean sediment

The uptake of authigenic hydrogen carbonate from the ocean and precipitating it in the sediment seems to play as well a major role in the carbon circle (Schrag et al., 2013). According to Kelemen (Kelemen and Manning, 2015) the carbon uptake by the sediment layer of the oceanic crust can be estimated to 13 to 23 Mt C/year. The carbon inventory consists of life and dead organic carbon, carbonate carbon and authigenic carbonate produced by excess alkalinity deriving mainly from sulphate reduction and silicate solution by reduced humic acids. According to Sun & Turchyn the formation of calcium carbonate and its burial in marine sediments accounts for about 80 % of the total carbon removed from the Earth surface (Sun and Turchyn, 2014). Meanwhile it seems possible to distinguish between marine formed sediment carbonate and authigenic carbonate (Zhao et al., 2016).

Accordingly, excess alkalinity is produced by dissolution of silicates like illite, kaolinite and fieldspars, volcanic ash, pyroxene or other silicate components of ocean sediments and even opal by Si complexation with reduced HA at methanogenic conditions (Meister et al., 2011; Roden and Edmonds, 1997; Solomon et al., 2014; Wallmann et al., 2008). Compensation by hydrogen carbonate induces authigenic precipitation of microbial dolomite (Roberts et al., 2004), Ca or Fe carbonate (Solomon et al., 2014; Vorhies and Gaines, 2009) (Dewangan et al., 2013; Merinero et al., 2008; Sun and Turchyn, 2014; Wallmann et al., 2008) and further minerals (Tribovillard et al., 2013).

As mentioned in chapter 4.1, the biological processes of chemical sediment reduction induced by the ISA fertilization changes NO_3^-, SO_4^{2-}, Fe(III), Mn(III/IV) and HCO_3^- to their deoxygenated and reduced species inclusive CH_4 and NH_4^+ generation, produces a pH increase and additional alkalinity. The alkalinity excess converts dissolved HCO_3^- into solid lime and dolomite (Berner et al., 1970; Krause et al., 2012; Luff and Wallmann, 2003; Raiswell and Fisher, 2004). The solid carbonates and CH_4 hydrate stabilize the sediment. Outside the polar permafrost region methane hydrates are stable below 300 m below sea level and at ocean temperatures of nearly 0 °C (Maekawa et al., 1995). The carbonate precipitation sequesters additional parts of CO_2, prevents the ocean water from acidifying and at last improves the CO_2 absorption by ocean water from the atmosphere. This again cools the troposphere.

The enhanced dissolution of silicates from the ISA induced by methanogenic sedimentation additionally compensates the enhanced alkalinity loss at the ocean surface attributed to the calcification due to foraminifera and coccolithofores phytoplankton growth by ISA fertilization.

4.3. Minimizing CH_4 emissions from sediments and igneous bedrock

The reaction product of oceanic crust minerals containing Fe(II) like Olivine and Pyrrotite with sea-water is hydrogen. Hydrogen is fermented by microbes with hydrogen carbonate into methane. The latter is known as constituent of the springs emitted by the ocean crust rocks (Früh-Green 2004).

Such and further methane emissions like anoxic sediments outside the methane hydrate stable pressure and temperature region induce de-oxygenation within the overlying water layer by methane emission (Römer et al., 2014; Yamamoto et al., 2014). CH_4 emissions are induced for instance by hydrothermal springs (Suess et al., 1999), sediment movement (Krastel et al., 2014; Paull et al., 2007), climate change induced seawater warming (Serov et al., 2015; Shakhova et al., 2005), changing ocean circulation (Berndt et al., 2014), ocean sediment subduction (Elvert et al., 2000; Fischer et al., 2013). At lower vertical sediment to ocean surface distances the CH_4 emissions reach the troposphere. Because the Arctic Ocean suffers at most from the climate change induced warming the CH_4 release within this region rise extraordinary (Phrampus et al., 2014). The most elevated Global surface-near oceanic methane concentrations are located within the Arctic Ocean and the arctic troposphere (Shakhova et al., 2008). This might be one of the reasons for the higher temperature rise of the Arctic region than the average surface Earth warming.

Within the sediment and within the suboxic ocean water column, methane is oxidized by sulphate. Iron is an accelerator of this microbial fermentation reaction (Sivan et al., 2014). The ocean water column and the underlying sediment having had contact with ISA-originating iron are elevated in their iron content. This has different cooling effects to the troposphere: at first the elevated iron content in the uppermost suboxic sediment reduces the methane content emitted by the sediment by anaerobic oxidation of methane by sulphate-reducing bacteria.

Next the iron content reduces the methane bubble-development within the sediment layer preventing catastrophic methane eruptions by sediment destabilization, methane bursts and sediment avalanches.

Third: elevated iron content prevents the ocean water column from CH_4-induced oxygen deficiency by the formation of ammonium. This oxygen deficiency prevention protects from generation of the extreme stable and very effective GHG N_2O (Naqvi et al., 2010).

The glacial age proved that in spite of the multiplicity of the cooling processes induced, they caused little disturbance to the ecosystems. This predestines ISA as a steering tool to prevent climate fluctuations like the recent climate warming mankind is suffering from. The present study aims to describe in chapter 5 the technical means to realize this climate engineering project by the ISA method.

Figures 6a and 6b illustrate respectively the differences between a poorly and a sufficiently mixed ocean.

Earth Syst. Dynam. Discuss., doi:10.5194/esd-2016-32, 2016
Manuscript under review for journal Earth Syst. Dynam.
Published: 10 August 2016

Earth System Dynamics
Discussions
Open Access

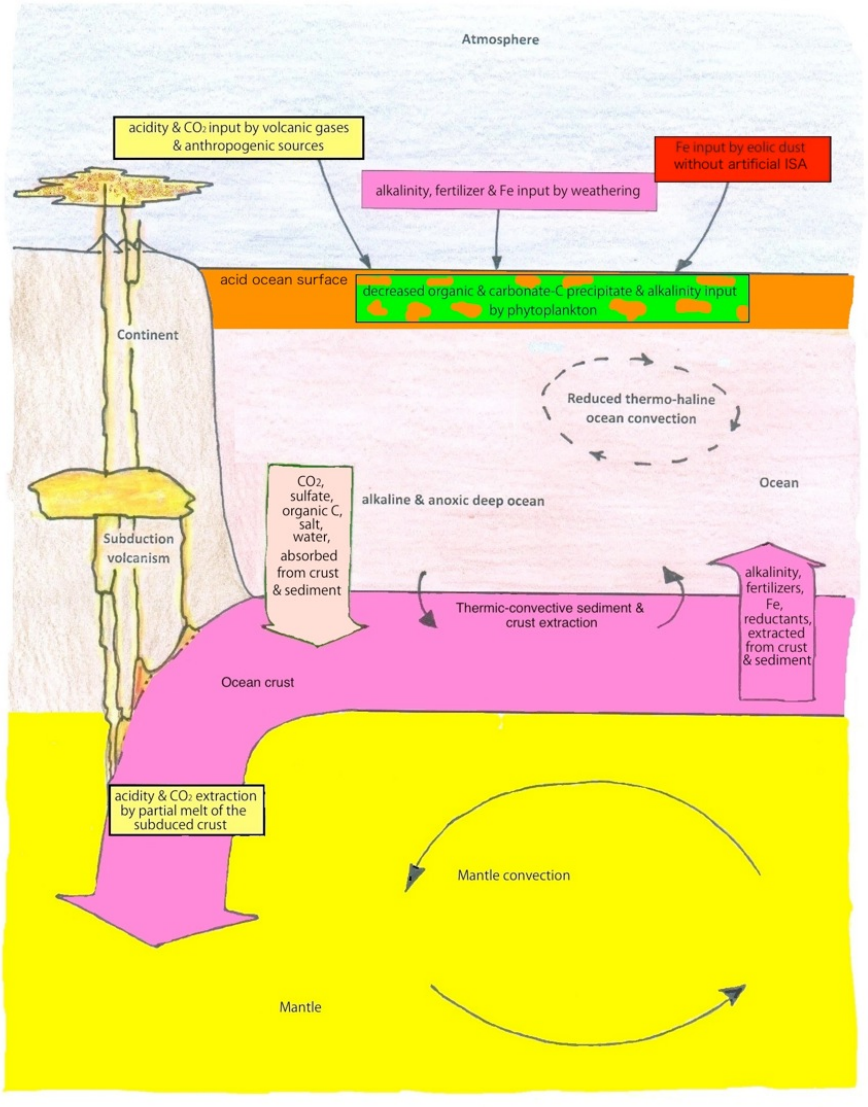

Earth Syst. Dynam. Discuss., doi:10.5194/esd-2016-32, 2016
Manuscript under review for journal Earth Syst. Dynam.
Published: 10 August 2016

Earth System Dynamics
Discussions
Open Access

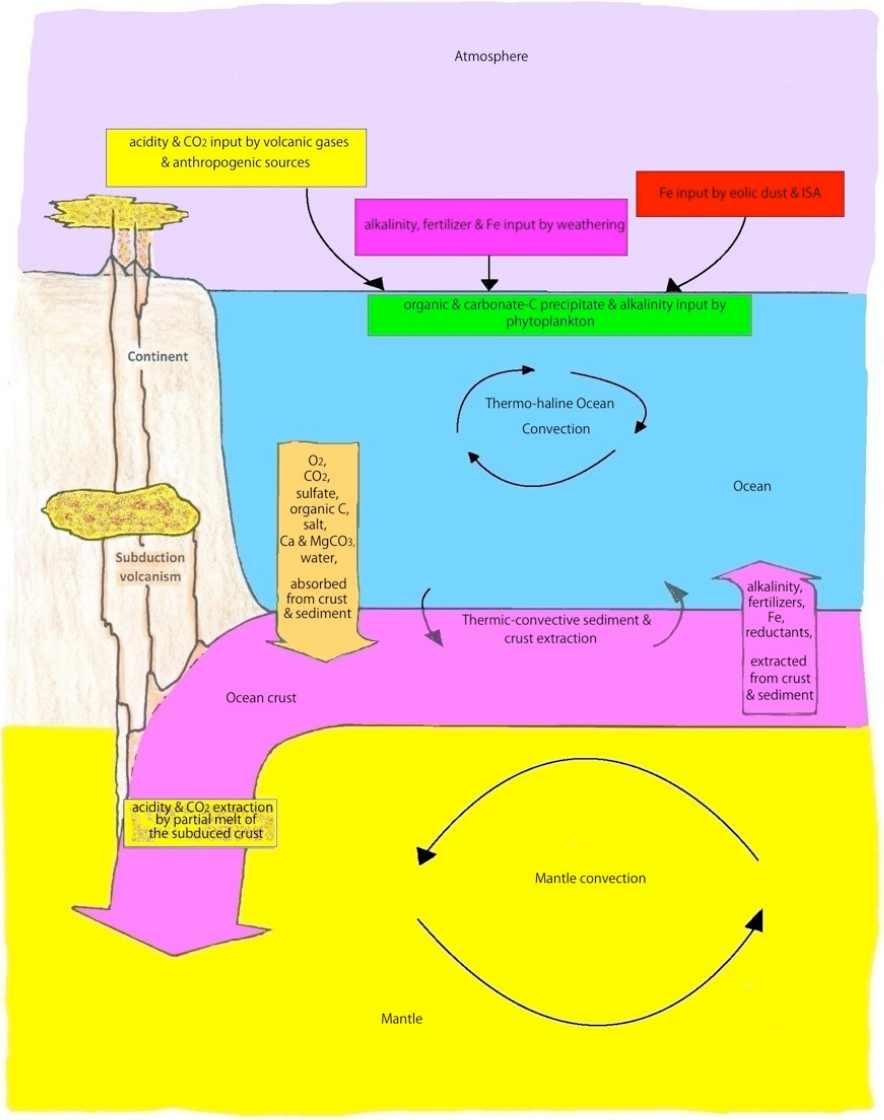

Figures 6a and 6b. The poorly mixed ocean has an acid surface balanced in CO_2, hydrogen carbonate and O_2 content with the atmosphere because these ingredients cannot be removed sufficiently from the surface to the basin bottom where hydrogen carbonate is precipitated in sediments and bedrock by the thermal convective sediment and crust extraction processes. The low O_2 transport rate to the deeper ocean ensures suboxic to

anoxic milieu below the surface layer. The acid-tolerant phytoplankton species have a lower production rate of organic carbon and a smaller production of carbon in the form of $CaCO_3$, because the fertilizer extracted from anaerobic sediments and bedrock does not arrive at the ocean surface. The organic carbon debris fraction precipitating as sediment layer in a poorly mixed ocean bottom is elevated compared to a sufficiently mixed ocean, because is the small oxidation rate during its trickling through the suboxic to anoxic water column. But this is by far no compensation of the low rate of hydrogen carbonate transfer from surface to bottom and its storage as dolomite and lime precipitate. As a result, the poorly mixed ocean has a decreased carbon transformation rate from atmosphere to ocean crust and sediment comparing to the sufficiently mixed ocean and will further accelerate the climate temperature rise.

This result is contradictious to the calculations of Duprat et al. (Duprat et al., 2016). They found within the iron containing melt water trail of the giant Antarctica that icebergs increased phytoplankton concentration. Duprat et al. assume that the iceberg induced carbon export increase by a factor of 5 to 10 within its influence locality and they expect an increase in carbon export by the expected increase of the iceberg production that has been prognosted (for instance Joughin et al. (Joughin et al., 2014)). We interpret the ongoing increase of icebergs and ice melt as a further severe warning sign that the ongoing destabilization might end soon in an insufficient mixed ocean.

The only artificially realizable restoration tool to change an insufficiently or poorly mixed ocean into a well mixed ocean is definitely by climate cooling. The ISA method appears to be the climate cooling method by means of choice, because it accelerates the conversion of atmospheric carbons into solid and even liquid carbons with the means of nature. Comparing to the artificial aerosol systems based on TiO_2 or H_2SO_4 (Pope et al., 2012), the sea-salt aerosol has advantages like better controllability and economy.

4.4. Modest iron effects onshore

The fertilizing role of African dust in the Amazon rainforest is well known (Yu et al., 2015b). On a basis of the 7-year average of trans-Atlantic dust transportation, Yu (Yu et al., 2015a) calculated that 182 Tg yr^{-1} dust leaves the coast of North Africa (15°W), of which 43 Tg yr^{-1} reaches America (75°W). The dust reaching the Caribbean and the Amazon come mainly of the northwestern Africa (Algeria, Mali, and Mauritania) (Gläser et al., 2015).

An average of dust deposition into the Amazon Basin over 7 years is estimated to be 29 (8–50) kg ha_{-1} yr_{-1} (Yu et al., 2015b), providing about to 23 (7–39) g ha_{-1} a_{-1} of phosphorus to fertilize the Amazon rainforest, together with Mg and Fe. Although not directly related to ISA, this dust deposition allows biomass fertilization and thus CO_2 removal from the atmosphere.

The wide spread tropical soils, mostly laterites, are deficient in phosphate and nitrogen but not in autochthon iron. The only exception to this is for all the epiphyte plants and the plants growing on the soil-free localities without any autochthon iron. These plants might gain profit from the ISA method. Such plant communities are localized for instance on top of the famous Tepuis (table mountains north of the Amazon basin near the borderlines of Brazil, Venezuela and Guyana) and on the tree branches in the rain forests without roots into the ground. From Köhler et al. (Köhler et al., 2007) the epiphytes flora on the tree branches of the rain forests may contain up to 16 t ha^{-1} (Costa Rica) up to 44 t ha^{-1} (Colombia) of epiphyte plant + humus dry weight on the tree branches.

The epiphytes but much more the Tepui plants would gain profit from ISA and even undissolved iron oxides, because plant roots and fungal hyphae secrete iron-solubilizing organic acids and complexants. Even microbial ferments have time enough to turn all kind of undissolvable Fe into dissolvable Fe.

Some rain forests like the Amazonian, benefit from sporadic dust plume fertilization of Saharan origin. Others may profit from an artificial ISA precipitation resulting in a significant additional epiphyte plant growth.

5. Estimations of the ISA demand by the ISA method

5.1. ISA can induce a significant CH_4 depletion

Wittmer (Wittmer et al., 2015a) reported that the ISA method is very efficient for °Cl generation. Hence, ISA allows depletion of greenhouse gas methane by separation prior cooling effect. Therefore, ISA appears to be a very promising cooling method with technical and economic stakes. But the answer depends strongly on the volume of ISA to be produced and emitted. Indeed, ISA plume should be released high enough in the troposphere to get sufficient distribution and residence time in combination with °Cl generation quantity.

Based on results of Fe photolysis induced °Cl production, Wittmer (Wittmer et al., 2015a) estimated the feasibility of CH_4 depletion by NaCl-diluted ISA. Wittmer found a °Cl emission of 1.9 x 10^5 °Cl/cm^3 at a Cl^-/Fe(III) molar ratio of 101 within the pH range of 2.1-2.3. The same °Cl generation was found at the suboptimal pH of 3.3 – 3.5 and at a Cl^-/Fe(III) molar ratio of 51. This Cl generation is four times higher than the reference which corresponds to a significant CH_4 lifetime reduction in the troposphere (Wittmer et al., 2015a). A pH range of around 2 corresponds to the natural aerosol pH within the oceanic boundary layer. The optimum efficiency of °Cl production by photolysis of ISA corresponds to pH 2, whatever the source of Cl^-, NaCl or gaseous HCl and whatever if ISA is an iron(III) oxide or an iron(III) chloride aerosol (Wittmer et al., 2015a).

5.2. ISA demand calculation

Current CH_4 depletion by °Cl is estimated from 3.3% (Platt et al., 2004) to 4.3% (Allan et al., 2007). According to the results of Wittmer (Wittmer et al., 2015a) at a Cl^-/Fe(III) molar ratio of 101, this amount would rise fourfold: from 13 to 17%.

1. Instead of using a Cl^-/Fe(III) molar ratio of 101, Wittmer used a Cl^-/Fe(III) ratio of 51 to perform calculations at the suboptimal pH of 3.3-3.5: 1.9 x 10^5 °Cl/cm^3 (Wittmer et al., 2015a);

Moreover, Wittmer made two wrong estimations:

2. There is no other tropospheric Cl^- source than sea-salt;
3. The global production rate of sea-salt aerosol Cl^- of 1785 Tg/year has to be doped with iron at a Cl^-/Fe(III) molar ratio of 51.

The calculations made with these wrong assumptions resulted in an iron demand of 56 Tg/year Fe(III) to obtain the desired CH_4 depletion effect (Wittmer et al., 2015a).

Whereas the calculations with the correct Cl^-/Fe(III) ratio of 101 results in a Fe(III) demand of only 18 Tg/year – still by the wrong assumption that there is no further Cl^- source than sea-salt.

ISA is produced from pyrogenic iron oxides. Pyrogenic oxides have particle sizes lower than 0.1µm. Diameters of the NaCl-diluted ISA particles of the Wittmer tests (Wittmer et al., 2015a) are round about 0.5µm. This confirms the test results of Wittmer et al. as calculation basis without any cut.

On the contrary, Wittmer made other two wrong assumptions:

4. ISA has the same particle size and corresponding surface range as sea-salt;
5. ISA has the same residence time as sea-salt aerosol in the troposphere

According to their coarse aerosol particle range, the residence time of sea-salt particles in the troposphere is inferior to 1 day (Jaenicke, 1980) while the artificial ISA particles with diameters lower than 0.5 µm have residence times in the troposphere of at least 10 days up to several weeks (Kumar et al., 2010; Penner et al., 2001). Analogue to CCN behavior in cloud processing (Rosenfeld et al., 2008) most of the small-sized ISA particles are protected by their small sizes from coagulation or coalescence with sea-salt aerosol particles. This effect prevents ISA from leaving the optimum active atomic chlorine emission conditions: low pH and low particle diameter range.

The residence time difference of more than one order of magnitude in comparison to sea-salt aerosol further reduces the Fe demand for ISA production from 18 Tg/year to less than 1.8 Tg/year.

6. The properties of the ISA particles produced by the most preferred ISA method variant are explained in chapter 4. Their difference to the NaCl-diluted ISA tested by Wittmer (Wittmer et al., 2015a) are: ISA particles are made of $FeCl_3$ x nH_2O undiluted by NaCl, or FeOOH coated by $FeCl_3$ x nH_2O undiluted by NaCl (Meyer-Oeste, 2010;

Oeste, 2009). The Cl^-/Fe(III) molar ratios of $FeCl_3$ x nH_2O are at 3 or even lower. The Cl^-/Fe(III) molar ratio of typical ISA particles is at least 30 times smaller than the molar Cl^-/Fe(III) ratio of 101 of the tested ISA by Wittmer (Wittmer et al., 2015a). This reduces the Fe demand for ISA production again at least by 1 order of magnitude from <1.8 Tg/year to about <0.2 Tg/year.

Additionally to the °Cl emission increase with increasing iron concentration in the tested aerosols, the results of Wittmer verify an increase in °Cl emission with decreasing pH (Wittmer et al., 2015a). According to Wittmer and Meyer-Oeste (Meyer-Oeste, 2010; Oeste, 2009), oxidic ISA aerosol particles may be generated free from any pH-buffering alkaline components. This hampers their pH decrease by air-borne HCl to the optimum pH around pH 2. Sea-salt buffering of the absorbed HCl (Sullivan et al., 2007) by the alkali and earthen alkali content of sea-salt aerosol can occur only by coagulation, most probable in a minor ISA particle fraction but not in the bulk. From the beginning of its action in the troposphere ISA keeps in the optimum °Cl emission mode: low pH, and high iron concentration levels.

Preferred ISA is produced by the ISA method variant 1 or variant 3 as described in chapter 4. Hence, ISA are composed of particles made by flame pyrolysis or iron salt vapor condensation. The mentioned ISA particles have diameters of 1/10 of the particle diameters of the Wittmer tests. These ISA particles have optimum chlorine activation efficiency:

- In an appropriate chloride dotation or chloride delivering environment;
- At a pH <2;
- If they are emitted above the tropospheric boundary layer.

Then the Fe demand may fall up even shorter than the calculated 0.2 Tg Fe/year because of their far extended surface area and far extended residence time in the atmosphere.

It has to be noted that this ISA demand calculation result refers only to the ISA cooling property according to CH_4 depletion; further cooling properties according to cloud albedo, depletion of CO_2, black and brown aerosol, ozone increase and further causes are still kept unconsidered.

Further oxidation activity on greenhouse gases and aerosols are induced by the °OH generation activity of ISA: Volcanic eruption plumes contain high concentrations of °Cl plus °OH (Baker et al., 2011) and are characterized by decreased CH_4 concentrations (Rose et al., 2006). Co-absorption of H_2O and HCl is the main reason of the generation of volcanic ash particle coats containing soluble Fe salts originating from insoluble Fe oxides and Fe silicates (Hoshyaripour et al., 2015; Martin et al., 2012). Gaseous HCl from the eruption plume entails Fe chlorides covering the surfaces of volcanic ash particles (Ayris et al., 2014). Therefore, it is reasonable that photolysis of those chlorides is the origin of both: °Cl and °OH generation in volcanic plumes.

Earth Syst. Dynam. Discuss., doi:10.5194/esd-2016-32, 2016
Manuscript under review for journal Earth Syst. Dynam.
Published: 10 August 2016

°OH can change from the liquid aerosol phase into gaseous phase (Nie et al., 2014). But by far, not as easy as °Cl can. Indeed, the Henry's law solubility constant of °OH is about one order of magnitude higher than that of °Cl and is in the same range than that of NH_3 (Sander, 2015). But when their hygroscopic water layer shrinks in dry air or by freezing, ISA particles might act as °OH emitters. These additional °OH emissions might further increase the CH_4 oxidation potential of volcanic ash or artificial ISA and thus reduce even more the Fe demand for ISA, though this has not been tested yet it cannot be ruled out.

In order to take care not to overstep the cooling effect too far, a reasonable goal might be to start the ISA method with a global ISA emission of 0.1 Tg Fe/year. This quantity corresponds to the magnitude of the actual Fe input from the atmosphere into the oceans under the form of soluble salt, which is estimated to be from 0.1 up to 0.26 Tg/year (Ito and Shi, 2015; Johnson and Meskhidze, 2013; Myriokefalitakis et al., 2014). Doubling or even tripling of this input quantity by the ISA method is of easy technical and economic feasibility as will been seen in chapter 6.

6. The ISA method: how to increase artificial iron emissions

Preceding calculation evidenced that the ISA method has the potential to cut back the rise of CH_4 and CO_2 and vice versa the small decline of atmospheric oxygen content (Keeling and Shertz, 1992; Manning and Keeling, 2006) because it acts by a bundle of chemical and physical means. The ISA method might retard, stop or even help to restore their contents to pre-industrial levels. By the ISA method, doubling or tripling of the ISA level in the troposphere seems to be possible by feasible technical and economical means.

Since 2004 proposals have been published (Oeste, 2015; Oeste and Ries, 2011) (Meyer-Oeste, 2010; Oeste, 2004, 2009) to modify combustion processes and flue gas emissions in the order to use them as ISA plume emission sources in the troposphere by traffic and power generating combustions and their warm uplifting flue gases. Predestined for the ISA method are any hot flue gas plumes emitted by ship and air traffic, fossil and sunshine power.

At least three variants of ISA production are proposed:

- Variant 1: Emission of flame pyrolytic FeOOH aerosol with particle diameters smaller than 100 nm (Buyukhatipoglu and Clyne, 2010; Kammler et al., 2001) as ISA precursor by co-combustion of organic iron or carbonyl iron additives with liquid or gaseous fuels or heating oils combusted in ship or and jet engines or by oil or gas combustors. Co-combustion of iron compounds is a possible measure in coal power stations and mixing the ISA precursor containing ~~oil~~ combustion flue gas to the coal combustion flue gas after the dry flue gas cleaning stage. Useful side effects of iron additives are fuel efficiency optimization and soot emission minimizing (Kim et al., 2008) ((Kasper et al., 1998; Madhu et al., 2015; Weiser et al.). The emitted FeOOH

aerosol plumes convert immediately into the ISA plume after leaving the emission sources because of the high reactivity of flame pyrolytic Fe oxides. The period to cover the flame pyrolytic FeOOH particle surface by HCl absorption from the gaseous phase with Fe(III) chlorides is several times shorter comparing to the generation of iron chlorides from natural iron oxide minerals in loess dust particles (Rubasinghege et al., 2010; Sullivan et al., 2007).

• Variant 2: Injection of vaporous ISA precursor iron compounds like $FeCl_3$ into a carrier gas. By contacting the carrier gas and/or the atmosphere the vaporous iron compounds condenses and/or converts by physical and/or chemical means directly into ISA. Contrary to all other ISA precursors, the sunlit $FeCl_3$ vapor becomes photo-reduced by concomitant generation of °Cl (Rustad and Gregory, 1980). Thus methane depleting °Cl emission can start even before this ISA precursor has changed into hydrated $FeCl_3$.

• Variant 3: Injection of ultrasonic nebulized aqueous $FeCl_3$ solution as ISA precursor into a carrier gas. By water evaporation from the aerosol droplets ISA becomes generated.

The preferred heights of ISA plume generation in the troposphere are 1000 m above ground or higher. There the ISA plumes have optimum conditions to spread over sufficient life-times. The necessary buoyancy to lift up the ISA plumes can be regulated by controlling their carrier gas temperatures. Uplift towers (Ming, 2016), vortex generators (Michaud and Renno, 2011) or tethered balloons (Davidson et al., 2012), (Kuo et al., 2012) are preferential means to direct ISA by carrier gas uplift to said heights.

Provision of the phytoplankton to optimize its growth with further nutrients like Mn, Zn, Co, Cu, Mo, B, Si and P by the ISA method is possible by at least the variants 1-3 of the ISA method by co-combustion, co-condensation or co-nebulizing.

Global fixing regulations of GHGs emission certificate prices, values, and ISA emission certificate credit values would be simple but effective measures for the quickest world-wide implementation of the ISA flue gas conditioning method.

7. Interaction of the ISA method with further measures to protect the environment

According to Wittmer & Zetzsch (Wittmer and Zetzsch, 2016) elevated HCl content in the atmosphere triggers the methane depleting coating of oxidic ISA precursors by photolytic active Fe(III) chlorides. Any measure triggering the reduction of the HCl content of the atmosphere would impair the effectiveness of the ISA method based on this kind of method.

In this sense all kind of measures to reduce the sulphur and NO_x content of the flue gas content of gaseous, liquid or gaseous fuels belongs would decrease the effectiveness of oxidic ISA precursors, because the S and NO_x oxidation products sulphuric acid aerosol and

gaseous nitric acid are the main producers of HCl by changing sea salt aerosol into sulphate and nitrate aerosol. Even the measures of reducing the energy production from fuel burning by changing to wind and photovoltaic energy would reduce this HCl source.

Sea salt aerosol even produce HCl after contact with organic aerosol and organic volatile matter because the latter generates acid oxidation products from the latter like oxalic acid (Drozd et al., 2014; Laskin et al., 2012; Wang et al., 2014a). A large fraction of organic aerosols and secondary organic aerosols originate from anthropogenic sources like combustions. The change to wind and photovoltaic energy would reduce even this HCl source.

The proposed CE measure of producing sulphuric acid aerosol within the stratosphere by inducing an albedo increase would increase the HCl content, during contact of the precipitating acid aerosol with tropospheric sea salt aerosol. Even the proposed CE measure of increasing the sea salt aerosol content of the troposphere by artificial sea salt aerosol as cloud whitening measure could be used as ISA method trigger if flue gas is used to elevate the sea salt aerosol.

8. Discussion and Conclusion

There is abundant literature on the many geoengineering methods that have been proposed to *"cool the Earth"* (Lackner, 2015; Zhang et al., 2014). In particular, the injection of sulphate aerosols into the stratosphere is the most studied method, as it mimics the episodic action of natural volcanoes (Pope et al., 2012); (Ming et al., 2014). Injected particles into the stratosphere reduce the radiative balance of Earth by scattering solar radiation back to space, so other nature and type of particles are envisioned with a wide range of side-effects (Jones et al., 2015).

The literature describes also many options to deliver this sulphates, their precursors (or other particles) to the stratosphere (Davidson et al., 2012). For instance, airplane delivery of the sulphate aerosols by the kerosene combustion process requires military jets because regular aircrafts only reach 10 km (30000 feet), and not the 20 km requested (Davidson et al., 2012).

In the case of ISA, the altitude needed to *"cool the Earth"* is much lower, as it is in the troposphere, not in the stratosphere, and the total quantities to deliver are 1 order of magnitude smaller. So air traffic might be a possible means of ISA delivery. But the global jet fuel consumption is about 240,000 t/year. Even by assuming the very high emission rate of 1 kg ISA precursor iron per ton of jet fuel, only 240 tons per year might be emitted. This seems far away from the order of magnitude of the target ISA emissions.

From the many other possible delivery strategies envisioned for SRM by stratospheric aerosols, many are not suited for ISA, like artillery, missiles and rockets (Davidson et al., 2012), because it will be cheaper and less polluting to make profit from the flue gas of a

reduced number of thermal power plants, that might be efficient enough to deliver the artificial iron aerosol needed over the boundary layer, in order to the aerosols to stay several days or weeks on the troposphere and be well distributed (Williams et al., 2002).

According to Luo (Luo et al., 2008), deposition of soluble iron from combustion already contributes from 20 to100% of the soluble iron deposition over many ocean regions.

As an example we calculated the possible production and emission of ISA respective the ISA precursor FeOOH aerosol using the flue gas of the German power station Niederaußem: with the input of 25 million t/year lignite (brown coal) this power station produces 3,600 MW. According to ISA production variant 1 (chapter 6) the ISA precursor FeOOH aerosol may be produced by burning of a ferrocene ($Fe(C_5H_5)_2$) oil solution containing 1 % ferrocene in a separate simple oil burner. The hot oil burner flue gas containing the ISA precursor FeOOH aerosol is injected and mixed into the cleaned power station flue gas. The power station flue gas emission rate is calculated to 9,000 m³ flue gas per ton lignite. Because the ISA precursor containing flue gas will be elevated to heights of more than 1000 m above ground, dust levels of the ISA precursor FeOOH aerosol of 20 mg/m³ flue gas seem to be acceptable. This allows a quantity of 180 g FeOOH/t of combusted lignite (9000 m³/t x 0,02 g/m³). At a lignite quantity of 25 million t/year, this corresponds to 4,500 t FeOOH/yr. FeOOH has an iron content of 63 %. This corresponds to a possible iron emission of 2,831 t/year or to a ferrocene consumption of 9,438 t/year.

Corresponding to this calculation about 100 of such huge power stations should have the ability to produce the sufficient ISA quantity of an equivalent of 200,000 to 300.000 t Fe/year. By a co-emission of HCl, for instance by co-burning of an organic HCl precursor, further optimization of the cooling capacity of the produced ISA is possible.

This example illustrates that ISA emission at only 100 power stations, or any similar ISA emission measures, is quite feasible compared to the alternative of CO_2 capture from the flue gas of 40 Gtons/yr, compression of the CO_2 until condensation to the liquid state and then storing the liquid CO_2 by injection into underground rock storage.

In order to increase the effectiveness of the buoyancy capacity of the power works the usual wet cooling tower might be replaced by a dry cooling tower to mix the dry and warm air emission from the cooling tower with the hot flue gas as additional buoyancy and due point reduction mean. Further the flue gas buoyancy may increase by increasing the flue gas temperature.

This or other simple techniques to realize ISA plumes may be used within the troposphere.

One delivery method seems promising and can easily be adapted to ISA method, is the use of tethered balloons (Davidson, 2012), and will cost much less as 1 or 2 km high will be sufficient for ISA emissions, requiring much lower pressures in the pipes, than for SO_2 delivery at 20 km high for the geoengineering method. Technical and economic feasibility

Earth Syst. Dynam. Discuss., doi:10.5194/esd-2016-32, 2016
Manuscript under review for journal Earth Syst. Dynam.
Published: 10 August 2016

have already been studied for the SPICE project (Kuo et al., 2012) which was planning to release sea water spay at 1 km high.

Also, as iron emissions only stay in the troposphere within weeks, compared to SRM sulphates in the stratosphere that are supposed to stay 1 or 2 years, in case any unintentional side effect or problem occurs, stopping the emissions is rapidly possible and the reversibility of its effects are much shorter than for solar radiation management by sulphates aerosols.

Other geoengineering strategies to cool the Earth, like carbon dioxide removal by iron fertilization (Williamson et al., 2012) have several pros and cons, like localized release, less dispersion, in a form that is not readily bio-available, resulting in restricted cooling effects, high expenses. The ISA method allows the use of the same atom of iron several times by catalytic and photocatalytic processes into the atmosphere, with different cooling effects (like albedo modification and enhancement of the methane destruction) and then reaches the oceans, with again further cooling effects like enhancement of the CO_2 carbon fixation. Figure 7 summarizes many of the cooling effects of the ISA method.

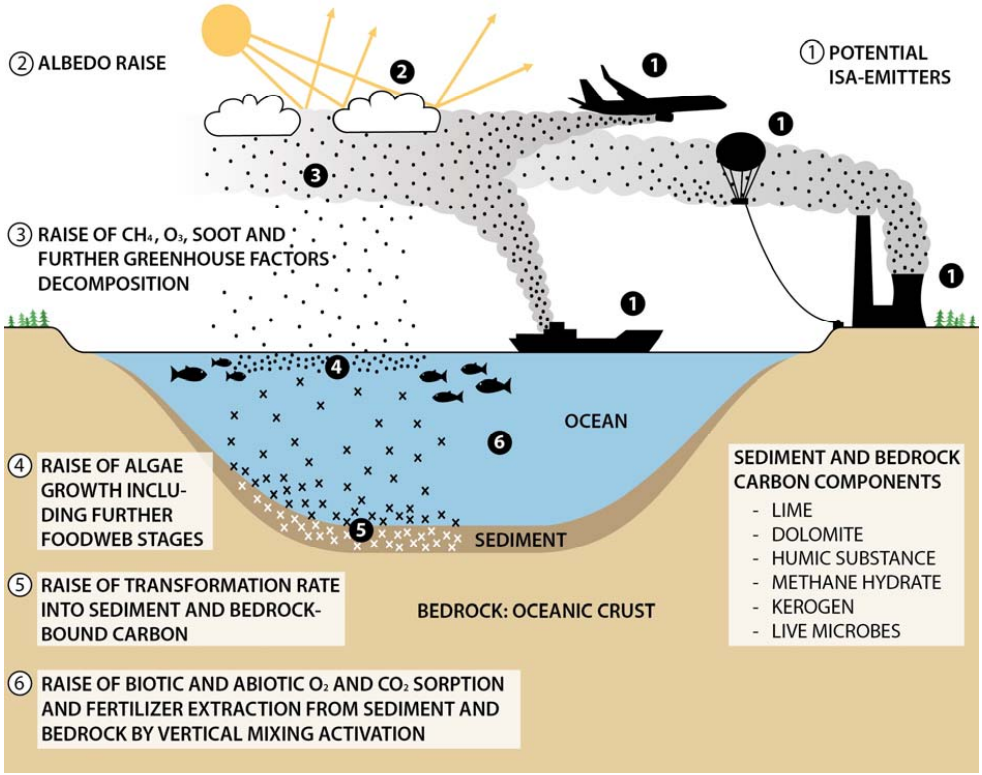

Figure 7. Summary of the principal cooling effects of the iron salt aerosols method proposed.

Why ISA appears to be better than ocean iron fertilization? For ocean iron fertilization several tons of Fe(II) are dispersed in a short time (hours) over only some km^2 of ocean with several drawbacks and a massive algae bloom can change the local biotopes. Meanwhile ISA releases iron continuously, over up to the entire 510 million km^2 of the Earth surface. The current iron inputs (in the form of soluble salts) into the oceans are estimated between 0.1 and 0.26 Tg/year per year (Ito and Shi, 2015; Johnson and Meskhidze, 2013; Myriokefalitakis et al., 2014). As the water surfaces cover nearly 72% of Earth surface (362 million km^2), if ISA delivers 1 Tg Fe/year evenly distributed (in addition to natural and anthropogenic current emissions), which is 4 times more than the expected needs (chapter 5.2), on average every km^2 of ocean receives 5.4 g Fe km^{-2} day^{-1} (1/510 tons of iron per km^2 per year).

As a conclusion: the ISA method is feasible even probably without environmental problems, because it relates to chemical and/or physical combustion processes occurring currently. The adjustable flue gas temperatures of different types of combustions are a means to lift the ISA plumes to optimal heights within the troposphere. Climate cooling by ISA involves the troposphere, dry solid surfaces, ocean, ocean sediment and ocean crust. Several GHG factors are controlled by ISA: CO_2, CH_4, tropospheric O_3, black carbon, dust, cloud albedo, and vertical ocean mixing.

Abbreviations:

Carbon capture and storage: CCS; Chlorine atom: °Cl; Cloud condensation nuclei: CCN; Intergovernmental Panel on Climate Change: IPPC; Iron salt: IS; Iron salt aerosols: ISA; Humic-like substances: HULIS; Hydroxyl radical: °OH; Ligand: L; Methane: CH_4; Mid-ocean rift: MOR; Secondary organic aerosol: SOA; Thermohaline circulation: THC; Volatile organic compounds: VOC.

Author contribution:

F. D. Oeste suggested the review idea and performed initial bibliographical search completed by R. de Richter. F. D. Oeste prepared the manuscript and the figures with contributions from all co-authors. T. Ming and S. Caillol also contributed to structuring the manuscript and English corrections.

Competing interests

The authors declare that they have no conflict of interest.

Acknowledgment:

This research was supported by the Scientific Research Foundation of Wuhan University of Technology (No. 40120237) and the ESI Discipline Promotion Foundation of WUT (No.35400664).

The co-authors would like to thanks Louise Phillips for grammatical corrections and re-reading.

Bibliography:

Al-Abadleh, H.A., 2015. Review of the bulk and surface chemistry of iron in atmospherically relevant systems containing humic-like substances. RSC Advances 5, 45785-45811.

Albani, S., Mahowald, N., Murphy, L., Raiswell, R., Moore, J., Anderson, R., McGee, D., Bradtmiller, L., Delmonte, B., Hesse, P., 2016. Paleodust variability since the Last Glacial Maximum and implications for iron inputs to the ocean. Geophysical Research Letters 43, 3944-3954.

Allan, W., Struthers, H., Lowe, D., 2007. Methane carbon isotope effects caused by atomic chlorine in the marine boundary layer: Global model results compared with Southern Hemisphere measurements. Journal of Geophysical Research: Atmospheres (1984–2012) 112.

Allen, C.C., Westall, F., Schelble, R.T., 2001. Importance of a martian hematite site for astrobiology. Astrobiology 1, 111-123.

Alt, J.C., Shanks, W.C., 2003. Serpentinization of abyssal peridotites from the MARK area, Mid-Atlantic Ridge: sulfur geochemistry and reaction modeling. Geochimica et Cosmochimica Acta 67, 641-653.

Alterskjær, K., Kristjánsson, J., 2013. The sign of the radiative forcing from marine cloud brightening depends on both particle size and injection amount. Geophysical Research Letters 40, 210-215.

Anderson, R.F., Barker, S., Fleisher, M., Gersonde, R., Goldstein, S.L., Kuhn, G., Mortyn, P.G., Pahnke, K., Sachs, J.P., 2014. Biological response to millennial variability of dust and nutrient supply in the Subantarctic South Atlantic Ocean. Philosophical Transactions of the Royal Society of London A: Mathematical, Physical and Engineering Sciences 372, 20130054.

Andreae, M., Gelencsér, A., 2006. Black carbon or brown carbon? The nature of light-absorbing carbonaceous aerosols. Atmospheric Chemistry and Physics 6, 3131-3148.

Ardon-Dryer, K., Huang, Y.-W., Cziczo, D., 2015. Laboratory studies of collection efficiency of sub-micrometer aerosol particles by cloud droplets on a single droplet basis. Atmospheric Chemistry and Physics Discussions 15, 6207-6236.

Ayris, P.M., Delmelle, P., Cimarelli, C., Maters, E.C., Suzuki, Y.J., Dingwell, D.B., 2014. HCl uptake by volcanic ash in the high temperature eruption plume: Mechanistic insights. Geochimica et Cosmochimica Acta 144, 188-201.

Bai, H., Jiang, W., Kotchey, G.P., Saidi, W.A., Bythell, B.J., Jarvis, J.M., Marshall, A.G., Robinson, R.A., Star, A., 2014. Insight into the mechanism of graphene oxide degradation via the photo-Fenton reaction. The Journal of Physical Chemistry C 118, 10519-10529.

Baker, A.K., Rauthe - Schöch, A., Schuck, T.J., Brenninkmeijer, C.A., van Velthoven, P.F., Wisher, A., Oram, D.E., 2011. Investigation of chlorine radical chemistry in the Eyjafjallajökull volcanic plume using observed depletions in non - methane hydrocarbons. Geophysical Research Letters 38.

Baker, A.K., Sauvage, C., Thorenz, U.R., Brenninkmeijer, C.A., Oram, D.E., van Velthoven, P., Zahn, A., Williams, J., 2015. Evidence for widespread tropospheric Cl chemistry in free tropospheric air masses from the South China Sea, EGU General Assembly Conference Abstracts, p. 10370.

Bakun, A., Black, B., Bograd, S.J., Garcia-Reyes, M., Miller, A., Rykaczewski, R., Sydeman, W., 2015. Anticipated effects of climate change on coastal upwelling ecosystems. Current Climate Change Reports 1, 85-93.

Barbusiński, K., 2009. Fenton reaction-controversy concerning the chemistry. Ecological chemistry and engineering 16, 347-358.

Bartels-Rausch, T., Jacobi, H.-W., Kahan, T.F., Thomas, J.L., Thomson, E.S., Abbatt, J.P., Ammann, M., Blackford, J.R., Bluhm, H., Boxe, C., 2014. A review of air–ice chemical and physical interactions (AICI): liquids, quasi-liquids, and solids in snow. Atmospheric Chemistry and Physics 14, 1587-1633.

Bauer, S.E., Menon, S., 2012. Aerosol direct, indirect, semidirect, and surface albedo effects from sector contributions based on the IPCC AR5 emissions for preindustrial and present - day conditions. Journal of Geophysical Research: Atmospheres (1984–2012) 117.

Belton, D.J., Deschaume, O., Patwardhan, S.V., Perry, C.C., 2010. A solution study of silica condensation and speciation with relevance to in vitro investigations of biosilicification. The Journal of Physical Chemistry B 114, 9947-9955.
Benz, M., Schink, B., Brune, A., 1998. Humic acid reduction by Propionibacterium freudenreichii and other fermenting bacteria. Applied and environmental microbiology 64, 4507-4512.
Bernardello, R., Marinov, I., Palter, J.B., Galbraith, E.D., Sarmiento, J.L., 2014a. Impact of Weddell Sea deep convection on natural and anthropogenic carbon in a climate model. Geophysical Research Letters 41, 7262-7269.
Bernardello, R., Marinov, I., Palter, J.B., Sarmiento, J.L., Galbraith, E.D., Slater, R.D., 2014b. Response of the ocean natural carbon storage to projected twenty-first-century climate change. Journal of Climate 27, 2033-2053.
Berndt, C., Feseker, T., Treude, T., Krastel, S., Liebetrau, V., Niemann, H., Bertics, V., Dumke, I., Dünnbier, K., Ferré, B., Graves, C., Gross, F., Hissmann, K., Hühnerbach, V., Krause, S., Liesner, K., Schauer, J., Steinle, L., 2014. Methane hydrates and global warming: Dissolution of hydrates off Svalbard caused by natural processes; . Pressemitteilung des GEOMAR Helmholz-Zentrum für Ozeanforschung Kiel Kiel
Berner, R.A., Scott, M.R., Thomlinson, C., 1970. Carbonate alkalinity in the pore waters of anoxic sediments. Limnology and Oceanography 15, 544-549.
Bintanja, R., Van Oldenborgh, G., Drijfhout, S., Wouters, B., Katsman, C., 2013. Important role for ocean warming and increased ice-shelf melt in Antarctic sea-ice expansion. Nature Geoscience 6, 376-379.
Bjorlykke, K., 2010. Petroleum geoscience: From sedimentary environments to rock physics. Springer Science & Business Media.
Blechschmidt, A.-M., Richter, A., Burrows, J., Kaleschke, L., Strong, K., Theys, N., Weber, M., Zhao, X., Zien, A., 2016. An exemplary case of a bromine explosion event linked to cyclone development in the Arctic. Atmospheric Chemistry and Physics 16, 1773-1788.
Bleicher, S., Buxmann, J., Sander, R., Riedel, T., Thornton, J., Platt, U., Zetzsch, C., 2014. The influence of nitrogen oxides on the activation of bromide and chloride in salt aerosol. Atmospheric Chemistry and Physics Discussions 14, 10135-10166.
Bond, D.R., Lovley, D.R., 2002. Reduction of Fe (III) oxide by methanogens in the presence and absence of extracellular quinones. Environmental Microbiology 4, 115-124.
Boucher, O., 2015. Biogeochemical Effects and Climate Feedbacks of Aerosols, Atmospheric Aerosols. Springer, pp. 247-269.
Boyd, P., Ellwood, M., 2010. The biogeochemical cycle of iron in the ocean. Nature Geoscience 3, 675-682.
Branch, T.A., DeJoseph, B.M., Ray, L.J., Wagner, C.A., 2013. Impacts of ocean acidification on marine seafood. Trends in ecology & evolution 28, 178-186.
Bruland, K., 2006. A review of the chemistries of redox sensitive elements within suboxic zones of oxygen minimum regions. Gayana (Concepc.) 70, 6-13.
Buyukhatipoglu, K., Clyne, A.M., 2010. Controlled flame synthesis of αFe2O3 and Fe3O4 nanoparticles: effect of flame configuration, flame temperature, and additive loading. Journal of Nanoparticle Research 12, 1495-1508.
Bykova, E., Dubrovinsky, L., Dubrovinskaia, N., Bykov, M., McCammon, C., Ovsyannikov, S., Liermann, H.-P., Kupenko, I., Chumakov, A., Rüffer, R., 2016. Structural complexity of simple Fe2O3 at high pressures and temperatures. Nature communications 7.
Capone, D.G., Hutchins, D.A., 2013. Microbial biogeochemistry of coastal upwelling regimes in a changing ocean. Nature geoscience 6, 711-717.
Carpenter, L.J., Archer, S.D., Beale, R., 2012. Ocean-atmosphere trace gas exchange. Chemical Society Reviews 41, 6473-6506.
Cartapanis, O., Bianchi, D., Jaccard, S.L., Galbraith, E.D., 2016. Global pulses of organic carbon burial in deep-sea sediments during glacial maxima. Nature communications 7.
Cassar, N., Laws, E.A., Bidigare, R.R., Popp, B.N., 2004. Bicarbonate uptake by Southern Ocean phytoplankton. Global Biogeochemical Cycles 18.
Charlson, R.J., Lovelock, J.E., Andreae, M.O., Warren, S.G., 1987. Oceanic phytoplankton, atmospheric sulphur, cloud albedo and climate. Nature 326, 655-661.
Charpentier, D., Buatier, M., Jacquot, E., Gaudin, A., Wheat, C., 2011. Conditions and mechanism for the formation of iron-rich Montmorillonite in deep sea sediments (Costa Rica margin): Coupling high resolution mineralogical characterization and geochemical modeling. Geochimica et Cosmochimica Acta 75, 1397-1410.
Chemizmu, K., Fentona, R., 2009. Fenton reaction-controversy concerning the chemistry. Ecological chemistry and engineering 16, 347-358.

Chen, C.-T.A., Lin, C.-M., Huang, B.-T., Chang, L.-F., 1996. Stoichiometry of carbon, hydrogen, nitrogen, sulfur and oxygen in the particulate matter of the western North Pacific marginal seas. Marine Chemistry 54, 179-190.

Claeys, M., Vermeylen, R., Yasmeen, F., Gómez-González, Y., Chi, X., Maenhaut, W., Mészáros, T., Salma, I., 2012. Chemical characterisation of humic-like substances from urban, rural and tropical biomass burning environments using liquid chromatography with UV/vis photodiode array detection and electrospray ionisation mass spectrometry. Environmental Chemistry 9, 273-284.

Coates, J.D., Ellis, D.J., Blunt-Harris, E.L., Gaw, C.V., Roden, E.E., Lovley, D.R., 1998. Recovery of humic-reducing bacteria from a diversity of environments. Applied and Environmental Microbiology 64, 1504-1509.

Coggon, R.M., Teagle, D., Harris, M., John, C., Smith-Duque, C., Alt, J., 2012. Why Does Calcium Carbonate Precipitate in the Ocean Crust?, AGU Fall Meeting Abstracts, p. 0545.

Conway, T., Wolff, E., Röthlisberger, R., Mulvaney, R., Elderfield, H., 2015. Constraints on soluble aerosol iron flux to the Southern Ocean at the Last Glacial Maximum. Nature communications 6.

Coogan, L.A., Gillis, K.M., 2013. Evidence that low - temperature oceanic hydrothermal systems play an important role in the silicate - carbonate weathering cycle and long - term climate regulation. Geochemistry, Geophysics, Geosystems 14, 1771-1786.

Cózar, A., Echevarría, F., González-Gordillo, J.I., Irigoien, X., Úbeda, B., Hernández-León, S., Palma, Á.T., Navarro, S., García-de-Lomas, J., Ruiz, A., 2014. Plastic debris in the open ocean. Proceedings of the National Academy of Sciences 111, 10239-10244.

Crutzen, P.J., 2006. Albedo enhancement by stratospheric sulfur injections: a contribution to resolve a policy dilemma? Climatic change 77, 211-220.

Crutzen, P.J., Oppenheimer, M., 2008. Learning about ozone depletion. Climatic Change 89, 143-154.

Cunningham, K.M., Goldberg, M.C., Weiner, E.R., 1988. Mechanisms for aqueous photolysis of adsorbed benzoate, oxalate, and succinate on iron oxyhydroxide (goethite) surfaces. Environmental science & technology 22, 1090-1097.

Daims, H., Lebedeva, E.V., Pjevac, P., Han, P., Herbold, C., Albertsen, M., Jehmlich, N., Palatinszky, M., Vierheilig, J., Bulaev, A., 2015. Complete nitrification by Nitrospira bacteria. Nature 528, 504-509.

Davidson, P., 2012. Up and away! TCE www.tcetoday.com, pp. 28-32.

Davidson, P., Burgoyne, C., Hunt, H., Causier, M., 2012. Lifting options for stratospheric aerosol geoengineering: advantages of tethered balloon systems. Philosophical Transactions of the Royal Society of London A: Mathematical, Physical and Engineering Sciences 370, 4263-4300.

De Laat, J., Le, G.T., Legube, B., 2004. A comparative study of the effects of chloride, sulfate and nitrate ions on the rates of decomposition of H2O2 and organic compounds by Fe (II)/H2O2 and Fe (III)/H2O2. Chemosphere 55, 715-723.

de Lavergne, C., Palter, J.B., Galbraith, E.D., Bernardello, R., Marinov, I., 2014. Cessation of deep convection in the open Southern Ocean under anthropogenic climate change. Nature Climate Change 4, 278-282.

de Richter, R., Caillol, S., 2011. Fighting global warming: the potential of photocatalysis against CO2, CH4, N2O, CFCs, tropospheric O3, BC and other major contributors to climate change. Journal of Photochemistry and Photobiology C: Photochemistry Reviews 12, 1-19.

de Richter, R., Ming, T., Caillol, S., Liu, W., 2016a. Fighting global warming by GHG removal: Destroying CFCs and HCFCs in solar-wind power plant hybrids producing renewable energy with no-intermittency. International Journal of Greenhouse Gas Control 49, 449-472.

de Richter, R., Ming, T., Shen, S., Caillol, S., 2016b. Fighting global warming by greenhouse gas removal: destroying atmospheric nitrous oxide thanks to synergies between two breakthrough technologies. Environmental Science and Pollution Research 23, 6119-6138.

Death, R., Wadham, J., Monteiro, F., Le Brocq, A., Tranter, M., Ridgwell, A., Dutkiewicz, S., Raiswell, R., 2014. Antarctic ice sheet fertilises the Southern Ocean. Biogeosciences 11, 2635-2643.

Demadis, K.D., Mavredaki, E., Somara, M., 2011. Additive-Driven Dissolution Enhancement of Colloidal Silica. 2. Environmentally Friendly Additives and Natural Products. Industrial & Engineering Chemistry Research 50, 13866-13876.

Dewangan, P., Basavaiah, N., Badesab, F., Usapkar, A., Mazumdar, A., Joshi, R., Ramprasad, T., 2013. Diagenesis of magnetic minerals in a gas hydrate/cold seep environment off the Krishna–Godavari basin, Bay of Bengal. Marine Geology 340, 57-70.

Dick, G.J., Anantharaman, K., Baker, B.J., Li, M., Reed, D.C., Sheik, C.S., 2015. The microbiology of deep-sea hydrothermal vent plumes: ecological and biogeographic linkages to seafloor and water column habitats. Hydrothermal microbial ecosystems, 79.

Dimitrova, K., Sarkisyan, A., Koleva, V., 2015. Vertical mussel reef farming: Exploring climate change solutions with economic and ecologic significance, Climate Engineering Research Symposium, Berlin.

Dorfman, J., Stoner, J., Finkenbinder, M., Abbott, M., Xuan, C., St-Onge, G., 2015. A 37,000-year environmental magnetic record of aeolian dust deposition from Burial Lake, Arctic Alaska. Quaternary Science Reviews 128, 81-97.
Dorn, R.I., 2009. The Rock Varnish Revolution: New Insights from Microlaminations and the Contributions of Tanzhuo Liu. Geography Compass 3, 1804-1823.
Drozd, G., Woo, J., Häkkinen, S., Nenes, A., McNeill, V.F., 2014. Inorganic salts interact with oxalic acid in submicron particles to form material with low hygroscopicity and volatility. Atmospheric Chemistry and Physics 14, 5205-5215.
Drushel, H.V., Hallum, J.V., 1958. The Organic Nature of Carbon Black Surfaces. II. Quinones and Hydroquinones by Coulometry at Controlled Potential. The Journal of Physical Chemistry 62, 1502-1505.
Duggen, S., Croot, P., Schacht, U., Hoffmann, L., 2007. Subduction zone volcanic ash can fertilize the surface ocean and stimulate phytoplankton growth: Evidence from biogeochemical experiments and satellite data. Geophysical Research Letters 34.
Duprat, L.P., Bigg, G.R., Wilton, D.J., 2016. Enhanced Southern Ocean marine productivity due to fertilization by giant icebergs. Nature Geoscience.
Eder, J.M., 1880. Über die Zersetzung des Eisenchlorides und einiger organischer Ferridsalze im Lichte. Monatshefte für Chemie/Chemical Monthly 1, 755-762.
Eder, J.M., 1906. Ausführliches Handbuch der Photographie, Erster Band, 2. Teil: Photochemie (die chemischen Wirkungen des Lichtes). Wilhelm Knapp.
Elvert, M., Suess, E., Greinert, J., Whiticar, M.J., 2000. Archaea mediating anaerobic methane oxidation in deep-sea sediments at cold seeps of the eastern Aleutian subduction zone. Organic Geochemistry 31, 1175-1187.
Enami, S., Sakamoto, Y., Colussi, A.J., 2014. Fenton chemistry at aqueous interfaces. Proceedings of the National Academy of Sciences 111, 623-628.
Evans, B.W., 2008. Control of the products of serpentinization by the Fe2+ Mg− 1 exchange potential of olivine and orthopyroxene. Journal of Petrology 49, 1873-1887.
Fenton, H., 1894. LXXIII.—Oxidation of tartaric acid in presence of iron. Journal of the Chemical Society, Transactions 65, 899-910.
Fischer, D., Mogollón, J.M., Strasser, M., Pape, T., Bohrmann, G., Fekete, N., Spiess, V., Kasten, S., 2013. Subduction zone earthquake as potential trigger of submarine hydrocarbon seepage. Nature Geoscience 6, 647-651.
Flanner, M.G., Zender, C.S., Randerson, J.T., Rasch, P.J., 2007. Present - day climate forcing and response from black carbon in snow. Journal of Geophysical Research: Atmospheres 112.
Früh - Green, G.L., Connolly, J.A., Plas, A., Kelley, D.S., Grobéty, B., 2004. Serpentinization of oceanic peridotites: implications for geochemical cycles and biological activity. The subseafloor biosphere at mid-ocean ridges, 119-136.
Fry, J.L., Draper, D.C., Barsanti, K.C., Smith, J.N., Ortega, J., Winkler, P.M., Lawler, M.J., Brown, S.S., Edwards, P.M., Cohen, R.C., 2014. Secondary organic aerosol formation and organic nitrate yield from NO3 oxidation of biogenic hydrocarbons. Environmental science & technology 48, 11944-11953.
Fujita, T., 1971. Concentration of major chemical elements in marine plankton. Geochemical Journal 4, 143-156.
Gammons, C., Parker, S., Nimick, D., 2007. Diel iron cycling in acidic rivers of southwestern Spain, Goechimica et Cosmochimica Acta. Pergamon - Elsevier Science Ltd, Oxford, England, pp. A305-A305.
Gaudin, A., Buatier, M., Beaufort, D., Petit, S., Grauby, O., Decarreau, A., 2005. Characterization and origin of Fe3+-montmorillonite in deep-water calcareous sediments (Pacific Ocean, Costa Rica margin). Clays and Clay Minerals 53, 452-465.
Ghio, A.J., Soukup, J.M., Dailey, L.A., Tong, H., Kesic, M.J., Budinger, G.S., Mutlu, G.k.M., 2015. Wood smoke particle sequesters cell iron to impact a biological effect. Chemical research in toxicology 28, 2104-2111.
Gläser, G., Wernli, H., Kerkweg, A., Teubler, F., 2015. The transatlantic dust transport from North Africa to the Americas—Its characteristics and source regions. Journal of Geophysical Research: Atmospheres 120.
Gopakumar, G., Belanzoni, P., Baerends, E.J., 2011. Hydroxylation catalysis by mononuclear and dinuclear iron oxo catalysts: a methane monooxygenase model system versus the Fenton reagent FeIVO (H2O) 52+. Inorganic chemistry 51, 63-75.
Graedel, T.E., Keene, W., 1996. The budget and cycle of Earth's natural chlorine. Pure and applied chemistry 68, 1689-1697.
Haas, S., Weber, N., Berry, A., Erich, E., 2014. Limestone powder carbon dioxide scrubber

as the technology for Carbon Capture and Usage. Cement International 3, 34-45.
Hadley, O.L., Kirchstetter, T.W., 2012. Black-carbon reduction of snow albedo. Nature Climate Change 2, 437-440.
Hammer, U.T., 1986. Saline lake ecosystems of the world. Springer Science & Business Media.
Hammond, C., Forde, M.M., Rahim, A., Hasbi, M., Thetford, A., He, Q., Jenkins, R.L., Dimitratos, N., Lopez - Sanchez, J.A., Dummer, N.F., 2012. Direct Catalytic Conversion of Methane to Methanol in an Aqueous Medium by using Copper - Promoted Fe - ZSM - 5. Angewandte Chemie International Edition 51, 5129-5133.
Hansen, J., Sato, M., Hearty, P., Ruedy, R., Kelley, M., Masson-Delmotte, V., Russell, G., Tselioudis, G., Cao, J., Rignot, E., 2015. Ice melt, sea level rise and superstorms: evidence from paleoclimate data, climate modeling, and modern observations that 2◦ C global warming is highly dangerous. Atmospheric Chemistry and Physics Discussions 15, 20059-20179.
Hauck, J., Köhler, P., Wolf-Gladrow, D., Völker, C., 2016. Iron fertilisation and century-scale effects of open ocean dissolution of olivine in a simulated CO2 removal experiment. Environmental Research Letters 11, 024007.
Hawkes, J.A., Connelly, D., Gledhill, M., Achterberg, E.P., 2013. The stabilisation and transportation of dissolved iron from high temperature hydrothermal vent systems. Earth and Planetary Science Letters 375, 280-290.
Hawkings, J.R., Wadham, J.L., Tranter, M., Raiswell, R., Benning, L.G., Statham, P.J., Tedstone, A., Nienow, P., Lee, K., Telling, J., 2014. Ice sheets as a significant source of highly reactive nanoparticulate iron to the oceans. Nature communications 5.
Hoffer, A., Kiss, G., Blazso, M., Gelencsér, A., 2004. Chemical characterization of humic - like substances (HULIS) formed from a lignin - type precursor in model cloud water. Geophysical research letters 31, L06115.
Holm, N.G., Neubeck, A., 2009. Reduction of nitrogen compounds in oceanic basement and its implications for HCN formation and abiotic organic synthesis. Geochem Trans 10.
Hoshyaripour, G., Hort, M., Langmann, B., 2015. Ash iron mobilization through physicochemical processing in volcanic eruption plumes: a numerical modeling approach. Atmospheric Chemistry and Physics 15, 9361-9379.
Hu, L., Yvon - Lewis, S.A., Butler, J.H., Lobert, J.M., King, D.B., 2013. An improved oceanic budget for methyl chloride. Journal of Geophysical Research: Oceans 118, 715-725.
Hungate, B., Danin, A., Pellerin, N., Stemmler, J., Kjellander, P., Adams, J., Staley, J., 1987. Characterization of manganese-oxidizing (MnII→ MnIV) bacteria from Negev Desert rock varnish: implications in desert varnish formation. Canadian Journal of Microbiology 33, 939-943.
Insua, T.L., Spivack, A.J., Graham, D., D'Hondt, S., Moran, K., 2014. Reconstruction of Pacific Ocean bottom water salinity during the Last Glacial Maximum. Geophysical Research Letters 41, 2914-2920.
Ito, A., Shi, Z., 2015. Delivery of anthropogenic bioavailable iron from mineral dust and combustion aerosols to the ocean. Atmospheric Chemistry and Physics Discussions 15, 23051-23088.
Ivarsson, M., Bengtson, S., Neubeck, A., 2016. The igneous oceanic crust–Earth's largest fungal habitat? Fungal Ecology 20, 249-255.
Jaccard, S.L., Galbraith, E.D., Martínez-García, A., Anderson, R.F., 2016. Covariation of deep Southern Ocean oxygenation and atmospheric CO2 through the last ice age. Nature 530, 207-210.
Jacobson, M.Z., 2002. Control of fossil - fuel particulate black carbon and organic matter, possibly the most effective method of slowing global warming. Journal of Geophysical Research: Atmospheres (1984–2012) 107, ACH 16-11-ACH 16-22.
Jaenicke, R., 1980. Atmospheric aerosols and global climate. Journal of Aerosol science 11, 577-588.
Jambeck, J.R., Geyer, R., Wilcox, C., Siegler, T.R., Perryman, M., Andrady, A., Narayan, R., Law, K.L., 2015. Plastic waste inputs from land into the ocean. Science 347, 768-771.
Janecky, D., Seyfried, W., 1986. Hydrothermal serpentinization of peridotite within the oceanic crust: experimental investigations of mineralogy and major element chemistry. Geochimica et Cosmochimica Acta 50, 1357-1378.
Jeong, D., Kim, K., Choi, W., 2012. Accelerated dissolution of iron oxides in ice. Atmospheric Chemistry and Physics 12, 11125-11133.
Jin, L., Zhang, P., Shao, T., Zhao, S., 2014. Ferric ion mediated photodecomposition of aqueous perfluorooctane sulfonate (PFOS) under UV irradiation and its mechanism. Journal of hazardous materials 271, 9-15.
Johnson, L., Eggleston, C., 2013. The photocatalytic actions of desert varnish. University of Wyoming, .
Johnson, M., Meskhidze, N., 2013. Atmospheric dissolved iron deposition to the global oceans: effects of oxalate-promoted Fe dissolution, photochemical redox cycling, and dust mineralogy. Geoscientific Model Development Discussions 6, 1901-1947.

Jones, A., Haywood, J., Jones, A., 2015. Climatic impacts of stratospheric geoengineering with sulfate, black carbon and titania injection. Atmospheric Chemistry & Physics Discussions 15.
Jorgensen, S.S., 1976. Dissolution kinetics of silicate minerals in aqueous catechol solutions. Journal of Soil Science 27, 183-195.
Joughin, I., Smith, B.E., Medley, B., 2014. Marine ice sheet collapse potentially under way for the Thwaites Glacier Basin, West Antarctica. Science 344, 735-738.
Kahan, T.F., Wren, S.N., Donaldson, D.J., 2014. A Pinch of Salt Is All It Takes: Chemistry at the Frozen Water Surface. Accounts of chemical research 47, 1587-1594.
Kalvelage, T., Lavik, G., Lam, P., Contreras, S., Arteaga, L., Löscher, C.R., Oschlies, A., Paulmier, A., Stramma, L., Kuypers, M.M., 2013. Nitrogen cycling driven by organic matter export in the South Pacific oxygen minimum zone. Nature geoscience 6, 228-234.
Kammler, H.K., Mädler, L., Pratsinis, S.E., 2001. Flame synthesis of nanoparticles. Chemical engineering & technology 24, 583-596.
Kappler, A., Benz, M., Schink, B., Brune, A., 2004. Electron shuttling via humic acids in microbial iron (III) reduction in a freshwater sediment. FEMS Microbiology Ecology 47, 85-92.
Karydis, V., Kumar, P., Barahona, D., Sokolik, I., Nenes, A., 2013. Assessing the Impact of Mineral Dust and Adsorption Activation on Cloud Droplet Formation, Advances in Meteorology, Climatology and Atmospheric Physics. Springer, pp. 515-520.
Kasper, M., Sattler, K., Siegmann, K., Matter, U., 1998. The effect of ferrocene addition on particle formation and burnout in combustion processes. Journal of Aerosol Science 29, S617-S618.
Kastner, M., 1999. Oceanic minerals: Their origin, nature of their environment, and significance. Proceedings of the National Academy of Sciences 96, 3380-3387.
Kawagucci, S., Chiba, H., Ishibashi, J.-i., Yamanaka, T., Toki, T., Muramatsu, Y., Ueno, Y., Makabe, A., Inoue, K., Yoshida, N., 2011. Hydrothermal fluid geochemistry at the Iheya North field in the mid-Okinawa Trough: Implication for origin of methane in subseafloor fluid circulation systems. Geochemical Journal 45, 109-124.
Kawamura, K., Umemoto, N., Mochida, M., Bertram, T., Howell, S., Huebert, B., 2003. Water - soluble dicarboxylic acids in the tropospheric aerosols collected over east Asia and western North Pacific by ACE - Asia C - 130 aircraft. Journal of Geophysical Research: Atmospheres (1984–2012) 108.
Keeling, R.F., Shertz, S.R., 1992. Seasonal and interannual variations in atmospheric oxygen and implications for the global carbon cycle. Nature 358, 723-727.
Kelemen, P.B., Manning, C.E., 2015. Reevaluating carbon fluxes in subduction zones, what goes down, mostly comes up. Proceedings of the National Academy of Sciences 112, E3997-E4006.
Kelemen, P.B., Matter, J., Streit, E.E., Rudge, J.F., Curry, W.B., Blusztajn, J., 2011. Rates and mechanisms of mineral carbonation in peridotite: natural processes and recipes for enhanced, in situ CO2 capture and storage. Annual Review of Earth and Planetary Sciences 39, 545-576.
Kelley, D.S., Karson, J.A., Früh-Green, G.L., Yoerger, D.R., Shank, T.M., Butterfield, D.A., Hayes, J.M., Schrenk, M.O., Olson, E.J., Proskurowski, G., 2005. A serpentinite-hosted ecosystem: the Lost City hydrothermal field. Science 307, 1428-1434.
Khalil, M., Moore, R., Harper, D., Lobert, J., Erickson, V.K., Keene, W., 1999. Natural emissions of chlorine-containing gases: Reactive Chlorine Emissions Inventory.
Khalil, M., Rasmussen, R., 1999. Atmospheric methyl chloride. Atmospheric Environment 33, 1305-1321.
Kiesgen de_Richter, R., Ming, T., Caillol, S., 2013. Fighting global warming by photocatalytic reduction of CO2 using giant photocatalytic reactors. Renewable and Sustainable Energy Reviews 19, 82-106.
Kim, D., Song, K., Kaushik, R., 2008. Fuel Additives for Particulate Matter/Dust Reduction. Asian Journal of Chemistry 20, 5797.
Kim, J.-S., Park, K., 2012. Atmospheric aging of Asian dust particles during long range transport. Aerosol Science and Technology 46, 913-924.
Kim, J.R., Santiano, B., Kim, H., Kan, E., 2013. Heterogeneous oxidation of methylene blue with surface-modified iron-amended activated carbon.
Kim, K., Choi, W., Hoffmann, M.R., Yoon, H.-I., Park, B.-K., 2010. Photoreductive dissolution of iron oxides trapped in ice and its environmental implications. Environmental science & technology 44, 4142-4148.
Klüpfel, L., Keiluweit, M., Kleber, M., Sander, M., 2014. Redox properties of plant biomass-derived black carbon (biochar). Environmental science & technology 48, 5601-5611.
Koch, D., Del Genio, A., 2010. Black carbon absorption effects on cloud cover, review and synthesis. Atmospheric Chemistry & Physics Discussions 10, 7323-7346.
Köhler, L., Tobón, C., Frumau, K.A., Bruijnzeel, L.S., 2007. Biomass and water storage dynamics of epiphytes in old-growth and secondary montane cloud forest stands in Costa Rica. Plant Ecology 193, 171-184.

Köhler, P., Abrams, J.F., Völker, C., Hauck, J., Wolf-Gladrow, D.A., 2013. Geoengineering impact of open ocean dissolution of olivine on atmospheric CO2, surface ocean pH and marine biology. Environmental Research Letters 8, 014009.
Köhler, P., Hartmann, J., Wolf-Gladrow, D.A., 2010. Geoengineering potential of artificially enhanced silicate weathering of olivine. Proceedings of the National Academy of Sciences 107, 20228-20233.
Köhler, P., Hauck, J., Völker, C., Wolf-Gladrow, D., 2015. The role of iron during the open ocean dissolution of olivine in a simulated CO2 removal experiment—enhanced weathering, ocean alkalinization, ocean fertilization.
Konhauser, K.O., Urrutia, M.M., 1999. Bacterial clay authigenesis: a common biogeochemical process. Chemical Geology 161, 399-413.
Kostka, J.E., Stucki, L.J.W., Nealson, K.H., Wu, J., 1996. Reduction of structural Fe (III) in smectite by a pure culture of the Fe-reducing bacterium Shewanella putrifaciens strain MR-1, Clays and Clay Minerals. Citeseer.
Krastel, S., Bialas, J., A, V., 2014. Im fragilen Gleichgewicht: Deutsch-Neuseeländisches Forscherteam entdeckt bisher unbekanntes Methanvorkommen bei der Untersuchung von instabilen untermeerischen Hängen; , Pressemitteilung 2/6/2014 des GEOMAR Helmholz-Zentrum für Ozeanforschung Kiel und Institut für Geowissenschaften der Christian-Albrechts-Universität zu Kiel vom 12.05.(2014), Kiel
Krause, S., Liebetrau, V., Gorb, S., Sánchez-Román, M., McKenzie, J.A., Treude, T., 2012. Microbial nucleation of Mg-rich dolomite in exopolymeric substances under anoxic modern seawater salinity: New insight into an old enigma. Geology 40, 587-590.
Kumar, P., Robins, A., Vardoulakis, S., Britter, R., 2010. A review of the characteristics of nanoparticles in the urban atmosphere and the prospects for developing regulatory controls. Atmospheric Environment 44, 5035-5052.
Kuo, K.A., Watson, I., Hunt, H.E., 2012. The SPICE project: an example of geoengineering research, Water and Climate: Policy Implementation Challenges; Proceedings of the 2nd Practical Responses to Climate Change Conference. Engineers Australia, p. 479.
Lackner, M., 2015. Geoengineering for Climate Stabilization. Springer, New York.
Lam, P.J., Bishop, J.K., 2008. The continental margin is a key source of iron to the HNLC North Pacific Ocean. Geophysical Research Letters 35.
Lamy, F., Gersonde, R., Winckler, G., Esper, O., Jaeschke, A., Kuhn, G., Ullermann, J., Martínez-Garcia, A., Lambert, F., Kilian, R., 2014. Increased dust deposition in the Pacific Southern Ocean during glacial periods. Science 343, 403-407.
Lana, A., Bell, T., Simó, R., Vallina, S.M., Ballabrera - Poy, J., Kettle, A., Dachs, J., Bopp, L., Saltzman, E., Stefels, J., 2011. An updated climatology of surface dimethlysulfide concentrations and emission fluxes in the global ocean. Global Biogeochemical Cycles 25.
Laskin, A., Moffet, R.C., Gilles, M.K., Fast, J.D., Zaveri, R.A., Wang, B., Nigge, P., Shutthanandan, J., 2012. Tropospheric chemistry of internally mixed sea salt and organic particles: Surprising reactivity of NaCl with weak organic acids. Journal of Geophysical Research: Atmospheres 117.
Latham, J., Bower, K., Choularton, T., Coe, H., Connolly, P., Cooper, G., Craft, T., Foster, J., Gadian, A., Galbraith, L., 2012a. Marine cloud brightening. Philosophical Transactions of the Royal Society of London A: Mathematical, Physical and Engineering Sciences 370, 4217-4262.
Latham, J., Parkes, B., Gadian, A., Salter, S., 2012b. Weakening of hurricanes via marine cloud brightening (MCB). Atmospheric Science Letters 13, 231-237.
Law, K.L., Morét-Ferguson, S.E., Goodwin, D.S., Zettler, E.R., DeForce, E., Kukulka, T., Proskurowski, G., 2014. Distribution of surface plastic debris in the eastern Pacific Ocean from an 11-year data set. Environmental science & technology 48, 4732-4738.
Le Bras, G., Platt, U., 1995. A possible mechanism for combined chlorine and bromine catalyzed destruction of tropospheric ozone in the Arctic. Geophysical research letters 22, 599-602.
Lenton, A., Sen Gupta, A., 2010. Carbon credits for oyster farming: fact or fiction?, Fish, p. 30.
Levin, Z., Teller, A., Ganor, E., Yin, Y., 2005. On the interactions of mineral dust, sea - salt particles, and clouds: A measurement and modeling study from the Mediterranean Israeli Dust Experiment campaign. Journal of Geophysical Research: Atmospheres (1984–2012) 110.
Levine, J.G., Wolff, E.W., Jones, A.E., Sime, L.C., 2011. The role of atomic chlorine in glacial - interglacial changes in the carbon - 13 content of atmospheric methane. Geophysical Research Letters 38.
Li, Q., Sun, H., Wang, J., 2010. Hydrochemical response of Epikarst Spring to rainfall: implications of nutrition element loss and groundwater pollution. Polish Journal of Environmental Studies 19, 441-448.

Liao, J., Huey, L.G., Liu, Z., Tanner, D.J., Cantrell, C.A., Orlando, J.J., Flocke, F.M., Shepson, P.B., Weinheimer, A.J., Hall, S.R., 2014. High levels of molecular chlorine in the Arctic atmosphere. Nature Geoscience 7, 91-94.
Lima, S.B., Borges, S.M.S., Rangel, M.d.C., Marchetti, S.G., 2013. Effect of iron content on the catalytic properties of activated carbon-supported magnetite derived from biomass. Journal of the Brazilian Chemical Society 24, 344-354.
Liu, T., Dorn, R.I., 1996. Understanding the spatial variability of environmental change in drylands with rock varnish microlaminations. Annals of the Association of American Geographers 86, 187-212.
Lovley, D.R., Blunt-Harris, E.L., 1999. Role of humic-bound iron as an electron transfer agent in dissimilatory Fe (III) reduction. Applied and environmental microbiology 65, 4252-4254.
Lovley, D.R., Fraga, J.L., Coates, J.D., Blunt - Harris, E.L., 1999. Humics as an electron donor for anaerobic respiration. Environmental Microbiology 1, 89-98.
Luff, R., Wallmann, K., 2003. Fluid flow, methane fluxes, carbonate precipitation and biogeochemical turnover in gas hydrate-bearing sediments at Hydrate Ridge, Cascadia Margin: numerical modeling and mass balances. Geochimica et Cosmochimica Acta 67, 3403-3421.
Luo, C., Mahowald, N., Bond, T., Chuang, P., Artaxo, P., Siefert, R., Chen, Y., Schauer, J., 2008. Combustion iron distribution and deposition. Global Biogeochemical Cycles 22.
Lyubetskaya, T., Korenaga, J., 2007. Chemical composition of Earth's primitive mantle and its variance: 1. Method and results. Journal of Geophysical Research: Solid Earth 112.
Machulek Jr, A., Moraes, J.E.F., Okano, L.T., Silvério, C.A., Quina, F.H., 2009. Photolysis of ferric ions in the presence of sulfate or chloride ions: implications for the photo-Fenton process. Photochemical & Photobiological Sciences 8, 985-991.
Mackinder, L., Wheeler, G., Schroeder, D., Riebesell, U., Brownlee, C., 2010. Molecular mechanisms underlying calcification in coccolithophores. Geomicrobiology Journal 27, 585-595.
Madhu, S., Nagaraju, J., Sridhar, P., 2015. Evaluation of four stroke diesel engine performance with ferrocene as fuel additive. International Journal & Magazine of Engineering, Technology, Management and Research 2, 2199-2204.
Maekawa, T., Itoh, S., Sakata, S., Igari, S.-i., Imai, N., 1995. Pressure and temperature conditions for methane hydrate dissociation in sodium chloride solutions. Geochemical Journal 29, 325-329.
Maher, B., Prospero, J., Mackie, D., Gaiero, D., Hesse, P., Balkanski, Y., 2010. Global connections between aeolian dust, climate and ocean biogeochemistry at the present day and at the last glacial maximum. Earth-Science Reviews 99, 61-97.
Maher, B.A., Dennis, P., 2001. Evidence against dust-mediated control of glacial–interglacial changes in atmospheric CO2. Nature 411, 176-180.
Mahowald, N.M., Baker, A.R., Bergametti, G., Brooks, N., Duce, R.A., Jickells, T.D., Kubilay, N., Prospero, J.M., Tegen, I., 2005. Atmospheric global dust cycle and iron inputs to the ocean. Global biogeochemical cycles 19.
Mahowald, N.M., Engelstaedter, S., Luo, C., Sealy, A., Artaxo, P., Benitez-Nelson, C., Bonnet, S., Chen, Y., Chuang, P.Y., Cohen, D.D., 2009. Atmospheric Iron Deposition: Global Distribution, Variability, and Human Perturbations*. Annual Review of Marine Science 1, 245-278.
Manning, A.C., Keeling, R.F., 2006. Global oceanic and land biotic carbon sinks from the Scripps atmospheric oxygen flask sampling network. Tellus B 58, 95-116.
Martin, J.H., 1990. Glacial-interglacial CO2 change: the Iron hypothesis. Paleoceanography 5, 1-13.
Martin, P., Loeff, M.R., Cassar, N., Vandromme, P., d'Ovidio, F., Stemmann, L., Rengarajan, R., Soares, M., González, H.E., Ebersbach, F., 2013. Iron fertilization enhanced net community production but not downward particle flux during the Southern Ocean iron fertilization experiment LOHAFEX. Global Biogeochemical Cycles 27, 871-881.
Martin, R., Wheeler, J., Ilyinskaya, E., Braban, C., Oppenheimer, C., 2012. The uptake of halogen (HF, HCl, HBr and HI) and nitric (HNO 3) acids into acidic sulphate particles in quiescent volcanic plumes. Chemical Geology 296, 19-25.
Martin, W., Russell, M.J., 2007. On the origin of biochemistry at an alkaline hydrothermal vent. Philosophical Transactions of the Royal Society of London B: Biological Sciences 362, 1887-1926.
Martínez-Garcia, A., Rosell-Melé, A., Jaccard, S.L., Geibert, W., Sigman, D.M., Haug, G.H., 2011. Southern Ocean dust-climate coupling over the past four million years. Nature 476, 312-315.
Martínez-García, A., Sigman, D.M., Ren, H., Anderson, R.F., Straub, M., Hodell, D.A., Jaccard, S.L., Eglinton, T.I., Haug, G.H., 2014. Iron fertilization of the Subantarctic Ocean during the last ice age. Science 343, 1347-1350.
Matrai, P., Keller, M., 1994. Total organic sulfur and dimethylsulfoniopropionate in marine phytoplankton: intracellular variations. Marine Biology 119, 61-68.
Matsunaga, K., Ohyama, T., Kuma, K., Kudo, I., Suzuki, Y., 1995. Photoreduction of manganese dioxide in seawater by organic substances under ultraviolet or sunlight. Water Research 29, 757-759.

Meister, P., Gutjahr, M., Frank, M., Bernasconi, S.M., Vasconcelos, C., McKenzie, J.A., 2011. Dolomite formation within the methanogenic zone induced by tectonically driven fluids in the Peru accretionary prism. Geology 39, 563-566.
Merinero, R., Lunar, R., Martínez-Frías, J., Somoza, L., Díaz-del-Río, V., 2008. Iron oxyhydroxide and sulphide mineralization in hydrocarbon seep-related carbonate submarine chimneys, Gulf of Cadiz (SW Iberian Peninsula). Marine and Petroleum Geology 25, 706-713.
Meyer-Oeste, F.-D., 2010. Method for Cooling the Troposphere. (Remark: [Wittmer, 2015] focus only to the side variant of claim 8). US Patent.
Meyer, J., Riebesell, U., 2015. Reviews and Syntheses: Responses of coccolithophores to ocean acidification: a meta-analysis. Biogeosciences (BG) 12, 1671-1682.
Michaud, L., Renno, N., 2011. the sky's the limit. Mechanical Engineering 133, 42.
Ming, T., 2016. Solar Chimney Power Plant Generating Technology. Academic Press, 246p. ISBN: 978-0-12-805370-6. .
Ming, T., de_Richter, R., Liu, W., Caillol, S., 2014. Fighting global warming by climate engineering: Is the Earth radiation management and the solar radiation management any option for fighting climate change? Renewable and Sustainable Energy Reviews 31, 792-834.
Mitchell, D.L., Finnegan, W., 2009. Modification of cirrus clouds to reduce global warming. Environmental Research Letters 4, 045102.
Monico, L., Janssens, K., Hendriks, E., Vanmeert, F., Van der Snickt, G., Cotte, M., Falkenberg, G., Brunetti, B.G., Miliani, C., 2015. Evidence for Degradation of the Chrome Yellows in Van Gogh's Sunflowers: A Study Using Noninvasive In Situ Methods and Synchrotron - Radiation - Based X - ray Techniques. Angewandte Chemie 127, 14129-14133.
Monnin, C., Chavagnac, V., Boulart, C., Ménez, B., Gérard, M., Gérard, E., Pisapia, C., Quemeneur, M., Erauso, G., Postec, A., 2014. Fluid chemistry of the low temperature hyperalkaline hydrothermal system of Prony Bay (New Caledonia). Biogeosciences 11, 5687-5706.
Moreno-Castilla, C., Lopez-Ramon, M., Carrasco-Marın, F., 2000. Changes in surface chemistry of activated carbons by wet oxidation. Carbon 38, 1995-2001.
Müller, M., Barcelos e Ramos, J., Schulz, K.G., Riebesell, U., Kazmierczak, J., Gallo, F., Mackinder, L., Li, Y., Nesterenko, P., Trull, T., 2015. Phytoplankton calcification as an effective mechanism to prevent cellular calcium poisoning. Biogeosciences Discussions 12, 12691-12712.
Müntener, O., 2010. Serpentine and serpentinization: A link between planet formation and life. Geology 38, 959-960.
Myriokefalitakis, S., Mihalopoulos, N., Baker, A., Kanakidou, M., 2014. The anthropogenic influence on Iron deposition over the oceans: a 3-D global modeling, EGU General Assembly Conference Abstracts, p. 8310.
Naqvi, S., Bange, H.W., Farias, L., Monteiro, P., Scranton, M., Zhang, J., 2010. Marine hypoxia/anoxia as a source of CH4 and N2O. Biogeosciences 7, 2159-2190.
Nayak, B., Das, S.K., Bhattacharyya, K.K., 2011. Detrital and authigenic (?) baddeleyite (ZrO2) in ferromanganese nodules of Central Indian Ocean Basin. Geoscience Frontiers 2, 571-576.
Nguyen, T.H., Ball, W.P., 2006. Absorption and adsorption of hydrophobic organic contaminants to diesel and hexane soot. Environmental science & technology 40, 2958-2964.
Nie, W., Ding, A., Wang, T., Kerminen, V.-M., George, C., Xue, L., Wang, W., Zhang, Q., Petäjä, T., Qi, X., 2014. Polluted dust promotes new particle formation and growth. Scientific reports 4.
Nielsen, S.G., Rehkämper, M., Teagle, D.A., Butterfield, D.A., Alt, J.C., Halliday, A.N., 2006. Hydrothermal fluid fluxes calculated from the isotopic mass balance of thallium in the ocean crust. Earth and Planetary Science Letters 251, 120-133.
Oelkers, E.H., Gislason, S.R., Matter, J., 2008. Mineral carbonation of CO2. Elements 4, 333-337.
Oeste, F.D., 1977. Die H2S-oxidation an aktiver kohle—ein elektrochemischer prozess? Carbon 15, 225-228.
Oeste, F.D., 2004. Climate cooling by interaction of artificial loess haze with seasalt haze induced by iron- or titanium-doped ship- and aircraft-fuel, Geo Leipzig 2004, Gemeinschaftstagung DGG und GGW, Universität Bremen, DE, p. 344.
Oeste, F.D., 2009. Controlling concentration of active materials necessary for life; air pollution control. US Patents 08/534535.
Oeste, F.D., 2015. The ISA method (IM), Climate Engineering Research Symposium 2015, Current State and Future Perspectives, Berlin.
Oeste, F.D., Ries, E., 2011. IOA, the CO2- and methane-carbon capturing process: Effective and secure carbon sequestration from troposphere into ocean sediment by flue gas conditioning of coal power plants. , 2nd ICEPE 2011 International Conference on Energy Process Engineering, Frankfurt am Main, Book of Extended Abstracts: Efficient carbon capture for coal power plants DECHEMA Gesellschaft für Chemische Technik & Biotechnologie e.V., Frankfurt am Main, Frankfurt pp. 207-209.

Ofner, J., Krüger, H.-U., Grothe, H., Schmitt-Kopplin, P., Whitmore, K., Zetzsch, C., 2011. Physico-chemical characterization of SOA derived from catechol and guaiacol–a model substance for the aromatic fraction of atmospheric HULIS. Atmospheric Chemistry and Physics 11, 1-15.
Oh, S.-Y., Chiu, P.C., 2009. Graphite-and soot-mediated reduction of 2, 4-dinitrotoluene and hexahydro-1, 3, 5-trinitro-1, 3, 5-triazine. Environmental science & technology 43, 6983-6988.
Ohman, L.-O., Nordin, A., Sedeh, I.F., Sjoberg, S., 1991. Equilibrium and Structural Studies of Silicon (IV) and Aluminium (III) in Aqueous Solution. 28. Formation of Soluble Silicic Acid-Ligand Complexes as Studied by Potentiometrie and Solubility Measurements. Acta chemica scandinavica 45, 335-341.
Ohshima, K.I., Fukamachi, Y., Williams, G.D., Nihashi, S., Roquet, F., Kitade, Y., Tamura, T., Hirano, D., Herraiz-Borreguero, L., Field, I., 2013. Antarctic Bottom Water production by intense sea-ice formation in the Cape Darnley polynya. Nature Geoscience 6, 235-240.
Ola, O., Maroto-Valer, M.M., 2015. Transition metal oxide based TiO 2 nanoparticles for visible light induced CO 2 photoreduction. Applied Catalysis A: General 502, 114-121.
Orcutt, B.N., Sylvan, J.B., Knab, N.J., Edwards, K.J., 2011. Microbial ecology of the dark ocean above, at, and below the seafloor. Microbiology and Molecular Biology Reviews 75, 361-422.
Oster, G.K., Oster, G., 1959. Photoreduction of Metal Ions by Visible Light1. Journal of the American Chemical Society 81, 5543-5545.
Osthoff, H.D., Roberts, J.M., Ravishankara, A., Williams, E.J., Lerner, B.M., Sommariva, R., Bates, T.S., Coffman, D., Quinn, P.K., Dibb, J.E., 2008. High levels of nitryl chloride in the polluted subtropical marine boundary layer. Nature Geoscience 1, 324-328.
Otto-Bliesner, B.L., Brady, E.C., Shields, C., 2002. Late Cretaceous ocean: coupled simulations with the national center for atmospheric research climate system model. Journal of Geophysical Research: Atmospheres 107.
Parekh, P., Follows, M.J., Boyle, E., 2004. Modeling the global ocean iron cycle. Global biogeochemical cycles 18.
Paull, C.K., Ussler, W., Dallimore, S.R., Blasco, S.M., Lorenson, T.D., Melling, H., Medioli, B.E., Nixon, F.M., McLaughlin, F.A., 2007. Origin of pingo - like features on the Beaufort Sea shelf and their possible relationship to decomposing methane gas hydrates. Geophysical Research Letters 34.
Pechtl, S., von Glasow, R., 2007. Reactive chlorine in the marine boundary layer in the outflow of polluted continental air: A model study. Geophysical research letters 34.
Pena, A.L., Segura E, R., Chan M, A., Hoggard E, P., 2014. Photodegradation of dichloromethane catalyzed by iron (III) chloride on silica gel. Current Catalysis 3, 35-38.
Penner, J.E., Andreae, M., Annegarn, H., Barrie, L., Feichter, J., Hegg, D., Jayaraman, A., Leaitch, R., Murphy, D., Nganga, J., 2001. Aerosols, their direct and indirect effects, Climate Change 2001: The Scientific Basis. Contribution of Working Group I to the Third Assessment Report of the Intergovernmental Panel on Climate Change. Cambridge University Press, pp. 289-348.
Perry, R.S., Kolb, V.M., Lynne, B.Y., Sephton, M.A., Mcloughlin, N., Engel, M.H., Olendzenski, L., Brasier, M., StaleyJr, J.T., 2005. How desert varnish forms?, Optics & Photonics 2005. International Society for Optics and Photonics, pp. 59060V-59060V-59012.
Phrampus, B.J., Hornbach, M.J., Ruppel, C.D., Hart, P.E., 2014. Widespread gas hydrate instability on the upper US Beaufort margin. Journal of Geophysical Research: Solid Earth 119, 8594-8609.
Piepenbrock, A., Behrens, S., Kappler, A., 2014. Comparison of humic substance-and Fe (III)-reducing microbial communities in anoxic aquifers. Geomicrobiology Journal 31, 917-928.
Pignatello, J.J., Oliveros, E., MacKay, A., 2006. Advanced oxidation processes for organic contaminant destruction based on the Fenton reaction and related chemistry. Critical reviews in environmental science and technology 36, 1-84.
Pillar, E.A., Camm, R.C., Guzman, M.I., 2014. Catechol oxidation by ozone and hydroxyl radicals at the air–water interface. Environmental science & technology 48, 14352-14360.
Pinto, I.S., Pacheco, P.H., Coelho, J.V., Lorençon, E., Ardisson, J.D., Fabris, J.D., de Souza, P.P., Krambrock, K.W., Oliveira, L.C., Pereira, M.C., 2012. Nanostructured δ-FeOOH: an efficient Fenton-like catalyst for the oxidation of organics in water. Applied Catalysis B: Environmental 119, 175-182.
Platt, U., Allan, W., Lowe, D., 2004. Hemispheric average Cl atom concentration from 13 C/12 C ratios in atmospheric methane. Atmospheric Chemistry and Physics 4, 2393-2399.
Polgári, M., Hein, J., Németh, T., Pál-Molnár, E., Vigh, T., 2013. Celadonite and smectite formation in the Úrkút Mn-carbonate ore deposit (Hungary). Sedimentary Geology 294, 157-163.
Pope, F., Braesicke, P., Grainger, R., Kalberer, M., Watson, I., Davidson, P., Cox, R., 2012. Stratospheric aerosol particles and solar-radiation management. Nature Climate Change 2, 713-719.
Postec, A., Quéméneur, M., Méline Bes, N.M., Benaïssa, F., Payri, C., Pelletier, B., Monnin, C., Guentas-Dombrowsky, L., Ollivier, B., Gérard, E., 2015. Microbial diversity in a submarine carbonate edifice from the serpentinizing hydrothermal system of the Prony Bay (New Caledonia) over a 6-year period. Frontiers in microbiology 6.

Pratt, K.A., Custard, K.D., Shepson, P.B., Douglas, T.A., Pöhler, D., General, S., Zielcke, J., Simpson, W.R., Platt, U., Tanner, D.J., 2013. Photochemical production of molecular bromine in Arctic surface snowpacks. Nature Geoscience 6, 351-356.
Pufahl, P., Hiatt, E., 2012. Oxygenation of the Earth's atmosphere–ocean system: a review of physical and chemical sedimentologic responses. Marine and Petroleum Geology 32, 1-20.
Raeisi, E., Karami, G., 1997. Hydrochemographs of Berghan karst spring as indicators of aquifer characteristics. Journal of Cave and Karst Studies 59, 112-118.
Rahmstorf, S., 2006. Thermohaline Ocean Circulation. Encyclopedia of Quaternary Sciences. Postdam Institute for Climate Impact Research 5.
Rahmstorf, S., Feulner, G., Mann, M.E., Robinson, A., Rutherford, S., Schaffernicht, E.J., 2015. Exceptional twentieth-century slowdown in Atlantic Ocean overturning circulation. Nature climate change 5, 475-480.
Raiswell, R., Fisher, Q., 2004. Rates of carbonate cementation associated with sulphate reduction in DSDP/ODP sediments: implications for the formation of concretions. Chemical Geology 211, 71-85.
Ramana, M., Ramanathan, V., Feng, Y., Yoon, S., Kim, S., Carmichael, G., Schauer, J., 2010. Warming influenced by the ratio of black carbon to sulphate and the black-carbon source. Nature Geoscience 3, 542-545.
Ramanathan, V., Carmichael, G., 2008. Global and regional climate changes due to black carbon. Nature geoscience 1, 221-227.
Ramanathan, V., Li, F., Ramana, M., Praveen, P., Kim, D., 2007. Atmospheric brown clouds: hemispherical and regional variations in long-range transport, absorption, and radiative forcing. J. Geophys. Res 112, D22S21.
Rast, W., Calcagno, A., Williams, W.D., 2001. The Watershed: Water from the Mountains into the Sea. Streams And Rivers: Water Flowing Over the Land Surface., in: Programme, U.U.N.e. (Ed.), Lakes and Reservoirs vol. 2, p. 36.
Resing, J.A., Sedwick, P.N., German, C.R., Jenkins, W.J., Moffett, J.W., Sohst, B.M., Tagliabue, A., 2015. Basin-scale transport of hydrothermal dissolved metals across the South Pacific Ocean. Nature 523, 200-203.
Riedel, T., Wolfe, G., Danas, K., Gilman, J., Kuster, W., Bon, D., Vlasenko, A., Li, S.-M., Williams, E., Lerner, B., 2014. An MCM modeling study of nitryl chloride (ClNO 2) impacts on oxidation, ozone production and nitrogen oxide partitioning in polluted continental outflow. Atmospheric Chemistry and Physics 14, 3789-3800.
Righi-Cavallaro, K.O., Roche, K.F., Froehlich, O., Cavallaro, M.R., 2010. Structure of macroinvertebrate communities in riffles of a Neotropical karst stream in the wet and dry seasons. Acta Limnologica Brasiliensia 22, 306-316.
Roberts, J.A., Bennett, P.C., González, L.A., Macpherson, G., Milliken, K.L., 2004. Microbial precipitation of dolomite in methanogenic groundwater. Geology 32, 277-280.
Roden, E., Edmonds, J., 1997. Phosphate mobilization in iron-rich anaerobic sediments: microbial Fe (III) oxide reduction versus iron-sulfide formation. Archiv für Hydrobiologie 139, 347-378.
Römer, M., Torres, M., Kasten, S., Kuhn, G., Graham, A.G., Mau, S., Little, C.T., Linse, K., Pape, T., Geprägs, P., 2014. First evidence of widespread active methane seepage in the Southern Ocean, off the sub-Antarctic island of South Georgia. Earth and Planetary Science Letters 403, 166-177.
Rose, W.I., Millard, G.A., Mather, T.A., Hunton, D.E., Anderson, B., Oppenheimer, C., Thornton, B.F., Gerlach, T.M., Viggiano, A.A., Kondo, Y., 2006. Atmospheric chemistry of a 33–34 hour old volcanic cloud from Hekla Volcano (Iceland): Insights from direct sampling and the application of chemical box modeling. Journal of Geophysical Research: Atmospheres (1984–2012) 111.
Rosenfeld, D., Andreae, M.O., Asmi, A., Chin, M., Leeuw, G., Donovan, D.P., Kahn, R., Kinne, S., Kivekäs, N., Kulmala, M., 2014. Global observations of aerosol - cloud - precipitation - climate interactions. Reviews of Geophysics 52, 750-808.
Rosenfeld, D., Freud, E., 2011. Number of activated CCN as a key property in cloud aerosol interactions or, more on simplicity in complex systems, WCRP First Open Science Conference, Denver, USA.
Rosenfeld, D., Lohmann, U., Raga, G.B., O'Dowd, C.D., Kulmala, M., Fuzzi, S., Reissell, A., Andreae, M.O., 2008. Flood or drought: how do aerosols affect precipitation? science 321, 1309-1313.
Rost, B., Riebesell, U., 2004. Coccolithophores and the biological pump: responses to environmental changes, Coccolithophores. Springer, pp. 99-125.
Rubasinghege, G., Lentz, R.W., Scherer, M.M., Grassian, V.H., 2010. Simulated atmospheric processing of iron oxyhydroxide minerals at low pH: roles of particle size and acid anion in iron dissolution. Proceedings of the National Academy of Sciences 107, 6628-6633.
Rustad, D., Gregory, N., 1980. Photoreduction of gaseous iron (III) chloride with sunlight and other light sources. Inorganic and Nuclear Chemistry Letters 16, 521-524.

Sadanaga, Y., Hirokawa, J., Akimoto, H., 2001. Formation of molecular chlorine in dark condition: Heterogeneous reaction of ozone with sea salt in the presence of ferric ion. Geophysical research letters 28, 4433-4436.
Salgado, P., Melin, V., Contreras, D., Moreno, Y., Mansilla, H.D., 2013. Fenton reaction driven by iron ligands. Journal of the Chilean Chemical Society 58, 2096-2101.
Salter, I., Schiebel, R., Ziveri, P., Movellan, A., Lampitt, R., Wolff, G.A., 2014. Carbonate counter pump stimulated by natural iron fertilization in the Polar Frontal Zone. Nature Geoscience.
Sander, R., 2015. Compilation of Henry's law constants (version 4.0) for water as solvent. Atmospheric Chemistry and Physics 15, 4399-4981.
Sander, R., Burrows, J., Kaleschke, L., 2006. Carbonate precipitation in brine–a potential trigger for tropospheric ozone depletion events. Atmospheric Chemistry and Physics 6, 4653-4658.
Sanna, A., Uibu, M., Caramanna, G., Kuusik, R., Maroto-Valer, M., 2014. A review of mineral carbonation technologies to sequester CO 2. Chemical Society Reviews 43, 8049-8080.
Santachiara, G., Prodi, F., Belosi, F., 2012. A review of thermo-and diffusio-phoresis in the atmospheric aerosol scavenging process. Part 1: Drop Scavenging. Atmospheric and Climate Sciences 2, 148-158.
Schrag, D.P., Higgins, J.A., Macdonald, F.A., Johnston, D.T., 2013. Authigenic carbonate and the history of the global carbon cycle. Science 339, 540-543.
Schrenk, M.O., Brazelton, W.J., Lang, S.Q., 2013. Serpentinization, carbon, and deep life. Rev Mineral Geochem 75, 575-606.
Serov, P., Portnov, A., Mienert, J., Semenov, P., Ilatovskaya, P., 2015. Methane release from pingo - like features across the South Kara Sea shelf, an area of thawing offshore permafrost. Journal of Geophysical Research: Earth Surface 120, 1515-1529.
Shakhova, N., Semiletov, I., Panteleev, G., 2005. The distribution of methane on the Siberian Arctic shelves: Implications for the marine methane cycle. Geophysical Research Letters 32.
Shakhova, N., Semiletov, I., Salyuk, A., Kosmach, D., 2008. Anomalies of methane in the atmosphere over the East Siberian shelf: Is there any sign of methane leakage from shallow shelf hydrates, Geophysical Research Abstracts, p. A01526.
Shindell, D., Kuylenstierna, J.C., Vignati, E., van Dingenen, R., Amann, M., Klimont, Z., Anenberg, S.C., Muller, N., Janssens-Maenhout, G., Raes, F., 2012. Simultaneously mitigating near-term climate change and improving human health and food security. Science 335, 183-189.
Sissmann, O., Brunet, F., Martinez, I., Guyot, F.o., Verlaguet, A., Pinquier, Y., Daval, D., 2014. Enhanced olivine carbonation within a basalt as compared to single-phase experiments: reevaluating the potential of CO2 mineral sequestration. Environmental science & technology 48, 5512-5519.
Sivan, O., Antler, G., Turchyn, A.V., Marlow, J.J., Orphan, V.J., 2014. Iron oxides stimulate sulfate-driven anaerobic methane oxidation in seeps. Proceedings of the National Academy of Sciences 111, E4139-E4147.
Six, K.D., Kloster, S., Ilyina, T., Archer, S.D., Zhang, K., Maier-Reimer, E., 2013. Global warming amplified by reduced sulphur fluxes as a result of ocean acidification. Nature Climate Change 3, 975-978.
Skinner, L., 2008. Facing future climate change: is the past relevant? Philosophical Transactions of the Royal Society of London A: Mathematical, Physical and Engineering Sciences 366, 4627-4645.
Slomp, C.P., Mort, H.P., Jilbert, T., Reed, D.C., Gustafsson, B.G., Wolthers, M., 2013. Coupled dynamics of iron and phosphorus in sediments of an oligotrophic coastal basin and the impact of anaerobic oxidation of methane.
Smetacek, V., Klaas, C., Strass, V.H., Assmy, P., Montresor, M., Cisewski, B., Savoye, N., Webb, A., d'Ovidio, F., Arrieta, J.M., 2012. Deep carbon export from a Southern Ocean iron-fertilized diatom bloom. Nature 487, 313-319.
Smetacek, V., Naqvi, S., 2008. The next generation of iron fertilization experiments in the Southern Ocean. Philosophical Transactions of the Royal Society of London A: Mathematical, Physical and Engineering Sciences 366, 3947-3967.
Solomon, E.A., Spivack, A.J., Kastner, M., Torres, M.E., Robertson, G., 2014. Gas hydrate distribution and carbon sequestration through coupled microbial methanogenesis and silicate weathering in the Krishna–Godavari basin, offshore India. Marine and Petroleum Geology 58, 233-253.
Song, P., Wang, Y., Pan, J., Xu, W., Zhuang, L., 2015. Structure-activity relationship in high-performance iron-based electrocatalysts for oxygen reduction reaction. Journal of Power Sources 300, 279-284.
Soreghan, G.S., Sur, S., Owens, J.D., Raiswell, R., Heavens, N.G., Natalie, M., Lyons, T.W., 2014. The potential biological impact of eolian delivery of reactive iron to late Paleozoic icehouse seas, 2014 GSA Annual Meeting in Vancouver, British Columbia.

Sousa, F.L., Thiergart, T., Landan, G., Nelson-Sathi, S., Pereira, I.A., Allen, J.F., Lane, N., Martin, W.F., 2013. Early bioenergetic evolution. Philosophical Transactions of the Royal Society of London B: Biological Sciences 368, 20130088.
Southworth, B.A., Voelker, B.M., 2003. Hydroxyl radical production via the photo-Fenton reaction in the presence of fulvic acid. Environmental science & technology 37, 1130-1136.
Spolaor, A., Vallelonga, P., Cozzi, G., Gabrieli, J., Varin, C., Kehrwald, N., Zennaro, P., Boutron, C., Barbante, C., 2013. Iron speciation in aerosol dust influences iron bioavailability over glacial - interglacial timescales. Geophysical Research Letters 40, 1618-1623.
Storelvmo, T., Kristjansson, J., Muri, H., Pfeffer, M., Barahona, D., Nenes, A., 2013. Cirrus cloud seeding has potential to cool climate. Geophysical Research Letters 40, 178-182.
Straub, K.L., Kappler, A., Schink, B., 2005. Enrichment and isolation of ferric - iron - and humic - acid - reducing bacteria. Methods in enzymology 397, 58-77.
Studebaker, M.L., Huffman, E., Wolfe, A., Nabors, L., 1956. Oxygen-containing groups on the surface of carbon black. Industrial & Engineering Chemistry 48, 162-166.
Suess, E., Torres, M., Bohrmann, G., Collier, R., Greinert, J., Linke, P., Rehder, G., Trehu, A., Wallmann, K., Winckler, G., 1999. Gas hydrate destabilization: enhanced dewatering, benthic material turnover and large methane plumes at the Cascadia convergent margin. Earth and Planetary Science Letters 170, 1-15.
Sullivan, R.C., Guazzotti, S.A., Sodeman, D.A., Tang, Y., Carmichael, G.R., Prather, K.A., 2007. Mineral dust is a sink for chlorine in the marine boundary layer. Atmospheric Environment 41, 7166-7179.
Sun, X., Turchyn, A.V., 2014. Significant contribution of authigenic carbonate to marine carbon burial. Nature Geoscience 7, 201-204.
Sur, S., Owens, J.D., Soreghan, G.S., Lyons, T.W., Raiswell, R., Heavens, N.G., Mahowald, N.M., 2015. Extreme eolian delivery of reactive iron to late Paleozoic icehouse seas. Geology 43, 1099-1102.
Swanson, K.A., 1988. The effect of dissolved catechol on the dissolution of amorphous silica in seawater. Pennsylvania State University.
Takashima, R., Nishi, H., Huber, B., LeckieE, M., 2006. Greenhouse world and the Mesozoic Ocean. The Oceanography Society 19, 82-92.
Taylor, L.L., Quirk, J., Thorley, R.M., Kharecha, P.A., Hansen, J., Ridgwell, A., Lomas, M.R., Banwart, S.A., Beerling, D.J., 2015. Enhanced weathering strategies for stabilizing climate and averting ocean acidification. Nature Climate Change.
Teixeira, A.P.C., Tristão, J.C., Araujo, M.H., Oliveira, L.C., Moura, F.C., Ardisson, J.D., Amorim, C.C., Lago, R.M., 2012. Iron: a versatile element to produce materials for environmental applications. Journal of the Brazilian Chemical Society 23, 1579-1593.
Thakur, R.S., Chaudhary, R., Singh, C., 2015. Influence of pH on photocatalytic reduction, adsorption, and deposition of metal ions: speciation modeling. Desalination and Water Treatment 56, 1335-1363.
Tréguer, P., Pondaven, P., 2000. Global change: silica control of carbon dioxide. Nature 406, 358-359.
Tribovillard, N., Du Châtelet, E.A., Gay, A., Barbecot, F., Sansjofre, P., Potdevin, J.-L., 2013. Geochemistry of cold seepage-impacted sediments: Per-ascensum or per-descensum trace metal enrichment? Chemical Geology 340, 1-12.
van Kessel, M.A., Speth, D.R., Albertsen, M., Nielsen, P.H., den Camp, H.J.O., Kartal, B., Jetten, M.S., Lücker, S., 2015. Complete nitrification by a single microorganism. Nature.
van Sebille, E., Wilcox, C., Lebreton, L., Maximenko, N., Hardesty, B.D., van Franeker, J.A., Eriksen, M., Siegel, D., Galgani, F., Law, K.L., 2015. A global inventory of small floating plastic debris. Environmental Research Letters 10, 124006.
Vione, D., Maurino, V., Minero, C., Pelizzetti, E., 2003. The atmospheric chemistry of hydrogen peroxide: A review. ANNALI DI CHIMICA-ROMA- 93, 477-486.
von Glasow, R., Sander, R., 2001. Variation of sea salt aerosol pH with relative humidity. Geophysical research letters 28, 247-250.
Vorhies, J.S., Gaines, R.R., 2009. Microbial dissolution of clay minerals as a source of iron and silica in marine sediments. Nature Geoscience 2.
Voss, M., Bange, H.W., Dippner, J.W., Middelburg, J.J., Montoya, J.P., Ward, B., 2013. The marine nitrogen cycle: recent discoveries, uncertainties and the potential relevance of climate change. Philosophical Transactions of the Royal Society B: Biological Sciences 368, 20130121.
Wallmann, K., Aloisi, G., Haeckel, M., Tishchenko, P., Pavlova, G., Greinert, J., Kutterolf, S., Eisenhauer, A., 2008. Silicate weathering in anoxic marine sediments. Geochimica et Cosmochimica Acta 72, 2895-2918.

Wang, B., O'Brien, R.E., Kelly, S.T., Shilling, J.E., Moffet, R.C., Gilles, M.K., Laskin, A., 2014a. Reactivity of liquid and semisolid secondary organic carbon with chloride and nitrate in atmospheric aerosols. The Journal of Physical Chemistry A 119, 4498-4508.
Wang, L., Yao, Y., Zhang, Z., Sun, L., Lu, W., Chen, W., Chen, H., 2014b. Activated carbon fibers as an excellent partner of Fenton catalyst for dyes decolorization by combination of adsorption and oxidation. Chemical Engineering Journal 251, 348-354.
Wang, P., Grover, S., Pruppacher, H., 1978. On the effect of electric charges on the scavenging of aerosol particles by clouds and small raindrops. Journal of the Atmospheric Sciences 35, 1735-1743.
Wang, S.H., Hsu, N.C., Tsay, S.C., Lin, N.H., Sayer, A.M., Huang, S.J., Lau, W.K., 2012. Can Asian dust trigger phytoplankton blooms in the oligotrophic northern South China Sea? Geophysical Research Letters 39.
Wang, Y., Lee, K.-H., Lin, Y., Levy, M., Zhang, R., 2014c. Distinct effects of anthropogenic aerosols on tropical cyclones. Nature Climate Change 4, 368-373.
Watson, A.J., Vallis, G.K., Nikurashin, M., 2015. Southern Ocean buoyancy forcing of ocean ventilation and glacial atmospheric CO2. Nature Geoscience.
Wayne, R.P., Poulet, G., Biggs, P., Burrows, J., Cox, R., Crutzen, P., Hayman, G., Jenkin, M., Le Bras, G., Moortgat, G., 1995. Halogen oxides: Radicals, sources and reservoirs in the laboratory and in the atmosphere. Atmospheric Environment 29, 2677-2881.
Weber, T., Cram, J.A., Leung, S.W., DeVries, T., Deutsch, C., 2016. Deep ocean nutrients imply large latitudinal variation in particle transfer efficiency. Proceedings of the National Academy of Sciences, 201604414.
Weiser, V., Eisenreich, N., Roth, E., Pfeil, A., Mechanisms of Soot Reduction in Diesel Pool Fire by Ferrocene.
Weller, C., Tilgner, A., Bräuer, P., Herrmann, H., 2014. Modeling the Impact of Iron–Carboxylate Photochemistry on Radical Budget and Carboxylate Degradation in Cloud Droplets and Particles. Environmental science & technology 48, 5652-5659.
Willey, J.D., Kieber, R.J., Seaton, P.J., Miller, C., 2008. Rainwater as a source of Fe (II)-stabilizing ligands to seawater. Limnology and Oceanography 53, 1678.
Williams, J., Reus, M.d., Krejci, R., Fischer, H., Ström, J., 2002. Application of the variability-size relationship to atmospheric aerosol studies: estimating aerosol lifetimes and ages. Atmospheric Chemistry and Physics 2, 133-145.
Williamson, P., Wallace, D.W., Law, C.S., Boyd, P.W., Collos, Y., Croot, P., Denman, K., Riebesell, U., Takeda, S., Vivian, C., 2012. Ocean fertilization for geoengineering: a review of effectiveness, environmental impacts and emerging governance. Process Safety and Environmental Protection 90, 475-488.
Wittmer, J., Bleicher, S., Ofner, J., Zetzsch, C., 2015a. Iron (III)-induced activation of chloride from artificial sea-salt aerosol. Environmental Chemistry 12, 461-475.
Wittmer, J., Bleicher, S., Zetzsch, C., 2015b. Iron (III)-Induced Activation of Chloride and Bromide from Modeled Salt Pans. The Journal of Physical Chemistry A 119, 4373–4385.
Wittmer, J., Zetzsch, C., 2016. Photochemical activation of chlorine by iron-oxide aerosol. Journal of Atmospheric Chemistry.
Wren, S., Donaldson, D., 2012. How does deposition of gas phase species affect pH at frozen salty interfaces? Atmospheric Chemistry and Physics 12, 10065-10073.
Wu, Y.-H., Liao, L., Wang, C.-S., Ma, W.-L., Meng, F.-X., Wu, M., Xu, X.-W., 2013. A comparison of microbial communities in deep-sea polymetallic nodules and the surrounding sediments in the Pacific Ocean. Deep Sea Research Part I: Oceanographic Research Papers 79, 40-49.
Xu, H.-Q., Hu, J., Wang, D., Li, Z., Zhang, Q., Luo, Y., Yu, S.-H., Jiang, H.-L., 2015. Visible-Light Photoreduction of CO2 in a Metal–Organic Framework: Boosting Electron–Hole Separation via Electron Trap States. Journal of the American Chemical Society 137, 13440-13443.
Yamamoto, A., Yamanaka, Y., Oka, A., Abe - Ouchi, A., 2014. Ocean oxygen depletion due to decomposition of submarine methane hydrate. Geophysical Research Letters 41, 5075-5083.
Yokouchi, Y., Noijiri, Y., Barrie, L., Toom-Sauntry, D., Machida, T., Inuzuka, Y., Akimoto, H., Li, H.-J., Fujinuma, Y., Aoki, S., 2000. A strong source of methyl chloride to the atmosphere from tropical coastal land. Nature 403, 295-298.
Yoshizawa, K., Shiota, Y., Yumura, T., Yamabe, T., 2000. Direct methane-methanol and benzene-phenol conversions on Fe-ZSM-5 zeolite: Theoretical predictions on the reaction pathways and energetics. The Journal of Physical Chemistry B 104, 734-740.
Young, C., Washenfelder, R., Edwards, P., Parrish, D., Gilman, J., Kuster, W., Mielke, L., Osthoff, H., Tsai, C., Pikelnaya, O., 2014. Chlorine as a primary radical: evaluation of methods to understand its role in initiation of oxidative cycles. Atmospheric Chemistry and Physics 14, 3427-3440.

Yu, H., Chin, M., Bian, H., Yuan, T., Prospero, J.M., Omar, A.H., Remer, L.A., Winker, D.M., Yang, Y., Zhang, Y., 2015a. Quantification of trans-Atlantic dust transport from seven-year (2007–2013) record of CALIPSO lidar measurements. Remote Sensing of Environment 159, 232-249.

Yu, H., Chin, M., Yuan, T., Bian, H., Remer, L.A., Prospero, J.M., Omar, A., Winker, D., Yang, Y., Zhang, Y., 2015b. The fertilizing role of African dust in the Amazon rainforest: A first multiyear assessment based on data from Cloud - Aerosol Lidar and Infrared Pathfinder Satellite Observations. Geophysical Research Letters 42, 1984-1991.

Zamaraev, K., 1997. Catalytic science and technology for environmental issues. Catalysis today 35, 3-13.

Zamaraev, K.I., Khramov, M.I., Parmon, V.N., 1994. Possible impact of heterogeneous photocatalysis on the global chemistry of the Earth's atmosphere. Catalysis Reviews—Science and Engineering 36, 617-644.

Zhang, H., McFarquhar, G.M., Cotton, W.R., Deng, Y., 2009. Direct and indirect impacts of Saharan dust acting as cloud condensation nuclei on tropical cyclone eyewall development. Geophysical Research Letters 36.

Zhang, Z., Moore, J.C., Huisingh, D., Zhao, Y., 2014. Review of geoengineering approaches to mitigating climate change. Journal of Cleaner Production.

Zhao, M.-Y., Zheng, Y.-F., Zhao, Y.-Y., 2016. Seeking a geochemical identifier for authigenic carbonate. Nature communications 7.

Zhou, X., Zhang, Y., Wang, C., Wu, X., Yang, Y., Zheng, B., Wu, H., Guo, S., Zhang, J., 2012. Photo-Fenton reaction of graphene oxide: a new strategy to prepare graphene quantum dots for DNA cleavage. Acs Nano 6, 6592-6599.

Zhu, X., Prospero, J.M., Savoie, D.L., Millero, F.J., Zika, R.G., Saltzman, E.S., 1993. Photoreduction of iron (III) in marine mineral aerosol solutions. Journal of Geophysical Research: Atmospheres (1984–2012) 98, 9039-9046.

Ziegler, M., Diz, P., Hall, I.R., Zahn, R., 2013. Millennial-scale changes in atmospheric CO2 levels linked to the Southern Ocean carbon isotope gradient and dust flux. Nature Geoscience 6, 457-461.

Zijlstra, H., 1995. 3. Early diagenesis of chalk, in: The sedimentology of chalk. Springer.

Zuberi, B., Johnson, K.S., Aleks, G.K., Molina, L.T., Molina, M.J., Laskin, A., 2005. Hydrophilic properties of aged soot. Geophysical research letters 32.